ADJUSTMENT OF SURFACE CHEMICAL AND PHYSICAL PROPERTIES WITH FUNCTIONALIZED POLYMERS TO CONTROL CELL ADHESION

A Dissertation

Presented to the Faculty of the Graduate School

of Cornell University

In Partial Fulfillment of the Requirements for the Degree of

Doctor of Philosophy

by

Zhaoli Zhou

January 2013

ADJUSTMENT OF SURFACE CHEMICAL AND PHYSICAL PROPERTIES WITH FUNCTIONALIZED POLYMERS TO CONTROL CELL ADHESION

Zhaoli Zhou, Ph. D.

Cornell University 2013

Cell-surface interaction is crucial in many cellular functions such as movement, growth, differentiation, proliferation and survival. In the present work, we have developed several strategies to design and prepare synthetic polymeric materials with selected cues to control cell attachment. To promote neuronal cell adhesion on the surfaces, biocompatible, non-adhesive PEG-based materials were modified with neurotransmitter acetylcholine functionalities to produce hydrogels with a range of porous structures, swollen states, and mechanical strengths. Mice hippocampal cells cultured on the hydrogels showed differences in number, length of processes and exhibited different survival rates, thereby highlighting the importance of chemical composition and structure in biomaterials. Similar strategies were used to prepare polymer brushes to assess how topographical cues influence neuronal cell behaviors. The brushes were prepared using the "grown from" method through surface-initiated atom transfer radical polymerization (SI-ATRP) reactions and further patterned via UV photolithography. Protein absorption tests and hippocampal neuronal cell culture of the brush patterns showed that both protein and neuronal cells can adhere to the patterns and therefore can be guided by the patterns at certain length scales.

We also prepared functional polymers to discourage attachment of undesirable cells on the surfaces. For example, we synthesized PEG-perfluorinated alkyl amphiphilic surfactants to modify polystyrene-*block*-poly(ethylene-ran-butylene)-*block*-polyisoprene (SEBI or K3) triblock

copolymers for marine antifouling/fouling release surface coatings. Initial results showed that the polymer coated surfaces can facilitate removal of *Ulva* sporelings on the surfaces. In addition, we prepared both bioactive and dual functional biopassive/bioactive antimicrobial coatings based on SEBI polymers. Incubating the polymer coated surfaces with gram-positive bacteria (*S. aureus*), gram-negative bacteria (*E. coli*) and marine bacteria (*C. marina*) species demonstrated that, unlike biopassive surfaces, the dual functionality polymer coated surfaces can significantly reduce both live and dead cells, without killing the cells in the culture media. The knowledge gained from those studies offers opportunities for further modification and potential applications of those types of polymers in the future.

BIOGRAPHICAL SKETCH

Zhaoli Zhou was born and grew up in Gansu, P. R. China, and she finished her undergraduate studies in the School of Chemistry and Chemical Engineering at Lanzhou University in China. Zhaoli came to U.S. in 2004, and enrolled in the graduate studies at the Department of Chemistry in Wake Forest University, North Carolina. Under the supervision of Dr. Bernard A. Brown II, Zhaoli completed her Master's degree in the field of Biochemistry and Protein X-ray Crystallography in 2007. After graduation, Zhaoli decided to pursue her Ph.D. in the Department of Chemistry and Chemical Biology at Cornell University. Working in the research laboratory of Prof. Christopher K. Ober, Zhaoli's research was focus on developing different types of polymers for surface modification and various biological applications. After completing her Ph.D. degree in fall 2012, Zhaoli set out to begin her professional career in the private sector in the U.S.

ACKNOWLEDGMENTS

First and foremost, I would like to use this opportunity to express my deepest gratitude to my thesis advisor and mentor Prof. Christopher K. Ober, who has been very patient and supportive through all the years of my PhD studies, and always given me great freedom to pursue independent work. His great personality and his dedication to his work and students have also been truly inspirational to me. I am also very grateful to Prof. Barbara Baird and Prof. Claudia Fischbach-Teschl for serving on my thesis committee and for always being there for me during my graduate studies. I would also like to give my special thanks to Dr. Herbert Geller and Dr. Nancy Geller in NIH, and my master's thesis advisor Dr. Bernard A. Brown II They have been great friends and mentors to me, I can't thank them enough for their guidance and advice in many difficult situations in my life.

It has been a great privilege to spend several years in Prof. Ober's group, and I would like to thank all group members for their help and friendship. In particular, I sincerely thank Prof. Xiao (Matthew) Hu, Prof. Cláudio dos Santos, and Prof. Jin Kyun Lee for sharing their experiences and giving great advice during my first couple of years in the lab. I would also like to thank people from Bard 360 office, past and present, Dr. Heloise Thérien-Aubin, Dr. Evan Lawrence Schwartz, Dr. Kui Xu and Lin Chen, for creating such a good atmosphere inside and outside the lab. I also thank Dr. Yosuke Hoshi, Dr. Youyong Xu, Liz Welch, and Alwin Wan for many times of help with my experiments. Also, it was a wonderful learning experience for me to work with Dr. Hee-Soo Yoo, Dr. Harihara Subramanian Sundaram, Dr. Youngjin Cho, David Calabrese and Justin Brian Steimle on antifouling projects; they let me understand the importance of teamwork. I would thank my dear friends Dr. Yeon Sook Chung and Christine Ouyang, their warm friendship certainly made Ithaca winters more tolerable.

I would also like to take this chance to thank my friends and collaborators who made this dissertation possible. Prof. Edward Kramer, Dr. Michael Dimitrou and Dr. Warren Taylor (UCSB) have kindly helped me with material preparation and characterization. Prof. Ester Angert and David Miller (Microbiology Department of Cornell) helped me with bacteria cell culturing studies. Dr. Panpan Yu and Dr. Bing Zhou (NIH) have helped me with neuronal cell cultures and taught me a lot about neurobiology. It was my pleasure to work with all of them and I am grateful for all their time and help. In addition, I would thank the Cornell Center for Materials Research (CCMR) stuffs, Dr. Yuanming Zhang, Anthony Condo, John Hunt, Kit Umbach, and Nanobiotechnology Center (NBTC) staff, Dr. Teresa Porri, and Penny Burke. They helped me solve many difficult problems in my experiments, and I truly enjoyed learning technical aspects of scientific research from them.

I would like to take this chance to thank my family in China, my father Zhong Zhou, my mother Jingfeng Li, my two beautiful sisters, Zhaoyu and Changxian Zhou, and my younger brother, Changke Zhou, for their unconditional love and constant support. I also want to express my deepest gratitude to Dr. Holly Brower, Jon Brower, and Dr. Udesh de Silva, they gave me a second family in the United states, standing right behind me with all their warmth, sensitivity, and understanding throughout all my graduate studies; their love and belief are the driving force for me to pursue my Ph.D. at Cornell.

TABLE OF CONTENTS

LIST OF FIGURES

LIST OF TABLES

CHAPTER ONE

SYNTHETIC POLYMERIC MATERIALS FOR CELL-SURFACE STUDIES

1.1 Introduction

Cell-surface interaction is a crucial event in many physiological processes and adhesion of cells on a surface plays an important role in a multitude of cellular functions such as movement, growth, differentiation, survival, and proliferation. Such interaction also represents a prerequisite for many cellular processes including cell-cell recognition, information transfer, and signaling. Cell interaction with surfaces can be both specific and non-specific. Specific interactions can be promoted by surfaces through their physical shape, topography, and chemical properties, and generally involve cell adhesion proteins and molecule recognition at the surface of cells, such as interactions between integrin receptors and the RGD motif (Arginine-Glycine-Aspartate) of proteins [1]. Many cells also have a tendency to physically adsorb onto solid substrates without specific receptor−recognition interactions (non-specific adsorption). Often non-specific adhesion of cells are undesirable, therefore under many circumstances surfaces are modified to have both enhanced specific binding or reduced non-specific binding. Moreover, artificial surfaces can be prepared to provide either cell repulsive or cell attractive characteristics [2]. The attractive interaction promotes cell adhesion, and can be represented by van-der-Waals forces, hydrogen bonding, acid-base interactions and hydrophobic interactions. The repulsive forces reduces cell adhesion, and can be caused by the presence of bound water molecules on polar moieties or steric hindrance due to the presence of hydrophilic, mobile macromolecules on the material or cell surface.

Synthetic polymeric materials play an essential and ubiquitous role in our daily lives due to their availability and wild range of desirable properties; their many key applications include food packaging, textiles and medical devices. Compared to naturally derived materials, they are also inexpensive, easy to synthesize, and many of their physical and chemical properties can be

precisely controlled. Recently, there is increased interest for researchers to use synthetic materials in interfaces; examples of such applications include biomedical implants that replace or improve lost or impaired vital body functions, biosensors for biomedical diagnostics, non-biofouling surfaces for the maritime industry or for device implants, polymers for controlled drug release, and templates for tissue engineering. All these processes require an understanding of the interactions between the synthetic surfaces and the biological environment. Surface modification used for controlling the interactions of protein and cells at the interface with synthetic materials can be divided into physical and chemical categories. Physical surface modifications include changes in surface roughness, surface charge, and mechanical properties [3]. Chemical modifications of surfaces include altered local surface chemistry, generation of functional groups or interaction with biomolecules (such as ECM proteins) and cells [4].

In this review chapter, we outline the types of synthetic polymers used for cell-surface studies, categorize strategies and methods used to prepare the surfaces, list experimental evidence which proves the effectiveness of the material – cellular interactions, and analyze the key factors in the development of polymers for specific cell-surface interactions. We primarily summarize the research area dealing with the use of surface cues on synthetic materials for cellular control with applications in the regeneration or repair of the nervous system, antifouling and fouling release marine surfaces, and surfaces for antimicrobial applications. Directions for future research and challenges in the development of those areas are also addressed.

1.2 Overview of Types of Synthetic Materials Used for Cell-Surface Studies

1.2.1 Hydrogels

Hydrogels are crosslinked, water-insoluble polymeric networks which have the capacity

to hold large amounts of water when placed in an aqueous environment. Hydrogels exhibit a variety of functional properties, such as swelling, mechanical, permeation, surface and optical properties, thus provide many applications in oil recovery, agriculture, and separation processes. They are also particularly suitable for biomedical and tissue engineering applications [5,6], because they show structural similarities to the macromolecular based components in the body and are considered biocompatible.

Based on various parameters, hydrogels can be classified into different categories [6,7]. They can be prepared from natural resources, such as collagen, gelatin, chitosan, and hyaluronic acid, or specifically synthesized homopolymers or copolymers, such as polyhydroxyethyl methacrylate (pHEMA) and polymethyl methacrylate (pMMA) hdyrogels. Based on the charge of the networks, hydrogels can be classified as neutral, anionic or cationic. According to their physical structures, amorphous, semicystalline, hydrogen-bonded, supramolecular, or hydrocolloidal hydrogels can be distinguished. Such classifications can also be made based on the porosity of the gels, including non-porous, micro-porous, macro-porous, and super-porous hydrogels. Depending on the nature of the crosslinking reactions, permanent hydrogels containing covalent bonds, while physical hydrogels may be formed due to physical interactions, such as molecular entanglement, ionic interactions and hydrogen bonding, to form crosslinked networks. In addition, conventional hydrogels absorb water when put in aqueous media and there is no change in the equilibrium swelling with changes of the environment, while “smart hydrogels” are “stimuli responsive”, they can change equilibrium swelling behavior with a change of the surrounding environment, such as pH, salt concentration, temperature, and electric field.

Most hydrogels are very hydrophilic due to the presence of hydrophilic chemical residues

within the polymer backbone or side chains, such as hydroxylic (-OH), carboxylic (-COOH), amidic (-CONH-), amine ($-NH_2$), sulphonic ($-SO_3H$) and other functional groups. Hydrogels with a significant amount of hydrophobic content can also be produced, just by blending or copolymerizing hydrophilic and hydrophobic monomers in the polymer precursors. The water holding capacity of hydrogels are often determined by the number of the hydrophilic groups and crosslinking density in the network; the higher the number of the hydrophilic groups and lower crosslinking density, the higher is the water holding capacity or increase in the equilibrium swelling capacity. The percentage swelling (S%) value, which is the difference between the weight of fully swollen gels (W_s) and the dry gels (W_d), is used to measure this water holding capacity and is expressed by the following equation [7]: $S\% = (W_s-W_d)/W_d \times 100$. Also, increased crosslinking density can increase the mechanical strength of the hydrogels, but at the same time decrease the elongation of the hydrogels, and as a result hydrogels become brittle.

Due to their capability of retaining high amounts of water and their rubbery nature, many hydrogels can capture numerous characteristics of the architecture and mechanics of the native cellular microenvironment and provide excellent biocompatibility, therefore can be used in scaffold engineering to closely resemble living tissue. Recent work has demonstrated that hydrogels can provide distinct efficacy as 3D matrices for cell culture [8], and they help to promote cell viability and direct cell adhesion, differentiation, proliferation and migration. Synthetic hydrogels such as PEG, poly(vinyl alcohol), and pHEMA are good candidates for this application, those hydrogels are inert in nature and allow facile tuning of mechanical properties, they are also highly reproducible and can be simply processed. Nanocomposite 3D scaffolds based on biodegradable hydrogels have also been developed by using different nano-structures and processing methods to provide robust and diverse scaffolds for cell culture. Hydrogels are

also highly attractive materials for developing synthetic ECM analogues since they can simulate the nature of most soft tissues [9]. However, application of synthetic hydrogels to tissue engineering is a complicated process, and in order to properly mimic the native cellular environment, it is necessary to rationally incorporate bio-inspired cues to provide multifunctional permissive surfaces with tailored bioactivity, structural and mechanical integrity as well as electrical conductivity, and their mechanical and chemical properties have to be tuned to the time and length scales of cell development. This likely requires multiple, orthogonal chemistries, and different fabrication techniques can also prove critical for the success of their applications [10].

1.2.2 Soluble Polymers, Proteins and Polypeptides

Poly(ethylene glycol)s or PEGs are water soluble macromolecules and are one of the most used synthetic materials because of their biocompatibility. Polymers based on PEG have also been widely used to resist nonspecific protein adsorption and subsequently cell attachment [11]. Although this behavior of PEG is not fully understood and is still an active area of research [12], it is believed that the dense solvated brush-like PEG structure uses a “steric repulsion” and a hydration layer *via* hydrogen bonding around molecular chains to shields surface charges and disallow interaction of proteins with the underlying surface [13]. Therefore, the molecular weight or chain length of PEG and its density on surfaces can contribute these protein and cell resistance effects [14]. Previous work [15] used long- and short-chain PEG based alkanethiol assemblies to investigate the differences in cell response. The results showed that longer PEG chains have higher resistance to protein adsorption and cell adhesion. Short PEG chains can still prevent adsorption; however, this can be observed only when the density and coverage of PEG on the surface is high.

Many other soluble synthetic polymers [16] that are not neutral and mostly bear either

positive or negative charges, such as poly-l-lysine (PLL), polypropylenimine (PPI), polypyrrole (PPy) and polyacrylic acid (PAA), have also been used as biomaterials for cell culture and have shown to be able to improve rat neuronal cell growth [17,18]. In addition, poly(ethylene imine) (PEI) has been used for complex formation with DNA and may pave the way for in situ transfection of cells in the field of tissue engineering [19]. These polycations and polyanions can be deposited on surfaces primarily by electrostatic forces to form thin films on the substrate surfaces. The layer-by-layer (LBL) technique [20] is a method that represents the alternating adsorption of oppositely charged polyelectrolytes from aqueous solution onto a surface. The adsorption steps can be repeated in cycles which lead to polyelectrolyte multilayer formation of adjustable composition and thickness. Some polyelectrolytes bear ionogenic groups, their charge depending on ambient conditions, so the adjustment and control of process parameters like pH value, ionic strength of the solutions as well as temperature can have a strong impact on their conformation, and hence those conditions have to be more carefully controlled to apply those soluble polymers on the surfaces through solution coating or LBL techniques.

In vivo, large extracellular matrix (ECM) proteins, such as collagen, laminin, or fibronectin, provide binding domains for cell adhesion, and they have also been shown to improve cell viability and function *in vitro* [21]. Today, protein engineering has evolved such that we can identify active peptide sequences from desired components of the ECM proteins, and incorporate them into synthetic polymers. This allows the controlled placement of specific binding domains of proteins, such as RGD, IKVAV, and YIGSR, onto an otherwise bio-inert background. For instance, modifying PEG scaffolds with pendent RGD, which is the known binding domain of fibronectin, has been shown to increase viability and adhesion of encapsulated cells [22]. Novel polymerization mechanisms, such as photointiated acrylate and thiol-ene

chemistries, also allow facile incorporation of peptides within routinely used synthetic polymers. Similar concepts can be extended to other functional peptide sequences, such as growth factors [23,24]. Furthermore, other biomolecules, such as micro RNAs (mRNA), small interfering RNAs (siRNA) and RNA aptamers, have also been incorporated in synthetic polymeric materials and induce specific cellular responses. Also, it is important to note that many biomacromolecules including DNA, RNA, proteins and polysaccharides are also polyelectrolytes [25], and hence they may be incorporated onto charged surfaces. The LBL method can also be applied to those polyelectrolytes to tailor the layer thickness and wettability of multilayers, and might be a useful tool to mimic the natural environment of cells and to regulate the adhesion of cells on those biomaterials.

1.2.3 Polymer Thin Films through Self-assembled Monolayers and Polymer Brushes

In biomedical applications, materials used for device making are often chosen because of their bulk properties, such as mechanical strength, porosity, and optical transparency requirements, without necessarily having the optimum surface properties, such as wettability, biocompatibility, corrosion resistance and friction. Surface modification and engineering were frequently followed in order to tailor the surface characteristics to meet specific needs without changing bulk properties.

Self-assembled monolayers (SAMs) provide surfaces with well-defined thin molecular films of biological or chemical moieties, and have stimulated much interest due to their flexibility of processing, molecular order, versatility, and simplicity [1]. Modern organic syntheses can be used to precisely control the molecular composition and properties of SAMs, making them one of the most attractive ways to obtain well-ordered organic surfaces. SAMs can

be prepared from solution using attachment of chlorosilanes, organosilioxanes, and thiolated molecules onto various surface with a high grafting density, as long as the anchor functionality is chosen correctly (e.g.: thiols on gold, silanes on glass, Si/SiO_2 and plasma oxidized polymers). Terminal groups with which SAMs have been used to functionalize surfaces include alcohols, alkanes, carboxylic acid, and primary amines [26]. Because of their well-characterized nature, SAMs are often used as the "gold standard" to present certain chemical functionalities for the investigation of interactions between surfaces and cells [27,28]. For example, various SAMs containing $-CH_3$-, $-OH$-, $-CO_2H$-, and $-(OCH_2CH_2)_3-OH$ were used to study bacterial adhesion resistance in real time [29]. Adhesion was found to be lowest on the $-(OCH_2CH_2)_3-OH$ surfaces, followed by $-OH$ surfaces, and on $-CO_2H$- and $-CH_3$ terminated SAMs, bacterial adhesion was much higher.

Polymer brushes are another class of surface modifiers that have been used to control and modify surface properties without altering a material's bulk characteristics [1]. In polymer brushes, long polymer chains are tethered by an end to a surface, and the tethering of the chains in proximity to each other forces the chains to stretch away from the surface hence avoid overlap. Commonly, brushes are prepared by grafting polymers to surfaces (or "grafted to"), either *via* chemical bond formation between reactive groups on the surface and reactive end groups, or by physisorption of block copolymers with 'sticky' segments. However, it is very difficult to achieve high grafting densities through the "grafted to" method, as a result of steric crowding of reactive surface sites by already adsorbed polymers, and the film thickness is limited by the molecular weight and conformation of the polymer in solution. 'Surface-initiated polymerizations' (also called "grafting from") [30] prepared polymer brushes from initiators bound to surfaces, is a powerful alternative to control of the functionality, density and thickness

of polymer brushes with almost molecular precision. First, the chosen substrate is modified with initiator-bearing SAMS. The initiator surfaces are then exposed to solutions containing catalyst, monomers, and solvent to start polymerization reactions. Ideally, the polymerization is surface-confined and no polymerization in solution should occur; thereby avoiding contaminating the surfaces with undesired structures [31,32]. This method has been used to grow poly(2-methacryloyloxy)propyl trimethylammonium bromide brushes [33], and the resulting brushes have showed good cell adhesion properties and long-term stability for neuronal culture.

Both SAMs and polymer brushes are powerful tools for surface functionalization and for controlling the biology-materials interface, and they offer complementary advantages to the field of biotechnology. While SAMs are easy of prepare, polymer brushes offer better mechanical and chemical robustness, coupled with a high degree of synthetic flexibility towards the introduction of a variety of functional groups. There is also an increasing interest of using functional or diblock copolymer brushes for 'smart' or responsive surfaces, which can change a physical properties upon an external trigger, such as heat, pH, or salt concentration.

Another advantage of polymer brushes over other surface modification methods is that they are well-suited for the fabrication of nano- or micro-patterned arrays with control over chemical functionality, shape, and feature dimension and inter-feature spacing on the micron and nanometer length scales. These characteristics make them very attractive for a variety of biotechnological applications including their use in molecular recognition, biosensing, protein separation and chromatography, combinatorial chemistry, scaffolds for tissue engineering, and micro- and nanofluidics. Particularly, "neuronal cell patterning" is an emerging area of study which uses the defined engineering methods to control the growth of neurons into networks. Polymer brushes have proved to be very useful to produce surfaces with either "topographical

patterns" induced by shapes and textures, or "chemical patterns" presented by different biochemical functional groups. They are of major interest in the field of cell-based biosensors, neuroelectronic circuits, neurological implants, and pharmaceutical testing [34].

It is important to characterize and analyze surfaces modified by self-assembled monolayers and polymer brushes to ensure the presence of different chemical functional groups, because the important roles they play in the interactions with cells. Infrared (IR) spectroscopy is a fast, simple and very useful tool to provide information about the chemical constituents (proteins, lipids, nucleic acids, polysaccharides, etc.) of surfaces. Chemical bonds showing IR signals include hydrocarbon chromophore (C-H, C-C, C=C), carbonyl chromophore (C=O, ketone, aldehyde, ester, carboxylic acid, acid anhydride, acyl halide, amides), alcohols and phenols (O-H), amines (N-H, C-N), unsaturated nitrogen compounds (C=N, N=N, N=C=N), halogen compounds (C-F, C-Cl, C-Br, C-I) and sulphur containing compounds (S-H, C=S, S=O). X-ray photoelectron spectroscopy (XPS) [35] is a more sophisticated analytical tool and is the most commonly used analysis technique to understand basic phenomena subsequent to surface modification [36]. It has very high surface sensitivity and elemental / molecular sensitivity, providing information on the chemical composition and chemical bonds on a surface. Atomic force microscopy (AFM) is another very versatile surface analysis tool for many research areas [37] and almost any surfaces. It is a profilometer that has proven to be a useful in determining the surface roughness of a substrate, giving rise to information on the quality of surface preparative techniques, or density of adsorbing species. AFM is also a powerful imaging technique to acquire sub-nanometer resolution of not only topographic data but also measurement of frictional force, surface modulus and a multitude of other properties such as surface energy and magnetism [38]. It is particularly useful for bio-surface interactions,

including proteins and living cells in an aqueous environment with minimal sample preparation [39,40]. In addition, Near Edge X-ray Absorption Fine Structure (NEXAFS) [41,42], ellipsometry, raman spectroscopy, secondary ion mass spectroscopy (SIMS), and surface plasmon resonance (SPR) are also frequently used in thin-film polymer characterization, and a detailed review of those techniques has been published [26]. By correlating information gathered from those techniques, a greater understanding of cell- surface interactions and their impact on the subsequent cellular behavior can be established.

1.2.4 Nanofibers, Nanoparticles and Others

The demand for many modern products has also driven the development of many other novel and advanced materials with nano-scale architecture. Because polymers at nano-scales show large conformational changes in response to small environmental stimuli and the ability to carry numerous active drugs [43], they may offer the promise of revolutionary improvements in tissue engineering, diagnosis, targeted drug delivery systems and cell behavior studies. For example, nanofibrous scaffolds [44] provide a 3D topology that better mimics the architecture formed by fibrillar ECM proteins, and provide a framework where the cells can directly interact with each other. Polymeric nanoparticles include nanospheres and nanocapsules, they are commonly used in drug delivery applications, in which therapeutic drugs can be adsorbed, dissolved, entrapped, encapsulated or covalently linked to the particles [45]. The synthetic polymers used to prepare nanoparticles include poly(lactic acid), poly(glycolic acid), poly(lactide-co-glycolide), poly(alkylcyanoacrylate), polyanhydride, and poly(biscarboxy-phenoxy propane-sebacic acid) (PCPP-SA). Natural polymers such as chitosan, alginate and gelatin have also been used [46]. More recently, novel nanoparticles such as solid-lipid

nanoparticles, micelles and dendrimers have been explored to possess low cytotoxicity and good physical stability [47,48].

1.3 Polymeric Materials Used in Cell-Surface Applications

1.3.1 Polymeric Biomaterials for Tissue Engineering

Biomaterials are those materials that are intended to be used to interact with biological systems and adapted for a medical application. The most important criterion for biomaterials is their biocompatibility, and they must elicit an appropriate host response in a specific application. Materials such as metal alloys, ceramics and biopolymers from natural resources have been used as biomaterials in history. Only recently, synthetic polymers as the newest type of novel biomaterial has gained attention for controlled drug delivery and tissue engineering [49]. This is mostly because of the development of organic chemistry that is able to use a variety of tailored compounds that can serve as monomer (building blocks) to be translated into polymers. Some of the most common trends to use synthetic polymeric materials as biomaterials include the usage of protein-repulsive surface modifiers like poly(ethylene glycol)s (PEGs), in order to avoid complement activation, platelet adhesion and local thrombosis. Poly(α-hydroxy acid)s derived from glycolic and/or lactic acid enantiomers, are regarded as the most attractive compounds and have been actually exploited clinically and commercially for many years in various surgical applications. Other macromolecular structures like poly(β-hydroxy butyric acid) or poly(β-hydroxyalkanoate)s, copolymerization with other monomers (ε-caprolactone, benzyl malolactonate) or PEG-based macromers have also been explored [49].

A major area involving synthetic polymeric biomaterials is neuronal tissue engineering in the CNS, where synthetic polymeric biomaterials, combined with advances in molecular biology,

Table 1.1: Various roles of biomaterials in brain repair, protection, and regeneration [55]. Reproduced with permission from Orive G, Anitua E, Pedraz JL, Emerich DF. Biomaterials for promoting brain protection, repair and regeneration. Nat Rev Neurosci. 2009;10:682-692. Copyright Nature Publishing Group, 2009.

Therapeutic strategy	Target	Obstacle	Potential biomaterial role
Neuroprotection	Reduce inflammation, excitotoxicity, apoptosis and secondary cell death	Poor drug stability or targeting	Polymers can be used to encapsulate drugs and/or proteins, providing long-term stability; surface peptides can be added to allow targeted (receptor-based) delivery; drug-loaded polymers can be injected intracerebrally
		Lack of control over duration and timing of delivery	Biomaterial-based drug delivery can provide sustained delivery of one or more compounds simultaneously or in a desired sequence
Cell transplantation or tissue engineering	Replace damaged neurons or tissues	Poor cell survival and integration	Biomaterials can be loaded with proteins that support survival and engraftment
	Provide sustained protein delivery	Need for a suitable immobilization system	Polymer encapsulation allows long-term survival of cells sourced from animals or human stem cells
Regeneration or reorganization	Promotion of neurite or axonal regrowth	Poor control over direction of growth of neurites	Polymer scaffolds can be manufactured with a surface topography, inclusion of proteins or surface ligands to control outgrowth of transplanted cells or ingrowth from host cells

genetic engineering, proteomics and genomics, play key roles in overcoming the inherent lack of protection, repair and regeneration abilities of neuronal tissues (Table 1.1). To date, synthetic biomaterials have been used as drugs or gene carriers for treatment of neurological disorders and brain tumors, scaffolds for promoting neuronal tissue regeneration, neural electrodes for restoration of lost neurological functions or shunt systems for hydrocephalus. At the same time, those systems were continuously improved with advances in cell-based therapeutics and regenerative medicine with promising results. For example, polymeric drug carries temporarily bound to drug molecules by labile junctions sometimes also in combination with ligands aimed at targeting specific receptors, provide sustained delivery of potential drug agents, such as proteins, genes and oligonucleotides, and therefore control the attachment, growth, and differentiation of cells [48,50,51]. Degradable polymers including microparticles, nanoparticles and more recently self-assembled systems like core-shell macromolecular micelles and multimolecule aggregates of amphiphilic polymeric systems [52] were introduced in this field in recent years, and they have effectively reduced the size of the medical devices. Polyelectrolyte

complexes involving genes for cell transfection and the use of polymeric carriers to defeat the cell defense system are also very popular. To date, poly-L-lysine (PLL), polyamidoamine dendrimer (PAMAM), polyethylenimine (PEI), PGA, PLA and PLGA, have been successfully used for gene delivery [53,54].

Despite the exciting findings of polymeric biomaterial systems used in tissue engineering, there are several major challenges to be overcome. For example, in those systems, investigation is often limited to a few early stage criteria, including polymer synthesis and characterization, and sometimes preliminary tests *in vitro* or *in vivo*. The lack of consideration for other criteria generally limits the practical interest of such work and precludes comparison with similar or different competing systems. For instance such factors include chemical and physico-chemical interactions between foreign polymeric surfaces with cell membranes, circulating macromolecules or chemical species like proteins, lipids and phospholipids in the physiological systems, and the evaluation of other macromolecules such as growth factors to cell adhesion and proliferation. Knowledge gained from those perspectives can increase our understanding of disease processes and may allow us to treat or reverse some underlying pathology in the future.

1.3.2 Polymeric Materials as Marine Antifouling Coatings

In the marine environment, biofouling on submerged surfaces by the settlement of a large variety of organisms poses serious threats to the safe and efficient operation of vessels, and consequently leads to enormous economic losses for maritime industries [56]. It is believed that the process of marine biofouling includes two key growth stages [57]. In the initial stage, a biofilm matrix is created by accumulation of adsorbed organic matter and the settlement and growth of pioneering colonizers, usually bacteria are dominant components of the primary colonizers owing to their high abundance in seawater [58]. The settled bacteria and other

colonizing microorganisms then secrete extracellular polymeric substances (EPS) to envelop and anchor them to the substrate thereby altering the local surface chemistry and dynamics, which can stimulate further settlement and growth of sessile marine organisms. In the subsequent stage, many other aquatic species, such as diatoms and algae, attach and proliferate on the biofilm platform (Figure 1.1).

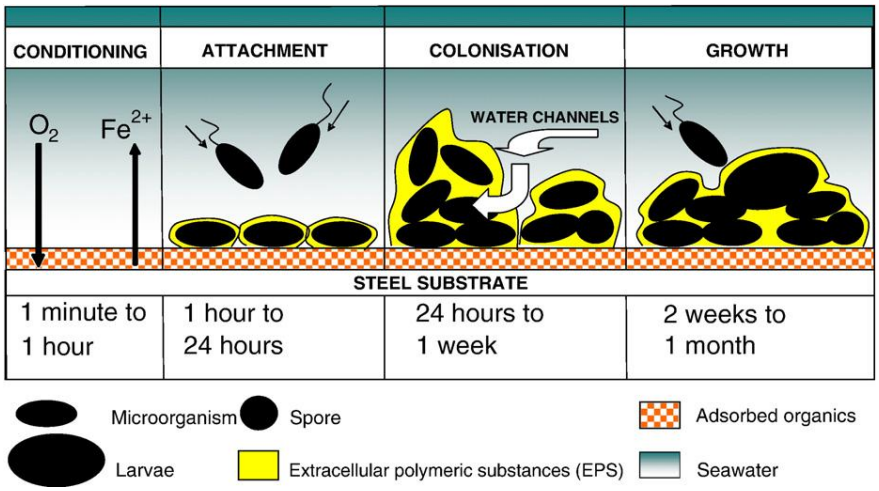

Figure 1.1: Schematic representation of several critical biofouling stages [57]. Reproduced with permission from Chambers LD, Stokes KR, Walsh FC, Wood RJK. Modern approaches to marine antifouling coatings. Surf Coat Tech. 2006;201:3642-52. Copyright Elsevier, 2006.

Polymers have been wildly used as coatings to protect engineered marine structures in a wide range of functions such as corrosion resistance, ease of maintenance, appearance, non-slip surfaces on decking as well as the prevention of fouling on the hull by unwanted marine organisms [57]. Historically, toxic antifoulants on ship hulls have been used to control fouling. But biocides such as lead, arsenic, mercury and their organic derivatives have been banned due to the environmental risks that they pose. Self-polishing copolymer techniques employing a similar heavy metal toxic (e.g. organotin) agent to deter marine organism growth was also banned due to severe shellfish deformities and the bioaccumulation of heavy metals in some

ducks, seals and fish [59,60]. Later on, booster biocides and terrestrial pesticides were used in antifouling coating systems but they have also been increasingly restricted [61,62], because those coatings are often not species specific to the detriment of non-target organisms. Those issues limit the further usage of those traditional coatings, and there is a constant need for new, robust, non-toxic, and environmentally friendly polymeric coatings.

A variety of non-leaching synthetic polymers have been prepared and investigated as an environmentally acceptable alternative to traditional toxic coatings and have met with variable success. One class of such polymer coatings is for fouling release coatings. Foul release coatings (FRCs) use an effective passive approach to fight against a broad spectrum of marine organisms; these materials combine critical surface free energy, low elastic modulus and = smoothness of the coating at the molecular level to degrade an organism's ability to generate a strong interfacial bond with the surfaces, so the organisms can be dislodged once a vessel is moving at high speed [63]. There are several major types of FRCs, including polydimethylsiloxane based hydrophobic surfaces [64,65], polyperfluoroether networks [66] and polymers containing fluorocarbon side chains [67,68], and these are all successful to some degree. Recently, amphiphilic polymer coated surfaces have shown promising results for a broad applicability for controlling biofouling. Amphililic polymers containing both hydrophobic (e.g., fluorinated or silicon based) and hydrophilic moieties in the polymer systems, when applied as coatings on a substrate, provide "ambiguous" surfaces that can inhibit fouling of various organisms. For example, a recent work [68] has developed a well-defined polystyrene-*block*-poly[(ethylene oxide)-*stat*-(allylglycidyl ether)] (PS-*b*-P(EO-*stat*-AGE)) statistical diblock terpolymer, the pendent alkene of the AGE units can be subsequently functionalized with hydrophobic perfluorooctane thiol *via* thiol-ene click chemistry. Protein adsorption studies demonstrated that the polymer coated surfaces can

effectively prevent nonspecific binding of proteins. In biological systems, settlement of spores of the green macroalga *Ulva* was significantly lower for the amphiphilic polymers compared to the polydimethylsiloxane elastomer standard. In addition, the attachment strength of sporelings (young plants) of *Ulva* was also reduced for the fAGE-containing polymers, affirming their potential as fouling-release coatings.

Zwitterionic polymers are viable alternatives to more traditional surfaces based on PEG as ultralow fouling coatings that are highly resistant to the attachment of marine organisms. Unlike the fouling release coatings, zwitterionic polymer coatings are designed to be resistant to the attachment of marine organisms under static conditions (antifouling). Polymer coatings based on phosphorylcholine, a major component of the outside surface of the erythrocyte membrane, has been demonstrated to be highly effective in reducing adsorption of proteins, cells, bacteria, and platelets [69,70]. Sulfobetaine-based polymers and carboxybetaine-based polymers are also ultralow fouling materials [71-76], and studies have demonstrated that these surfaces are highly resistant to non-specific protein adsorption even from undiluted blood plasma and serum, and they are also highly resist bacterial adhesion/biofilm formation [74]. Particularly, zwitterionic sulfobetaine methacrylate (SBMA) polymer brushes prepared by surface-initiated atom transfer radical polymerization have shown to be not-toxic in solution, and they are highly resistant against both *Ulva* and diatoms attachment [76]. Considering their effectiveness and stability, zwitterionic polymers are promising candidates as environmentally benign, effective, durable, and low-cost ultralow fouling coatings.

A more recent strategy to prepare antifouling coatings is to use a biomimetic approach that deals with bio-inspired designs [77]. Within the marine ecosystem, organisms have both physical and chemical methods to protect themselves from the harmful process of biofouling,

and they often provide inspiration to study the relationship between polymer chemical composition, architecture, surface density, and antifouling performance. Those studies can lead to the identification of new polymers with improved antifouling performance, including long-term durability in the marine environment [78]. For example, one of nature's most notorious fouling organisms, mussels, achieve opportunistic attachment to surfaces by way of a set of unique adhesive proteins, or 'bio-glues' [79]. Mimics of mussel adhesive proteins (MAPs) have been used in the form of chemical conjugates with antifouling polymers for conferring fouling resistance to surfaces. One typical example uses simple constructs of linear PEGs end-functionalized with DOPA (3,4-dihydroxyphenylalanin, an important residue found in MAPs) residues (mPEG-DOPA) [80]. The DOPA containing PEGs were used to treat Au surfaces and assessed by fibroblasts cell attachment, the results showed that the polymer-modified area is entirely cell-free. Recently, organic synthesis has been proven to be essential in preparing a variety of molecules that can present surface structures in nature with improved properties. For example, peptoids are unnatural mimics of peptides that have a protein-like backbones, with side chain derivatization on the amide nitrogen instead of the α-carbon [81], and are currently being explored as peptide mimics and for use in biofouling surface preparation. In one study [82], peptidomimetic polymer (PMP1) was synthesized on a solid phase amide resin by first synthesizing the adhesive peptide anchor with a standard Fmoc strategy followed by synthesis of a 20-mer N-methoxyethyl glycine peptoid using the submonomer protocol (Figure 1.2). The PMP1 was found to be highly soluble in aqueous solutions and adsorbed strongly onto Ti surfaces by simple immersion of the substrate into the polymer solution. Protein adsorption experiments showed that the amount of protein absorbed on the coated surface is similar to that adsorbed onto PEG coatings. Remarkably, the PMP1-modified surfaces exhibited low levels of

fibroblast cell attachment for over 5 months under frequent challenge with fresh serum and cells, demonstrating the excellent protein resistance and fouling resistance of the peptidomimetic polymers.

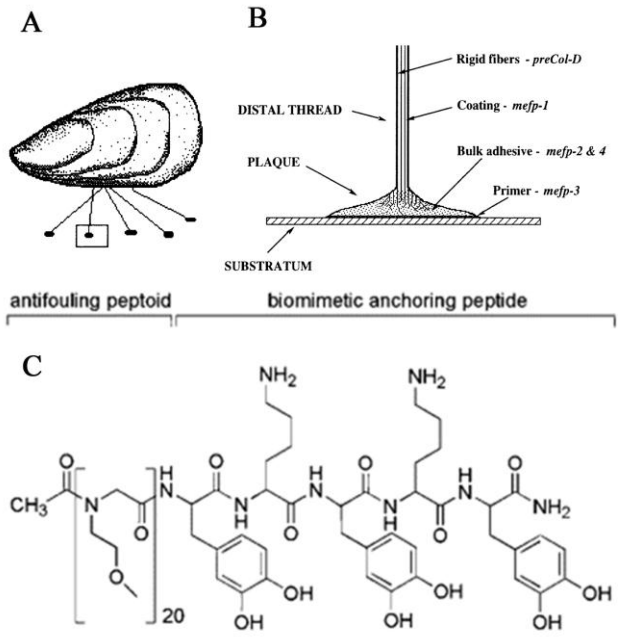

Figure 1.2: (A) The common mussel, M. edulis, adheres to substrates via byssal threads and adhesive plaques, which (B) contain varying amounts of DOPA [79] Waite JH. Reverse engineering of bioadhesion in marine mussels. Ann N.Y. Acad Sci. 1999;875:301-9. Copyright John Wiley & Sons. 2006. (C) antifouling peptidomimetic polymer containing DOPA segment [82]. Reproduced with permission from Statz AR, Meagher RJ, Barron AE, Messersmith PB. New peptidomimetic polymers for antifouling surfaces. J Am Chem Soc. 2005;127:7972-73. Copyright American Chemical Society, 2005.

1.3.3 Polymeric Antimicrobial Materials

Bacterial colonization and infection on material surfaces is an unwanted event in many circumstances. In the case of implanted materials and medical devices, bacterial infection is a common cause of severe inflammation which finally can result in biomaterial implant failure [83,84] and cause high rates of mortality [85]. In a marine environment, bacteria and

microorganisms attached on a submerged surface causes the formation of biofilms [86,87], which in turn can facilitate settlement of other sessile marine organisms, eventually posing serious threats to the safe and efficient operation of vessels and equipment, consequently leading to enormous economic losses for maritime industries [56].

Because of the ever-growing demand for healthy living and environmental concerns, there is a substantial industrial and commercial interest in polymeric materials with antifouling and antimicrobial properties. Two major categories of surface modification with materials were developed to meet this goal: biopassive and bioactive surface preparations [88]. Biopassive surface coatings reduce the adsorption of proteins and the adhesion of bacteria, without killing the bacteria or microorganisms. e.g., by coating with thin layers of poly(ethylene glycol) (PEG). In contrast, the bioactive surfaces can kill the bacteria on contact [89,90], e.g., substance immobilized with antibiotics and antimicrobial agents [91,92], such as quaternary ammonium compounds, silver ions, or iodine [93-95]. In particular, quaternary ammonium compounds have a broad spectrum of antimicrobial activity against both gram-positive and gram-negative bacteria [96]. When covalently attached to polymers, quaternary ammonium compounds offer many advantages compared with their small-molecule counterparts [97], such as that they are nonvolatile, chemically more stable, have long-term high antimicrobial activity, and display antimicrobial activity without permeating through skin [98,99]. Some polymeric coatings also attempt to combine both biopassive and bioactive mechanisms of antibacterial action; however, extra care has to be taken to design such dual functional coatings to ensure that contact between the antimicrobial moiety and bacteria are not prevented by the biopassive units in a polymer system.

“Smart” surfaces exhibiting stimuli-responsive properties have been used recently to

fabricate temperature - switchable surfaces between bactericidal and bacteria repellent surface properties [100]. One successful example is thermo-responsive copolymer brushes based on MEO_2 MA, hydroxyl-terminated oligo(ethylene glycol) methacrylate and 2- hydroxyethyl methacrylate (HEMA) [101]. An antimicrobial peptide magainin-I was grafted on the hydroxyl groups of the brushes (Figure 1.3). The responsive brushes were then tested against Gram-positive (*L. ivanovii)* and Gram-negative (*E. coli*) bacteria. The bioassays were performed at different temperatures and the results showed that the surface properties of the peptide-functionalized brushes have changed from dominantly bactericidal at 26 °C to predominantly non-adhesive when the temperature becomes higher than the collapse transition temperature (T_{coll}).

It has been suggested that host defense peptides act as broad spectrum, fast-killing antibiotics because they can fold into facially amphiphilic secondary structures by binding to biomembranes [102], and many amphiphilic synthetic polymers have the membrane-disrupting abilities and have been utilized in preparing chemical disinfectants and biocides [103]. A number of polymeric disinfectants have been prepared with side chains containing cationic quaternary ammonium salt units modified with long hydrophobic alkyl chains (6-12 carbons), including derivatives of conventional synthetic polymers, such as poly(vinyl pyridine), poly(vinyl alcohol), polyacrylate, and polystyrene [103,104]. It appears that optimization of the amphiphilic balance between cationic charge and hydrophobicity is a stringent design requirement for those materials. At appropriate ratios, their amphiphilic structures may reach an optimal balance between the selective binding to bacteria and the ability of polymers to insert into and breakdown the cell membrane, and ultimately lead to cell death.

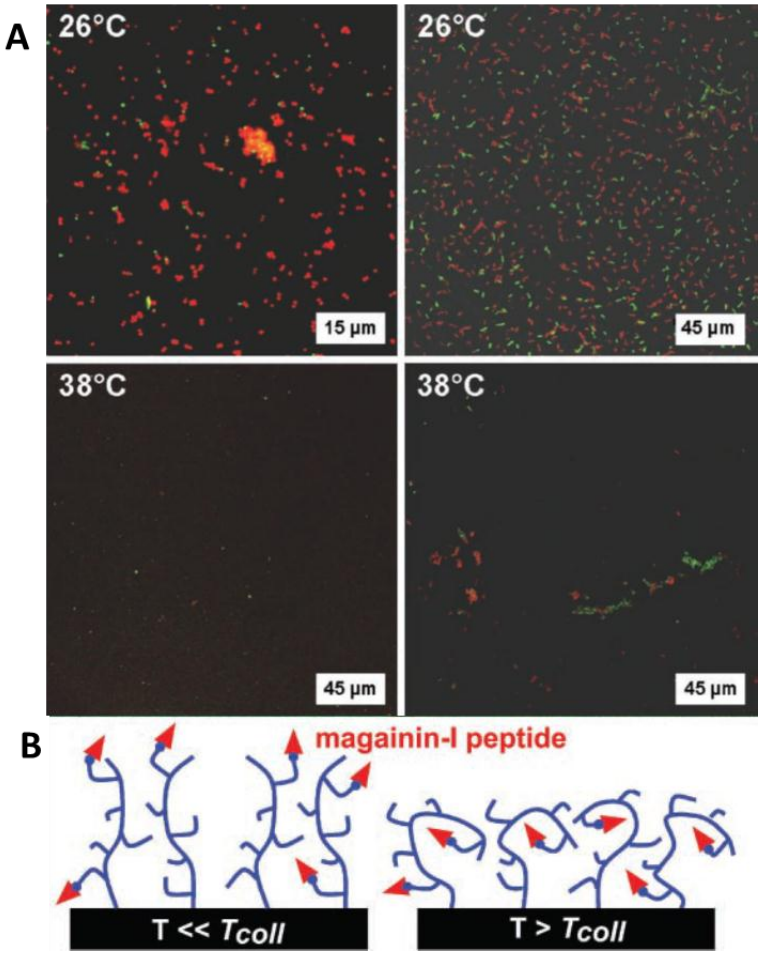

Figure 1.3: Antimicrobial polymers with magainin-I-peptides**.** A) (MAG-Cys)-functionalized P(MEO_2MA_{50}-$HOEGMA_{20}$-$HEMA_{30}$) brush incubated in the presence of *L. ivanovii* (left) or *E. coli* (right) and subsequently stained with the LIVE/DEAD viability kit; samples incubated at 26 °C (top) and 38°C (down). B) Schematic drawing of the (Biotinyl-MAG-Cys)-grafted Poly(MEO_2MA_{50}-$HOEGMA_{20}$-$HEMA_{30}$) brushes [101] and brush conformation well below and slightly above T_{coll}. Reproduced with permission from Laloyaux X, Fautre E, Blin T, Purohit V, Leprince J, Jouenne T, et al. Temperature-Responsive Polymer Brushes Switching from Bactericidal to Cell-Repellent. Adv Mater. 2010;22:5024-5028. Copyright John Wiley & Sons, 2010.

However, polymeric disinfectants often lack selectivity, showing both high antimicrobial activity and hemolytic activity, therefore limiting their clinical and medicinal utility. Extensive optimization has been carried out to obtain polymers that display potent antimicrobial activity combined with minimal or no toxicity to human cells. For example, study has shown that copolymers consisting of flexible polymer backbones and random amphiphilic sequences have

antimicrobial activity comparable to that of natural peptides, but with relatively reduced toxicity compared to that of high MW polymers and the toxin melittin. PEGylation has also been used to achieve the required amphiphilic balance and involves conjugation of electrically neutral hydrophilic moieties to polymeric disinfectants in order to alleviate their hemolytic properties. The prevention of protein adsorption by the physicochemical properties of PEG molecules would be expected to maintain the efficacy of positively charged chemical functions in killing bacteria on contact. Previously, cationic pyridinium group-containing monomers were coupled to wafer surfaces via Michael addition to surface-bound amino groups. This type of surface modification allowed attachment of a high amount of streptococcal cells, but killed attached bacterial cells on contact [105]. Recently, hydrophilic oligo(ethylene glycol) methacrylates and quaternary ammonium groups were used as side chains to prepare propylene-oxide-based antimicrobials, and the functionalized polymers showed low cytotoxicity toward human red blood cells, indicating good prospects for biocompatibility, while retaining effective antimicrobial behavior, highlighting their potential as therapeutic agents [106].

In summary, because of the low manufacturing cost and diversity of chemical structures, synthetic polymers offer many advantages and allow the production of antimicrobial materials on industrial scales. However, many structural features in those antimicrobial polymers have not been assessed systematically, including the roles of polymer backbone structure, flexibility/rigidity, copolymer microstructure, and macromolecular architectures. More detailed structure−activity studies aimed at delineating the effects of those parameters would improve our understanding of the biophysical basis for the observed activities and would facilitate future design strategies.

1.4 Material Physical Properties Influence Cell Responses

1.4.1 Surface Free Energy and Wettability

When a surface is placed in a particular environment, chemical groups at the surface tend to interact with other molecules or atoms approaching the surface in the environment. The ability of surfaces to enter into such interactions can be expressed by surface free energy. The types of forces or interactions in the process include van der Waals forces, polar interactions, electrostatic interaction, hydrophobic interactions and hydrogen bonding, depending on the chemistry of both the surface and the environment. Surface free energy is probably the most important physico-chemical property of a surface [107], as it indicates the tendency of that substratum to enter into various types of interactions spontaneously, and determines the suitability of the surface for adhesion events. The work of adhesion (W_{sl}) is defined as the work required to separate the liquid (the adhesive) from a solid (the substratum) [108] and is equal to the sum of the surface free energy of the solid (γ_s) and the surface tension of the liquid (γ_l) minus the interfacial tension between the solid and the liquid (γ_{sl}): $W_{sl} = \gamma_s + \gamma_l - \gamma_{sl}$. Thus, the lower the surface free energy of the solid (γ_s) the weaker is the adhesion, and studies have shown that minimal long-term adhesion is associated with surfaces having initial surface tensions between 20 and 30 dynes/cm (mN/m). This factor was used to select low energy surfaces to function as foul-release coatings [109] [78].

Hydrophobicity (low wettability) and hydrophilicity (high wettability) are also commonly used to describe surfaces and have been widely cited as a key factors in determining protein and cell-surface interactions. In general, hydrophobicity increases with a decrease in surface free energy, although the terms are not strictly interchangeable. Therefore, hydrophobic material surfaces are usually more resistant to microbial adhesion than hydrophilic ones [110,111]. For

example, it was shown that hydrophobic methyl-terminated alkanethiol SAMs on gold induce minimal cell attachment and cannot support spreading and formation of focal contacts by mouse fibroblasts [112]. There are also many contrary reports in the preference of bacteria associated with specific surfaces. For example, Dexter et al. reported fewer bacteria adhering to a low surface energy, hydrophobic materials (silicone elastomer) compared to a high surface energy materials (glass) [113], while studies of Fletcher et al. suggested that both freshwater and marine bacteria attach preferentially to hydrophobic surfaces [114]. However, the majority of these studies have been conducted with different strains of bacteria, and adhesion is dependent on the individual species or strain as well as the physiological state of the organism, and bacteria may have separate adhesion mechanisms for hydrophilic and hydrophobic surfaces [115]. Measurement of water contact angle (WCA) is the most common way to quantitatively measure a surface wettability (hydrophobicity or hydrophilicity), it is a fast, surface sensitive tool to differentiate between changes occurring on a substrate as a result of a treatment [116]. By using a range of different liquids, it can also be used to calculate the surface energy. However, it does not offer information on the identity or concentration surface species, many different chemical functional groups may give rise to the same contact angle.

1.4.2 Surface Mechanical Properties

The mechanical properties of a cell's environment can convey significant control over cell characteristics, since different cellular environments vary greatly in stiffness *in vivo*, with the brain presenting a much softer matrix than that of muscle or bone. Therefore, it is important to characterize mechanical properties of materials for their specific applications. For examples, in cell culture experiments, soft, flexible substrates can inhibit attachment and spreading, while solid surfaces may promote them [117]. Mouse hippocampal neurons exhibit variable neuronal

morphological differentiation and glial survival on substrates of variable stiffness [118], and neurons prefer softer surfaces (~ 100-500 Pa), and in contrast glial cell attachment was promoted on stiffer surfaces (~ 1 KPa to 10 KPa), and cell spreading, self-renewal, and differentiation were inhibited on substrata with moduli of 10 Pa. In the collagen matte with a gradient of stiffness [119], neurites from chick dorsal root ganglia explants were found to grow considerably longer towards the softer end of the gradient compared to stiffer or untreated collagen sheets. Others have reported a threshold response to substrate stiffness, such as Leach et al. who observed that PC-12 neurons extended few outgrowths being relatively short in length with little branching on soft substrates (~10 Pa) although neurons on stiffer materials (~102–104 Pa) had more outgrowths, being longer and highly branched. Above a threshold level of ~102 Pa no significant differences were observed [120]. Clearly surface mechanical elasticity is of significant importance in terms of neuronal cell behavior. Synthetic hydrogels are ideal to prepare substrates with tunable elastic stiffness by varying the ratio monomer to cross-linking agent. Polyacrylamide (PA) gels [121,122] for instance can be prepared having elasticity in the range 0.1–100 kPa. The wide stiffness range makes this system appealing to many researchers in this field, as it is can be adjusted to mimic hard tissues such as bone (E~30 kPa) through to soft tissues such as brain (E~0.5 kPa). Other materials have extended this range such as polydimethylsiloxane (E~10–1000 kPa) and collagen gels (E~0.001–1 kPa).

The surface modulus also determines the effectiveness of marine fouling release coatings; the application thickness of silicone coatings is typically 150 μm in comparison with 75 μm for fluoropolymers [123]. The thickness of the coating allows for the coating modulus to be controlled. A thicker low modulus coating is more successful as it requires less energy to fracture the bond between the foulant/coating. Removal of the attached organism occurs through a

peeling fracture mechanism as opposed to the shearing mechanism associated with the harder, thinner coatings of the fluoropolymer coatings.

1.4.3 Surface Topography and Preparation Techniques

The effect of the substrate morphology on cell adhesion and consequent cell reactions has been studied for many decades, and it is known that topographical surface cues can provoke distinct cellular reaction regarding adhesion, morphology, cytoskeletal arrangement, migration, proliferation, surface antigen display and gene expression [124,125]. Surface topographies can comprise scale (micro- and nanometer scale), type (e.g. ridges and grooves) and distribution (randomly or regularly distributed). One particular example of how surface features can influence cell behavior is neuronal cell patterning, where surface topography was used to understand how surface properties can direct the attachment and subsequent directional migration and growth of neuronal cells. It has been suggested that topographical cues may stimulate neurite growth by triggering various intracellular pathways through receptors and molecules such as integrins, tyrosine kinases in focal adhesions, actin and calcium channels [126]. The dimensions of surface features could also induce neural differentiation of stem cells. Human bone marrow mesenchymal stem cells responded to different nanopattern designs with specific changes of their microtubule organization, and in the case of surface topography featuring grooves with width/spacing of 40/30 μm [127,128], stem cell alignment, elongation and neuronal-like cell differentiation was observed.

Nano- and micro-fabrication techniques are useful tools to prepare surface patterns with precise scale control of the biochemical, topographical, micromechanical properties, as well as the vicinity of the cells [129]. They are also very useful in the area that presents stimuli for a cell in spatially and temporally defined regions for the study of cellular signals [130]. Surface

patterning techniques can be divided in two major categories according to the manufacturing of "top-down" and "bottom-up" approaches. "Top-down" methods include some of the most common and well-used lithographic techniques, such as electron-beam lithographic techniques[131], focused ion beam lithography, optical projection lithography, X-ray lithography, electron and ion projection lithography, and extreme UV lithography [132]. In lithographic processing, a light sensitive polymer, or photoresist either cross-links (negative resist) or deteriorates (positive resist) on action of exposure, is irradiated through a master pattern presented on a semi-transparent mask. The resist can then be removed leaving either a metalized pattern on the surface or patterned etched areas. Therefore, lithography processing allows potentially unlimited copies to be created from a single master. However, resolution of "top-down" approaches is determined by the wavelength of light used during irradiation, and these techniques generally require expensive equipment and also a certain lack of flexibility. The "bottom up" method benefit basically from interactions between molecules or colloidal particles to assemble discrete nanoscale structures in two or three dimensions [133], it allows for a strict control on the physicochemical properties of a surface and represents a versatile method for the production of a variety of surfaces. It also shows good promise for sub-100-nm feature fabrication [134]. Techniques for "bottom-up" method include nanoimprinting, micro-contact printing, soft-lithography, near field optical lithography and proximity probe lithography, and also self-assembly procedures such as Langmuir-Blodgett films or the layer-by-layer method. Most of these techniques are less costly and easier to handle.

In addition, some other methods, such as electrospun fibers, nanotubes, and particles assembled on a surface have also shown promise for the fabrication of desired surface topographies to control cell attachment and alignment [26]. However, although modern

technologies allow for fabrication of highly ordered and defined topographic surfaces, there is limited understanding of the spatial as well as the temporal constraints on cellular response and regulation. More progress in the understanding of cell adhesion on different substrates by controlling topography, chemistry, or growth factors has to be made. It is believed that both micro- or nanofabrication tools as well as materials science are needed to be successful in achieving this goal.

1.4.4 Surface Charges and Polarity

Cell surfaces are predominantly negatively charged, while artificial surfaces can possess either negative or positive surface charges; therefore, electrostatic interactions can play an important role in determining the biological response to surfaces. Positively charged surfaces promote cell adhesion, while negatively charged surfaces reduce it [135]. For example, positively charged surfaces such as those containing amine groups are widely regarded to promote the adhesion of neural cells, and in some cases they also interfere with cell signaling pathways. Poly-L-lysine (PLL) coated substrates promote the adhesion of neurons and allow neural networks to establish [136], whilst polyethyleneimine (PEI) enhances the adhesion and proliferation rates above that observed for other positively charged polymers [137]. However, although surface charge can be a dominant factor in determining biological interaction with surfaces, limiting the consideration of cell–surface interactions to charge states alone can lead to shortfalls in explaining the behavior of cell adhesion and migration [26]. In addition, cells adhere to the surfaces through electrostatic interactions can be strongly affected by ionic strength. At high ionic strength cell attachment is strong, since electrostatic force becomes negligible and van-der-Waals attraction dominates [138]. Furthermore, polar or charged functional groups in the synthetic polymers, such as amino or carboxylic groups, are strongly related to the wettability

of the materials, therefore affect the cell growth and function, while apolar groups like methyl group may merely inhibit cellular attachment, growth, and function [139].

1.4.5 Electrical and Magnetic Properties

The response of electrical and magnetic stimuli is a basic phenomenon in living systems. Particularly, in the peripheral nervous system (PNS) and central nervous system (CNS), electrical conductance of matrices for the culture of neural networks is of importance, not only for the continued development of better quality tissue regeneration, but also for the advancement of prostheses for the nervous system. Thus, over the past decades, some fields of research have intensively studied the electrical or magnetic effects on the development of cells, the electrochemotherapy, and the development of ultramicroelectrodes studying cell mechanisms or the search for new culture substrates. Currently, the effect on cell adhesion, migration, and orientation in response to electrical stimuli has been documented using a 2D culture system [140]. In particular, electroactive polymers (EAPs) become an intriguing research area and have been shown to play important roles in stimulating either the proliferation or differentiation of various cell types [141,142], and have been used as a useful tool for biological and biomedical applications, such as biosensors, tissue engineering and particularly for neural probe applications. Conductive polymers such as polypyrrole (PPy) and polyaniline (PANi) can be used alone or in combination with biopolymers that allow tailoring of the level of conductivity in a controlled manner, and they have been most widely used as scaffold materials in neural probes for the treatment of neural degenerative diseases such as Parkinson's or retinal, contributing to a new generation of biomaterials [143]. Recent advances have also been made in combining electrical stimulus polymer with biodegradable materials as new scaffold for tissue engineering. For example, through the condensation and polymerization of hydroxyl-capped poly(L-lactide)

(PLA) and carboxyl-capped aniline pentamer (AP), the copolymer exhibited excellent electroactivity, solubility and biodegradability and under electrical stimulations, also have demonstrated good adhesion and proliferation characteristics of C6 cells, and furthermore electrical stimulus was capable to accelerate rat neuronal pheochromocytoma PC-12 cell differentiation [144].

Electrical conductivity and good magnetic properties of the polymers could be also modulated by introducing electrically conductive nanocomposites, such as metal nanoparticles (e.g. silver, gold) and carbon nanostructures (e.g. nanotubes, graphene, nanofibers) [145]. The latter can be classified based on their structure and nanoscale dimensions such as zero-dimensional structures (fullerenes, diamond clusters), one-dimensional (carbon nanotubes, carbon nanofibers, diamond nanorods), two-dimensional (graphite sheets, diamond nanoplatelets) and three-dimensional structures (nanocrystalline diamond films, fullerite) [146]. Among those novel nanostructures, carbon nanotubes (CNT) are considered to be the ideal reinforcing agents for high-strength polymer composites, because of their mechanical strength, high electrical conductivity, and high aspect ratio [146,147].

1.4.6 Protein Absorption

Under physiological conditions, the presence of proteins in the surrounding body fluid prevents direct cell contact with a material surface. From in vitro studies, when cell culture is carried out in serum containing media, a protein layer may be adsorbed to the surface within a small fraction of a second, and thus cells do not directly contact the bare surface. Adsorption of protein on the surface occurs through similar interactions as cell adhesion, since proteins represent copolymers of different amino acids, they may carry both acidic and basic groups, and also hydrophilic and hydrophobic moieties, so they are both amphoteric and amphiphilic.

Depending on the isolectric points, they may possess positive or negative net charge under physiological conditions. Consequently, proteins absorb to almost all types of material surfaces except on those that are highly hydrophilic with tight water binding, such as PEG, or phosphatidylcholine [75,148]. Protein adsorption on surfaces may alter the physicochemical properties of underlying surfaces significantly, for example, the contact angle values may be brought closer to a narrow range of hydrophilic values, which in turn greatly influences subsequent cell adhesion [149-151].

The protein adsorption processes are complicated, and the factors governing protein−surface interactions are determined by the physical state of the material, protein properties, and solution environment. Surface hydrophobicity is expected to play a major role in protein adsorption, which is often accompanied and complicated further by a range of conformational changes and denatured states by many different microenvironments. Protein adsorption measurements are carried out mostly in real time by using methods that measure dielectric properties of an interface such as surface plasmon resonance (SPR) spectroscopy, waveguide interferometry, ellipsometry, and those that measure changes in the resonance frequency of a piezoelectric material such as the quartz crystal microbalance (QCM) and surface acoustic wave and acoustic plate mode devices. Detailed reviews of SPR and SPR−fluorescence [152], and QCM [153] as bioanalytical techniques for real-time measurements have also been published. Alternatively, fluorescence measurements and enzyme-linked immunoassay (ELISA)-type fluorescence amplification assays [1] also provide insightful data, but mostly for binding in the equilibrium state on surfaces.

1.4.7 Roughness

The roughness of a surface has also an impact on cell adhesion; it is easier to introduce

using various abrasive or electrochemical techniques and is almost unavoidable since it can be easily formed during the processing of most materials. In general, cells attach better on rougher surfaces than on smooth surfaces [154,155]. However, variations have been observed between research groups on the systematic investigation of cell response to varying degrees of roughness, probably due to the different cell types employed in their studies [156]. For example, studies have found that osteoblasts preferred rough surfaces whilst fibroblasts favored smooth surfaces. Proliferation response was distinctly different between the two cell-types investigated, with osteoblast proliferation significantly enhanced on rougher surfaces whilst fibroblasts showed the opposite trend. The morphology trend of both cell types however was similar, being more rounded on rough surfaces whilst spreading as roughness decreased.

1.5 Conclusion

Modification of surfaces for cell control has progressed over past decades, and a large number of synthetic polymeric materials have been explored in this area. They have provided a large degree of surface heterogeneity regarding to the type and distribution of bioactive functional groups, the presence of hydrophilic and hydrophobic groups, different surface charges and roughness, etc. Many synthetic polymers have been specifically prepared as either cell adhesive or cell repulsive materials, largely based on the chemical composition and structure presented in the systems. Surface topographical cues on those polymer surfaces are also critical parameters in determining the ability for cells to adhere, migrate, proliferate, grow and differentiate. With the advances in organic chemistry and materials science that produce ever more sophisticated synthetic and characterization approaches, and the advances in the molecular biology and cell biology, more well-defined surfaces can be prepared and characterized, which

will undoubtedly lead to major advances in many research fields including therapeutic materials and other industry applications.

However, the study of cell-surface interactions is still a young and very fertile field, and our understanding of biological processes at the interface with synthetic materials remains in its infancy. No complete molecular-level understanding of cell-surface interactions exists to date. Developing a meaningful understanding of how to rationally design polymeric materials for different applications will require significant advances in materials development, as well as a clear understanding of the types of cells and appropriate target biological responses. It is now well accepted that the characteristics of the substratum which influence subsequent adhesive events are: (1) the chemical characteristics of the clean surface; (2) physical features such as topography and roughness; and (3) biological features such as protein absorption and bacterial films. To induce specific cell binding properties and minimize the non-specific background interferences on a synthetic surface, a material has to provide all the proper surface cues. Although many contemporary synthetic materials possess excellent physical and chemical properties, however, many may still need to be modified in ways that cell attachment, adhesion and spreading on the surfaces can be controlled. It is also vital to be able to systematically vary the relevant surface chemistries with nano-or micro-scale topographies, and explore cell behavior trends on different surfaces. Collaborative efforts between organic chemists, cell biologists, materials scientists and biomedical engineers are critical for answering some key questions and promoting interdisciplinary research in this field.

REFERENCES

[1] Senaratne W, Andruzzi L, Ober CK. Self-assembled monolayers and polymer brushes in biotechnology: Current applications and future perspectives. Biomacromolecules. 2005;6:2427-48.

[2] Bongrand P, Capo C, Depieds R. Physics of Cell-Adhesion. Prog Surf Sci. 1982;12:217-85.

[3] Goddard JM, Hotchkiss JH. Polymer surface modification for the attachment of bioactive compounds. Prog Polym Sci. 2007;32:698-725.

[4] Leach JK. Multifunctional cell-instructive materials for tissue regeneration. Regen Med. 2006;1:447-55.

[5] Bushetti SS, Singh V, Raju SA, Atharjaved, Veermaram. Stimuli Sensitive Hydrogels: A Review. Indian J Pharm Educ. 2009;43:241-50.

[6] Van Vlierberghe S, Dubruel P, Schacht E. Biopolymer-Based Hydrogels As Scaffolds for Tissue Engineering Applications: A Review. Biomacromolecules. 2011;12:1387-408.

[7] Pal K, Banthia AK, Majumdar DK. Polymeric Hydrogels: Characterization and Biomedical Applications. Des Monomers Polym. 2009;12:197-220.

[8] Tibbitt MW, Anseth KS. Hydrogels as Extracellular Matrix Mimics for 3D Cell Culture. Biotechnol Bioeng. 2009;103:655-63.

[9] Dawson E, Mapili G, Erickson K, Taqvi S, Roy K. Biomaterials for stem cell differentiation. Adv Drug Deliver Rev. 2008;60:215-28.

[10] Elbert DL. Liquid-liquid two-phase systems for the production of porous hydrogels and hydrogel microspheres for biomedical applications: A tutorial review. Acta Biomater. 2011;7:31-56.

[11] Zheng J, Li LY, Tsao HK, Sheng YJ, Chen SF, Jiang SY. Strong repulsive forces between protein and oligo (ethylene glycol) self-assembled monolayers: A molecular simulation study. Biophys J. 2005;89:158-66.

[12] Sharma S, Johnson RW, Desai TA. XPS and AFM analysis of antifouling PEG interfaces for microfabricated silicon biosensors. Biosens Bioelectron. 2004;20:227-39.

[13] Feldman K, Hahner G, Spencer ND, Harder P, Grunze M. Probing resistance to protein adsorption of oligo(ethylene glycol)-terminated self-assembled monolayers by scanning force microscopy. J Am Chem Soc. 1999;121:10134-41.

[14] Tziampazis E, Kohn J, Moghe PV. PEG-variant biomaterials as selectively adhesive protein templates: model surfaces for controlled cell adhesion and migration. Biomaterials. 2000;21:511-20.

[15] Zhu B, Eurell T, Gunawan R, Leckband D. Chain-length dependence of the protein and cell resistance of oligo(ethylene glycol)-terminated self-assembled monolayers on gold. J Biomed Mater Res. 2001;56:406-16.

[16] Boura C, Menu P, Payan E, Picart C, Voegel JC, Muller S, et al. Endothelial cells grown on thin polyelectrolyte mutlilayered films: an evaluation of a new versatile surface modification. Biomaterials. 2003;24:3521-30.

[17] Boura C, Muller S, Vautier D, Dumas D, Schaaf P, Voegel JC, et al. Endothelial cell - interactions with polyelectrolyte multilayer films. Biomaterials. 2005;26:4568-75.

[18] Boura C, Muller S, Voegel JC, Schaaf P, Stoltz JF, Menu P. Behaviour of endothelial cells seeded on thin polyelectrolyte multilayered films: A new biological scaffold. Clin Hemorheol Micro. 2005;33:269-75.

[19] Remy-Kristensen A, Clamme JP, Vuilleumier C, Kuhry JG, Mely Y. Role of endocytosis in the transfection of L929 fibroblasts by polyethylenimine/DNA complexes. Bba-Biomembranes. 2001;1514:21-32.

[20] Crespilho FN, Zucolotto V, Oliveira ON, Nart FC. Electrochemistry of Layer-by-Layer Films: a review. Int J Electrochem Sc. 2006;1:194-214.

[21] Weber LM, Hayda KN, Anseth KS. Cell-Matrix Interactions Improve beta-Cell Survival and Insulin Secretion in Three-Dimensional Culture. Tissue Eng Pt A. 2008;14:1959-68.

[22] Nuttelman CR, Tripodi MC, Anseth KS. Synthetic hydrogel niches that promote hMSC viability. Matrix Biol. 2005;24:208-18.

[23] Kaneda N, Talukder AH, Nishiyama H, Koizumi S, Muramatsu T. Midkine, a heparin-binding growth differentiation factor, exhibits nerve cell adhesion and guidance activity for neurite outgrowth in vitro. J Biochem-Tokyo. 1996;119:1150-56.

[24] Povlsen GK, Berezin V, Bock E. Neural cell adhesion molecule-180-mediated homophilic binding induces epidermal growth factor receptor (EGFR) down-regulation and uncouples the inhibitory function of EGFR in neurite outgrowth. J Neurochem. 2008;104:624-39.

[25] Tang ZY, Wang Y, Podsiadlo P, Kotov NA. Biomedical applications of layer-by-layer assembly: From biomimetics to tissue engineering. Adv Mater. 2006;18:3203-24.

[26] Roach P, Parker T, Gadegaard N, Alexander MR. Surface strategies for control of neuronal cell adhesion: A review. Surf Sci Rep. 2010;65:145-73.

[27] Mrksich M, Chen CS, Xia YN, Dike LE, Ingber DE, Whitesides GM. Controlling cell attachment on contoured surfaces with self-assembled monolayers of alkanethiolates on gold. P Natl Acad Sci USA. 1996;93:10775-78.

[28] Mrksich M, Whitesides GM. Using self-assembled monolayers to understand the interactions of man-made surfaces with proteins and cells. Annu Rev Bioph Biom. 1996;25:55-78.

[29] Tegoulia VA, Cooper SL. Staphylococcus aureus adhesion to self-assembled monolayers: effect of surface chemistry and fibrinogen presence. Colloid Surface B. 2002;24:217-28.

[30] Edmondson S, Osborne VL, Huck WTS. Polymer brushes via surface-initiated polymerizations. Chem Soc Rev. 2004;33:14-22.

[31] Yoshikawa C, Goto A, Tsujii Y, Fukuda T, Yamamoto K, Kishida A. Fabrication of high-density polymer brush on polymer substrate by surface-initiated living radical polymerization. Macromolecules. 2005;38:4604-10.

[32] Lego B, Francois M, Skene WG, Giasson S. Polymer Brush Covalently Attached to OH-Functionalized Mica Surface via Surface-Initiated ATRP: Control of Grafting Density and Polymer Chain Length. Langmuir. 2009;25:5313-21.

[33] Ruhe J, Yano R, Lee JS, Koberle P, Knoll W, Offenhausser A. Tailoring of surfaces with ultrathin polymer films for survival and growth of neurons in culture. J Biomat Sci-Polym E. 1999;10:859-74.

[34] DiDonato M, Hsu HF, Narindrasorasak S, Que L, Sarkar B. Copper-induced conformational changes in the N-terminal domain of the Wilson disease copper-transporting ATPase. Biochemistry-Us. 2000;39:1890-96.

[35] McArthur SL. Applications of XPS in bioengineering. Surf Interface Anal. 2006;38:1380-85.

[36] Beamson G, Briggs D. High-Resolution Monochromated X-Ray Photoelectron-Spectroscopy of Organic Polymers - a Comparison between Solid-State Data for Organic Polymers and Gas-Phase Data for Small Molecules. Mol Phys. 1992;76:919-36.

[37] Giessibl FJ. Advances in atomic force microscopy. Rev Mod Phys. 2003;75:949-83.

[38] Magonov SN, Reneker DH. Characterization of polymer surfaces with atomic force microscopy. Annu Rev Mater Sci. 1997;27:175-222.

[39] Horber JKH, Miles MJ. Scanning probe evolution in biology. Science. 2003;302:1002-05.

[40] Gadegaard N. Atomic force microscopy in biology: technology and techniques. Biotech Histochem. 2006;81:87-97.

[41] Ade H. Compositional and orientational characterization of polymeric systems with X-ray microscopy. Trends Polym Sci. 1997;5:58-66.

[42] Unger WES, Lippitz A, Woll C, Heckmann W. X-ray absorption spectroscopy (NEXAFS) of polymer surfaces. Fresen J Anal Chem. 1997;358:89-92.

[43] Astete CE, Kumar CSSR, Sabliov CM. Size control of poly(D,L-lactide-co-glycolide) and poly(D,L-lactide-co-glycolide)-magnetite nanoparticles synthesized by emulsion evaporation technique. Colloid Surface A. 2007;299:209-16.

[44] Silva GA, Czeisler C, Niece KL, Beniash E, Harrington DA, Kessler JA, et al. Selective differentiation of neural progenitor cells by high-epitope density nanofibers. Science. 2004;303:1352-55.

[45] Lockman PR, Mumper RJ, Khan MA, Allen DD. Nanoparticle technology for drug delivery across the blood-brain barrier. Drug Dev Ind Pharm. 2002;28:1-13.

[46] Zhong YH, Bellamkonda RV. Biomaterials for the central nervous system. J R Soc Interface. 2008;5:957-75.

[47] Blasi P, Glovagnoli S, Schoubben A, Ricci M, Rossi C. Solid lipid nanoparticles for targeted brain drug delivery. Adv Drug Deliver Rev. 2007;59:454-77.

[48] Kaur IP, Bhandari R, Bhandari S, Kakkar V. Potential of solid lipid nanoparticles in brain targeting. J Control Release. 2008;127:97-109.

[49] Vert M. Polymeric biomaterials: Strategies of the past vs. strategies of the future. Prog Polym Sci. 2007;32:755-61.

[50] Cherian AK, Rana AC, Jain SK. Self-assembled carbohydrate-stabilized ceramic nanoparticles for the parenteral delivery of insulin. Drug Dev Ind Pharm. 2000;26:459-63.

[51] Lian T, Ho RJY. Trends and developments in liposome drug delivery systems. J Pharm Sci. 2001;90:667-80.

[52] Domurado D, Vert M. Bioresorbable polyelectrolyte amphiphiles as nanosized carriers for lipophilic drug solubilization and delivery. J Biomat Sci-Polym E. 2007;18:287-301.

[53] Kang HC, Lee M, Bae YH. Polymeric gene carriers. Crit Rev Eukar Gene. 2005;15:317-42.

[54] Bronich T. Multifunctional Polymeric Carriers for Gene and Drug Delivery. Pharm Res-Dordr. 2010;27:2257-59.

[55] Orive G, Anitua E, Pedraz JL, Emerich DF. Biomaterials for promoting brain protection, repair and regeneration. Nat Rev Neurosci. 2009;10:682-692.

[56] Yebra DM, Kiil S, Dam-Johansen K. Antifouling technology - past, present and future steps towards efficient and environmentally friendly antifouling coatings. Prog Org Coat. 2004;50:75-104.

[57] Chambers LD, Stokes KR, Walsh FC, Wood RJK. Modern approaches to marine antifouling coatings. Surf Coat Tech. 2006;201:3642-52.

[58] Dang HY, Lovell CR. Bacterial primary colonization and early succession on surfaces in

marine waters as determined by amplified rRNA gene restriction analysis and sequence analysis of 16S rRNA genes. Appl Environ Microb. 2000;66:467-75.

[59] Champ MA. A review of organotin regulatory strategies, pending actions, related costs and benefits. Sci Total Environ. 2000;258:21-71.

[60] Terlizzi A, Fraschetti S, Gianguzza P, Faimali M, Boero F. Environmental impact of antifouling technologies: state of the art and perspectives. Aquat Conserv. 2001;11:311-17.

[61] Thomas KV, Fileman TW, Readman JW, Waldock MJ. Antifouling paint booster biocides in the UK coastal environment and potential risks of biological effects. Mar Pollut Bull. 2001;42:677-88.

[62] Konstantinou IK, Albanis TA. Worldwide occurrence and effects of antifouling paint booster biocides in the aquatic environment: a review. Environ Int. 2004;30:235-48.

[63] Brady RF, Singer IL. Mechanical factors favoring release from fouling release coatings. Biofouling. 2000;15:73-81.

[64] Marabotti I, Morelli A, Orsini LM, Martinelli E, Galli G, Chiellini E, et al. Fluorinated/siloxane copolymer blends for fouling release: chemical characterisation and biological evaluation with algae and barnacles. Biofouling. 2009;25:481-93.

[65] Martinelli E, Suffredini M, Galli G, Glisenti A, Pettitt ME, Callow ME, et al. Amphiphilic block copolymer/poly(dimethylsiloxane) (PDMS) blends and nanocomposites for improved fouling-release. Biofouling. 2011;27:529-41.

[66] Hu ZK, Finlay JA, Chen L, Betts DE, Hillmyer MA, Callow ME, et al. Photochemically Cross-Linked Perfluoropolyether-Based Elastomers: Synthesis, Physical Characterization, and Biofouling Evaluation. Macromolecules. 2009;42:6999-7007.

[67] Li XF, Andruzzi L, Chiellini E, Galli G, Ober CK, Hexemer A, et al. Semifluorinated aromatic side-group polystyrene-based block copolymers: Bulk structure and surface orientation studies. Macromolecules. 2002;35:8078-87.

[68] Dimitriou MD, Zhou ZL, Yoo HS, Killops KL, Finlay JA, Cone G, et al. A General Approach to Controlling the Surface Composition of Poly(ethylene oxide)-Based Block Copolymers for Antifouling Coatings. Langmuir. 2011;27:13762-72.

[69] Iwata R, Suk-In P, Hoven VP, Takahara A, Akiyoshi K, Iwasaki Y. Control of nanobiointerfaces generated from well-defined biomimetic polymer brushes for protein and cell manipulations. Biomacromolecules. 2004;5:2308-14.

[70] Iwasaki Y, Sawada S, Ishihara K, Khang G, Lee HB. Reduction of surface-induced inflammatory reaction on PLGA/MPC polymer blend. Biomaterials. 2002;23:3897-903.

[71] Zhang Z, Chao T, Chen SF, Jiang SY. Superlow fouling sulfobetaine and carboxybetaine polymers on glass slides. Langmuir. 2006;22:10072-77.

[72] Zhang Z, Chen SF, Chang Y, Jiang SY. Surface grafted sulfobetaine polymers via atom transfer radical polymerization as superlow fouling coatings. J Phys Chem B. 2006;110:10799-804.

[73] Zhang Z, Chen SF, Jiang SY. Dual-functional biomimetic materials: Nonfouling poly(carboxybetaine) with active functional groups for protein immobilization. Biomacromolecules. 2006;7:3311-15.

[74] Cheng G, Zhang Z, Chen SF, Bryers JD, Jiang SY. Inhibition of bacterial adhesion and biofilm formation on zwitterionic surfaces. Biomaterials. 2007;28:4192-99.

[75] Ladd J, Zhang Z, Chen S, Hower JC, Jiang S. Zwitterionic polymers exhibiting high resistance to nonspecific protein adsorption from human serum and plasma. Biomacromolecules. 2008;9:1357-61.

[76] Zhang Z, Finlay JA, Wang LF, Gao Y, Callow JA, Callow ME, et al. Polysulfobetaine-Grafted Surfaces as Environmentally Benign Ultralow Fouling Marine Coatings. Langmuir. 2009;25:13516-21.

[77] Tamerler C, Dincer S, Heidel D, Zareie MH, Sarikaya M. Biomimetic multifunctional molecular coatings using engineered proteins. Prog Org Coat. 2003;47:267-74.

[78] Clare AS, Rittschof D, Gerhart DJ, Maki JS. Molecular Approaches to Nontoxic Antifouling. Invertebr Reprod Dev. 1992;22:67-76.

[79] Waite JH. Reverse engineering of bioadhesion in marine mussels. Ann N.Y. Acad Sci. 1999;875:301-9.

[80] Dalsin JL, Hu BH, Lee BP, Messersmith PB. Mussel adhesive protein mimetic polymers for the preparation of nonfouling surfaces. J Am Chem Soc. 2003;125:4253-58.

[81] Simon RJ, Kania RS, Zuckermann RN, Huebner VD, Jewell DA, Banville S, et al. Peptoids - a Modular Approach to Drug Discovery. P Natl Acad Sci USA. 1992;89:9367-71.

[82] Statz AR, Meagher RJ, Barron AE, Messersmith PB. New peptidomimetic polymers for antifouling surfaces. J Am Chem Soc. 2005;127:7972-73.

[83] Mack D, Rohde H, Harris LG, Davies AP, Horstkotte MA, Knobloch JKM. Biofilm formation in medical device-related infection. Int J Artif Organs. 2006;29:343-59.

[84] Rosentritt M, Hahnel S, Groger G, Muhlfriedel B, Burgers R, Handel G. Adhesion of Streptococcus mutans to various dental materials in a laminar flow chamber system. J Biomed Mater Res B. 2008;86B:36-44.

[85] Shin GY, Manuel RJ, Ghori S, Brecker S, Breathnach AS. Molecular technique identifies the pathogen responsible for culture negative infective endocarditis. Heart. 2005;91.

[86] Ehrlich GD, Hu FZ, Lin Q, Costerton JW, Post JC. Intelligent implants to battle biofilms. Asm News. 2004;70:127-33.

[87] Hall-Stoodley L, Costerton JW, Stoodley P. Bacterial biofilms: From the natural environment to infectious diseases. Nat Rev Microbiol. 2004;2:95-108.

[88] Charnley M, Textor M, Acikgoz C. Designed polymer structures with antifouling-antimicrobial properties. React Funct Polym. 2011;71:329-34.

[89] Klibanov AM. Permanently microbicidal materials coatings. J Mater Chem. 2007;17:2479-82.

[90] Schofield WCE, Badyal JPS. A Substrate-Independent Approach for Bactericidal Surfaces. Acs Appl Mater Inter. 2009;1:2763-67.

[91] Desai NP, Hossainy SFA, Hubbell JA. Surface-Immobilized Polyethylene Oxide for Bacterial Repellence. Biomaterials. 1992;13:417-20.

[92] Roosjen A, Busscher HJ, Nordel W, van der Mei HC. Bacterial factors influencing adhesion of Pseudomonas aeruginosa strains to a poly(ethylene oxide) brush. Microbiol-Sgm. 2006;152:2673-82.

[93] Kohnen W, Jansen B. Polymer materials for the prevention of catheter-related infections. Zbl Bakt-Int J Med M. 1995;283:175-86.

[94] Medlin J. Germ warfare. Environ Health Persp. 1997;105:290-92.

[95] Shearer AEH, Paik JS, Hoover DG, Haynie SL, Kelley MJ. Potential of an antibacterial ultraviolet-irradiated nylon film. Biotechnol Bioeng. 2000;67:141-46.

[96] Kawabata N, Nishiguchi M. Antibacterial Activity of Soluble Pyridinium-Type Polymers. Appl Environ Microb. 1988;54:2532-35.

[97] Kenawy ER, Abdel-Hay FI, El-Raheem A, El-Shanshoury R, El-Newehy MH. Biologically active polymers: synthesis and antimicrobial activity of modified glycidyl methacrylate polymers having a quaternary ammonium and phosphonium groups. J Control Release. 1998;50:145-52.

[98] Cakmak I, Ulukanli Z, Tuzcu M, Karabuga S, Genctav K. Synthesis and characterization of novel antimicrobial cationic polyelectrolytes. Eur Polym J. 2004;40:2373-79.

[99] Yudovin-Farber I, Golenser J, Beyth N, Weiss EI, Domb AJ. Quaternary Ammonium Polyethyleneimine: Antibacterial Activity. J Nanomater. 2010.

[100] Stuart MAC, Huck WTS, Genzer J, Muller M, Ober C, Stamm M, et al. Emerging applications of stimuli-responsive polymer materials. Nat Mater. 2010;9:101-13.

[101] Laloyaux X, Fautre E, Blin T, Purohit V, Leprince J, Jouenne T, et al. Temperature-Responsive Polymer Brushes Switching from Bactericidal to Cell-Repellent. Adv Mater. 2010;22:5024-5028.

[102] Palermo EF, Kuroda K. Structural determinants of antimicrobial activity in polymers which mimic host defense peptides. Appl Microbiol Biot. 2010;87:1605-15.

[103] Tashiro T. Antibacterial and bacterium adsorbing macromolecules. Macromol Mater Eng. 2001;286:63-87.

[104] Kenawy ER, Worley SD, Broughton R. The chemistry and applications of antimicrobial polymers: A state-of-the-art review. Biomacromolecules. 2007;8:1359-84.

[105] Muller R, Eidt A, Hiller KA, Katzur V, Subat M, Schweikl H, et al. Influences of protein films on antibacterial or bacteria-repellent surface coatings in a model system using silicon wafers. Biomaterials. 2009;30:4921-29.

[106] Chakrabarty S, King A, Kurt P, Zhang W, Ohman DE, Wood LF, et al. Highly Effective, Water-Soluble, Hemocompatible 1,3-Propylene Oxide-Based Antimicrobials: Poly[(3,3-quaternary/PEG)-copolyoxetanes]. Biomacromolecules. 2011;12:757-69.

[107] Fletcher M, Marshall KC. Bubble Contact-Angle Method for Evaluating Substratum Interfacial Characteristics and Its Relevance to Bacterial Attachment. Appl Environ Microb. 1982;44:184-92.

[108] Lindner E, Arias E. Surface Free-Energy Characteristics of Polyfluorinated Silane Films. Langmuir. 1992;8:1195-98.

[109] Callow ME, Fletcher RL. The Influence of Low Surface-Energy Materials on Bioadhesion - a Review. Int Biodeter Biodegr. 1994;34:333-48.

[110] An YH, Friedman RJ. Concise review of mechanisms of bacterial adhesion to biomaterial surfaces. J Biomed Mater Res. 1998;43:338-48.

[111] Chandra J, Patel JD, Li J, Zhou GY, Mukherjee PK, McCormick TS, et al. Modification of surface properties of biomaterials influences the ability of Candida albicans to form biofilms. Appl Environ Microb. 2005;71:8795-801.

[112] McClary KB, Ugarova T, Grainger DW. Modulating fibroblast adhesion, spreading, and proliferation using self-assembled monolayer films of alkylthiolates on gold. J Biomed Mater Res. 2000;50:428-39.

[113] Dexter SC. Influence of Substratum Critical Surface-Tension on Bacterial Adhesion - Insitu Studies. J Colloid Interf Sci. 1979;70:346-54.

[114] Fletcher M, Marshall KC. Are Solid-Surfaces of Ecological Significance to Aquatic Bacteria. Adv Microb Ecol. 1982;6:199-230.

[115] Paul JH, Jeffrey WH. Evidence for Separate Adhesion Mechanisms for Hydrophilic and Hydrophobic Surfaces in Vibrio-Proteolytica. Appl Environ Microb. 1985;50:431-37.

[116] Morgenthaler S, Zink C, Spencer ND. Surface-chemical and -morphological gradients. Soft Matter. 2008;4:419-34.

[117] Pelham RJ, Wang YL. Cell locomotion and focal adhesions are regulated by substrate flexibility. P Natl Acad Sci USA. 1997;94:13661-65.

[118] Saha K, Keung AJ, Irwin EF, Li Y, Little L, Schaffer DV, et al. Substrate Modulus Directs Neural Stem Cell Behavior. Biophys J. 2008;95:4426-38.

[119] Sundararaghavan HG, Monteiro GA, Firestein BL, Shreiber DI. Neurite Growth in 3D Collagen Gels With Gradients of Mechanical Properties. Biotechnol Bioeng. 2009;102:632-43.

[120] Leach JB, Brown XQ, Jacot JG, DiMilla PA, Wong JY. Neurite outgrowth and branching of PC12 cells on very soft substrates sharply decreases below a threshold of substrate rigidity. J Neural Eng. 2007;4:26-34.

[121] Pelham RJ, Wang YL. Cell locomotion and focal adhesions are regulated by the mechanical properties of the substrate. Biol Bull. 1998;194:348-49.

[122] Wang YL, Pelham RJ. Preparation of a flexible, porous polyacrylamide substrate for mechanical studies of cultured cells. Method Enzymol. 1998;298:489-96.

[123] Brady RF. A fracture mechanical analysis of fouling release from nontoxic antifouling coatings. Prog Org Coat. 2001;43:188-92.

[124] Curtis ASG, Clark P. The Effects of Topographic and Mechanical-Properties of Materials on Cell Behavior. Crit Rev Biocompat. 1990;5:343-62.

[125] Gates BD, Xu QB, Stewart M, Ryan D, Willson CG, Whitesides GM. New approaches to nanofabrication: Molding, printing, and other techniques. Chem Rev. 2005;105:1171-96.

[126] Dalby MJ. Topographically induced direct cell mechanotransduction. Med Eng Phys. 2005;27:730-42.

[127] Biggs MJ, Richards RG, Dalby MJ. Nanotopographical modification: a regulator of cellular function through focal adhesions. Nanomedicine : nanotechnology, biology, and medicine. 2010;6:619-33.

[128] Martino S, D'Angelo F, Armentano I, Kenny JM, Orlacchio A. Stem cell-biomaterial interactions for regenerative medicine. Biotechnology advances. 2012;30:338-51.

[129] Folch A, Toner M. Microengineering of cellular interactions. Annu Rev Biomed Eng. 2000;2:227-+.

[130] Raghavan S, Chen CS. Micropatterned environments in cell biology. Adv Mater. 2004;16:1303-13.

[131] Klopp JM, Pasini D, Byers JD, Willson CG, Frechet JMJ. Microlithographic assessment of a novel family of transparent and etch-resistant chemically amplified 193-nm resists eased on cyclopolymers. Chem Mater. 2001;13:4147-53.

[132] Bretagnol F, Valsesia A, Sasaki T, Ceccone G, Colpo P, Rossi F. Direct nanopatterning of 3D chemically active structures for biological applications. Adv Mater. 2007;19:1947-+.

[133] Ahn SJ, Kaholek M, Lee WK, LaMattina B, LaBean TH, Zauscher S. Surface-initiated polymerization on nanopatterns fabricated by electron-beam lithography. Adv Mater. 2004;16:2141-+.

[134] von Werne TA, Germack DS, Hagberg EC, Sheares VV, Hawker CJ, Carter KR. A versatile method for tuning the chemistry and size of nanoscopic features by living free radical polymerization. J Am Chem Soc. 2003;125:3831-38.

[135] Vitte J, Benoliel AM, Pierres A, Bongrand P. Regulation of cell adhesion. Clin Hemorheol Micro. 2005;33:167-88.

[136] Lakard S, Herlem G, Propper A, Kastner A, Michel G, Valles-Villarreal N, et al. Adhesion and proliferation of cells on new polymers modified biomaterials. Bioelectrochemistry. 2004;62:19-27.

[137] Lakard S, Herlem G, Valles-Villareal N, Michel G, Propper A, Gharbi T, et al. Culture of neural cells on polymers coated surfaces for biosensor applications. Biosens Bioelectron. 2005;20:1946-54.

[138] Trommler A, Gingell D, Wolf H. Red Blood-Cells Experience Electrostatic Repulsion but Make Molecular Adhesions with Glass. Biophys J. 1985;48:835-41.

[139] Keselowsky BG, Collard DM, Garcia AJ. Surface chemistry modulates fibronectin conformation and directs integrin binding and specificity to control cell adhesion. J Biomed Mater Res A. 2003;66A:247-59.

[140] Wang E, Zhao M, Forrester JV, McCaig CD. Bi-directional migration of lens epithelial cells in a physiological electrical field. Experimental eye research. 2003;76:29-37.

[141] Kerns JM, Fakhouri AJ, Weinrib HP, Freeman JA. Electrical-Stimulation of Nerve Regeneration in the Rat - the Early Effects Evaluated by a Vibrating Probe and Electron-Microscopy. Neuroscience. 1991;40:93-107.

[142] Basser PJ. Focal Magnetic Stimulation of an Axon. Ieee T Bio-Med Eng. 1994;41:601-06.

[143] Rivers TJ, Hudson TW, Schmidt CE. Synthesis of a novel, biodegradable electrically conducting polymer for biomedical applications. Adv Funct Mater. 2002;12:33-37.

[144] Huang LH, Zhuang XL, Hu J, Lang L, Zhang PB, Wang YS, et al. Synthesis of biodegradable and electroactive multiblock polylactide and aniline pentamer copolymer for tissue engineering applications. Biomacromolecules. 2008;9:850-58.

[145] Sun S, Titushkin I, Cho M. Regulation of mesenchymal stem cell adhesion and orientation in 3D collagen scaffold by electrical stimulus. Bioelectrochemistry. 2006;69:133-41.

[146] Dottori M, Armentano I, Fortunati E, Kenny JM. Production and Properties of Solvent-Cast Poly(epsilon-caprolactone) Composites with Carbon Nanostructures. J Appl Polym Sci. 2011;119:3544-52.

[147] Bianco A, Del Gaudio C, Baiguera S, Armentano I, Bertarelli C, Dottori M, et al. Microstructure and cytocompatibility of electrospun nanocomposites based on poly(epsilon-caprolactone) and carbon nanostructures. Int J Artif Organs. 2010;33:271-82.

[148] Li LY, Chen SF, Zheng J, Ratner BD, Jiang SY. Protein adsorption on oligo(ethylene glycol)-terminated alkanethiolate self-assembled monolayers: The molecular basis for nonfouling behavior. J Phys Chem B. 2005;109:2934-41.

[149] Schwender N, Huber K, Al Marrawi F, Hannig M, Ziegler C. Initial bioadhesion on surfaces in the oral cavity investigated by scanning force microscopy. Appl Surf Sci. 2005;252:117-22.

[150] Muller R, Groger G, Hiller KA, Schmalz G, Ruhl S. Fluorescence-based bacterial overlay method for simultaneous in situ quantification of surface-attached bacteria. Appl Environ Microb. 2007;73:2653-60.

[151] Muller R, Ruhl S, Hiller KA, Schmalz G, Schweikl H. Adhesion of eukaryotic cells and Staphylococcus aureus to silicon model surfaces. J Biomed Mater Res A. 2008;84A:817-27.

[152] Neumann T, Johansson ML, Kambhampati D, Knoll W. Surface-plasmon fluorescence spectroscopy. Adv Funct Mater. 2002;12:575-86.

[153] Janshoff A, Galla HJ, Steinem C. Piezoelectric mass-sensing devices as biosensors - An alternative to optical biosensors? Angew Chem Int Edit. 2000;39:4004-32.

[154] Korovessis PG, Deligianni DD, Lenke LG. Role of surface roughness of titanium versus hydroxyapatite on human bone marrow cells response. J Spinal Disord Tech. 2002;15:175-83.

[155] Diener A, Nebe B, Luthen F, Becker P, Beck U, Neumann HG, et al. Control of focal adhesion dynamics by material surface characteristics. Biomaterials. 2005;26:383-92.

[156] Kunzler TP, Drobek T, Schuler M, Spencer ND. Systematic study of osteoblast and fibroblast response to roughness by means of surface-morphology gradients. Biomaterials. 2007;28:2175-82.

CHAPTER TWO

THE ROLE OF HYDROGELS WITH TETHERED ACETYLCHOLINE FUNCTIONALITY ON THE ADHESION AND VIABILITY OF HIPPOCAMPAL NEURONS AND GLIAL CELLS

***** Zhaoli Zhou, Panpan Yu, Herbert M. Geller,and Christopher K. Ober. *Biomaterials* **2012**, 33, 2473-2481.

ABSTRACT

In neural tissue engineering, designing materials with the right chemical cues is crucial in providing a permissive microenvironment to encourage and guide neuronal cell attachment and differentiation. Modifying synthetic hydrogels with biologically active molecules has become an increasingly important route in this field to provide a successful biomaterial and cell interaction. This study presents a strategy of using the monomer 2-methacryloxyethyl trimethylammonium chloride (MAETAC) to provide tethered neurotransmitter acetylcholine-like functionality with a complete 2-acetoxy-N,N,N-trimethylethanaminium segment, thereby modifying the properties of commonly used, non-adhesive PEG-based hydrogels. The effect of the functional monomer concentration on the physical properties of the hydrogels was systematically studied, and the resulting hydrogels were also evaluated for mice hippocampal neural cell attachment and growth. Results from this study showed that MAETAC in the hydrogels promotes neuronal cell attachment and differentiation in a concentration-dependent manner, different proportions of MAETAC monomer in the reaction mixture produce hydrogels with different porous structures, swollen states, and mechanical strengths. Growth of mice hippocampal cells cultured on the hydrogels showed differences in number, length of processes and exhibited different survival rates. Our results indicate that chemical composition of the biomaterials is a key factor in neural cell attachment and growth, and integration of the appropriate amount of tethered neurotransmitter functionalities can be a simple and effective way to optimize existing biomaterials for neuronal tissue engineering applications.

Keywords: PEG-based hydrogels, Neurotransmitters, Acetylcholine functionality, Concentration-dependent manner

2.1 Introduction

Injuries to the brain and spinal cord cause some of the most severe and widespread public health problems. According to the Center for Disease Control (CDC), several million people suffer from disabilities caused by brain damage each year in the U.S. alone. The causes of the damage include a wide range of conditions such as traumatic brain injury, stroke, chronic neurodegenerative disease, infections, hypoxia, and poisoning. These result in the loss of specific populations of neurons as well as connections between neurons and the development of defined psychiatric or neurological symptoms. Unfortunately, there are currently no therapies available to fully restore lost function or slow ongoing neurodegeneration in the damaged brain.

However, in recent years, knowledge of the factors influencing nerve reconstruction has increased, new surgical techniques and equipment have been developed, and experimental work in the field has made great progress. For example, neural tissue engineering [1-3] as a newly emerging field, involving the use of cells to promote nerve regeneration and to repair damage caused to nerves, provides a promising approach to repair segmental nerve defects. However, in order for cells to maintain their tissue-specific functions, a substrate material must be inserted to aid in organization of cells and the directed growth of neuronal processes [3-5]. For this application the choice of scaffolding material is crucial for success, and a number of different natural and synthetic materials have been explored that effect nerve regeneration and repair.

Compared to natural materials, synthetic materials have become increasingly important in this field, since their scaffold architectures, chemical composition, physical properties, and biochemical properties are controllable and reproducible, and each of the properties can also be tailored for specific applications. In particular, synthetic hydrogels have drawn interest as *in vitro* and *in vivo* research models for the study of neural tissue engineering applications [4], because

they have many advantages over alternative scaffold materials, such as high oxygen and nutrient permeability. They also have low interfacial tensions which minimize barriers to cells migrating into the scaffold from surrounding soft tissue, or processes from cells within or out of the material crossing the scaffold-tissue boundary [6]. Furthermore, hydrogels are able to retain aqueous solutions encapsulated with drugs, growth factors and cells for desired functioning *in vivo*. Numerous synthetic hydrogels have been explored for drug delivery and nerve regeneration applications, and they may hold key roles in overcoming the inherent insufficiency of protection, repair and regeneration of the brain [7,8].

To date, due to availability and biocompatibility of the precursors, methacrylate based hydrogels and polyethylene glycol (PEG) based hydrogels remain the most important classes of synthetic hydrogels for CNS applications. However, a major drawback of these types of hydrogels is low protein and cell attachment: they alone cannot support cell adhesion and tissue formation due to their bio-inert nature. Cell attachment to these hydrogels is facilitated by modifying them with other molecules to create synthetic templates that can mimic some of the properties of a natural tissue matrix, such as extracellular matrix (ECM) proteins (laminin, fibronectin, or vitronectin) or short adhesive peptides (RGDS, IKVAV or YIGSR) derived from these molecules [9,10]. Modifying PEG based hydrogels with small functional biologically active molecules also provides an alternate route to give positive cues for successful biomaterial and cell interactions [11,12]. An important class of biomolecules in the nervous system is the neurotransmitters, which play important roles in cell communication, differentiation and survival [13,14]. Studies have shown that both surface-tethered and directly integrated neurotransmitters in polymers can induce specific neuronal responses [15-17]. Immobilized rat chondrocytes directly encapsulated in tyramine-substituted hyaluronan hydrogels remained

metabolically active and behaved similar to cells cultured in monolayers [18]. Substantial improvement in neuronal outgrowth have been observed for neuronal cells on a bioactive polymer based on dopamine compared to tissue culture polystyrene, laminin, and poly-D-lysine [15]. Particularly, acetylcholine (ACh), as the first neurotransmitter, has been widely studied for its role in synaptic transmission [19,20], and it has been shown to regulate neuronal development and enhance neurite outgrowth [21-23]. However, studies using ACh functionality in synthetic hydrogels are limited, and the use of a structure that contains the complete acetylecholine functionality (2-acetoxy-N,N,N-trimethylethanaminium) segments is desirable to understand how immobilized acetylcholine neurotransmitter interact with neuronal cells.

In the current work, we designed and synthesized biomimetic hydrogels with a tethered acetylcholine structure to promote interaction between neuronal cells and material surfaces. 2-methacryloxyethyl trimethylammonium chloride (MAETAC) was chosen as a monomer to provide the ACh functionality (Figure 2.1). We systematically investigated a complete concentration range of MAETAC in the synthetic hydrogels by controlling the feeding volume ratio of MAETAC to PEGMA monomers in the prepolymerization solution (ranges from 90.0% to 1.0%, and the molar ratio ranges from 92.2% to 1.0%). We investigated the effect of MAETAC concentration on equilibrium swelling and mechanical properties of the hydrogels. The effect of these parameters on neuron and glial cell attachment and growth was demonstrated by seeding these hydrogels with cells derived from the mouse hippocampus.

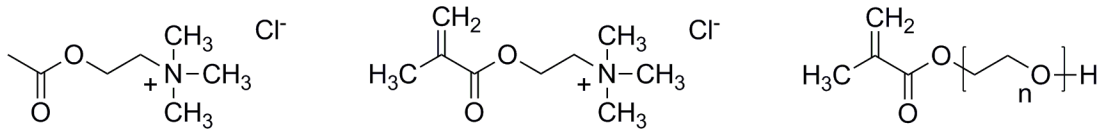

Figure 2.1: Chemical structures of ACh, MAETAC and PEG monomers. (a) neurotransmitter acetylcholine chloride (2-acetoxy-N,N,N-trimethylethanaminium), monomers (b) ([2-(methacryloyloxy) ethyl]-trimethylammonium chloride (MAETAC) and (c) Polyethylene glycol methacrylate (PEGMA). (a) and (b) share common functional group except (b) contains a methyl-vinyl group which can be used for photopolymerization reaction.

2.2 Materials and Methods

2.2.1 Synthesis of Hydrogels

Random copolymer poly(MAETAC-PEGMA) hydrogels were produced by photopolymerizing monomers MAETAC and PEGMA (Sigma-Aldrich, St. Louis, MO) at various ratios (Table 1). In all experiments, the crosslinking agent ethylene glycol dimethylacrylate (EGDMA; Sigma-Aldrich, St. Louis, MO) concentration is 0.1% (v/v) to the polymerization solution, and photoinitiator 2, 2-Dimethoxy-2-Phenylacetophenone (Irgacure 651; Sigma-Aldrich, St. Louis, MO) was 53.0 mM. We synthesized the hydrogel by pipetting the mixed monomer solution between two Parafilm®-covered optical glass slides separated by a 1-mm-thick spacer. The entire assembly was exposed to UV light (365 nm, 1.8 mW/cm^2) using a hand-held UV lamp (Spectroline; Westbury, NY) for 5 min. Following polymerization at room temperature, hydrogels were peeled off the Parafilm®-covered glass surface (7.6 cm diameter × 0.45cm thick, transmittance 95% at 365 nm, Esco Products, Oak Ridge, NJ). Subsequently, the gels were thoroughly washed in large quantities of distilled water for 2 days to remove unreacted monomers with periodic replacement of the water used for leaching. After washing, the hydrogel

disks were cut out using a 10 mm Arch punch (10 mm diameter, McMaster-Carr, New Brunswick, NJ). Hydrogel disks were then stored in deionized water until use.

2.3 Physical Characterization of Hydrogels

Hydrogel disks were dehydrated using lyophilization for elemental analysis and scanning electron microscopy (SEM). The fully swollen hydrogel samples were put in a freeze-dryer and shock-frozen in liquid nitrogen for 10 min. The samples were then dried under vacuum at less than 1 mm Hg for 24 h. Elemental analysis for weight percentage of C, H, N of the dried hydrogels was performed by Quantitative Technologies, Inc. (QTI). For SEM experiment, the dehydrated hydrogel samples were freshly cut with a sharp blade, and then mounted on SEM stubs and sputter coated with gold for 30 s. The morphologies and pore structures of the cross-sections of the gold-coated hydrogel samples were observed under SEM (Leica 440) at 10 KV.

To measure the equilibrium swelling ratio, the fully swollen hydrogel samples were weighed after excess surface water was gently removed by blotting with Kimwipes, and then freeze-dried and weighed again. Each measurement was repeated at least three times. The equilibrium water content was calculated from the change in mass of the samples before and after freeze-drying by the following equation [24-26]: $EWC\% = (1- W_d/W_s) \times 100$, and the swelling ratio was determined according to the following equation [25]: $\text{Swelling Ratio} = (W_s - W_d)/W_d$, where W_s is the weight of the swollen gel and W_d is the weight of the freeze dried gel, respectively.

Mechanical properties of hydrogels were tested using a DMA 2980 (TA Instruments) in submersion compression method. The hydrogel sample disks (10 mm) were submerged in deionized (DI) water for measurements. Tests were performed in controlled force mode and the

preload force was 0.01 N. The data was analyzed by calculating the compression modulus from the slope of the linear region on the plot of stress-strain curve, and each sample has been measured three times.

2.3.1 Hippocampal Cell Culture on Hydrogels

Procedures used in animal experiments were processed through institutional animal care. All hydrogel samples were autoclaved for 30 min before the experiments, and all cell culture experiments were carried out in 24 well plates. One day before culture, hydrogel samples in 24-well plates were rinsed twice in neuronal culture medium consisting of Neurobasal-A (Gibco/BRL, Bethesda, MD) supplemented with B27 (2%, v/v; Gibco), and then equilibrated in the medium overnight until cell plating.

Hippocampal neuronal cultures were prepared by Dr. Panpan Yu (NIH, Dr. Herbert M. Geller's lab) through enzymatic dissociation of hippocampi removed from postnatal day 0 mouse pups as previously described [27]. Briefly, after removal of the meanings of the cerebral hemispheres, hippocampi were dissected out, chopped into small pieces and digested with 0.125% trypsin (Gibco) for 15 min at 37°C. The tissue was then dissociated into a single cell suspension by triturating. The cells were plated at a density of 40,000 cells/well onto the hydrogel samples. The cells were cultured in Neurobasal-A medium supplemented with B27 and maintained for 3 days before fixation. Each experiment was performed in triplicate and repeated 3 times.

2.3.2 Cell Viability, Immunostaining and Statistical Analysis

Cell viability was measured using the standard LIVE/DEAD Viability/Cytotoxicity

Assay Kit from Invitrogen (Eugene, OR). After 3 days of culture, each hydrogel sample was placed in 1 ml growth media with 0.5 µL calcein substrate and 2 µL ethidium homodimer substrate, and incubated at 37°C for 20 min. Cell viability and distribution were visualized using a Nikon Eclipse 800 fluorescence microscope. Five random fields of each sample were imaged on both green and red channels and the number of live and dead cells was counted manually for each image. The number of live cells divided by the total number of live and dead cells was defined as the fractional viability.

For immunostaining experiments, cells on hydrogel samples were fixed after three days of culture with 4% paraformaldehyde (Sigma-Aldrich) in phosphate buffered saline (PBS, pH7.4, Sigma-Aldrich) for 20 min at room temperature, and then rinsed three times with PBS buffer. The samples were then prepared for immunostaining by blocking and permeabilizing in 10% normal goat serum (NGS; Sigma-Aldrich) and 0.1% Triton-X100 (v/v, PBS-T, Sigma-Aldrich) in PBS for 1 h at room temperature. Samples were exposed to the primary antibodies, mouse monoclonal anti-β-tubulin III (1:1000, Sigma-Aldrich) and rabbit polyclonal anti-GFAP (1:1000, DAKO) diluted in PBS-T buffer containing 2% NGS and incubated overnight at 4°C. On the following day, the samples were then washed with PBS-T buffer thoroughly. The cells were then incubated for 1.5 h at room temperature with AlexaFluor488-congugated goat anti-mouse IgG (1:1000, Molecular Probes) and AlexaFluor®568 goat anti-rabbit IgG (1:1000, Molecular Probes) diluted in PBS-T containing 2% NGS, followed by incubation with DAPI (1:1000, Molecular Probes) in PBS buffer for 5 min at room temperature. After rinsing with PBS five times, and 5 min each time, images of cultures were obtained using the fluorescence microscope. The images were analyzed using ImageJ (available at http://rsbweb.nih.gov/ij/) to determine the number of neurons and astrocytes in each random field. All data are reported for triplicate samples.

Statistical analyses were performed by one-way ANOVA followed by Turkey post hoc test. Results were considered statistically significant if $p<0.05$.

Table 2.1: Hydrogel preparation and analysis. Feeding ratios of monomer MAETAC to monomer PEGMA in the prepolymerization solutions for the preparation of hydrogel samples and elemental analysis of these samples. The prepared hydrogel samples showed different appearance according to the feeding ratio of the two monomers. Note the elemental composition of MAETAC ($C_9H_{18}NO_2Cl$, Mw = 207.7) is as follows: C: 52.0%; H: 8.7%; and N: 6.7%. v/v, w/w, and n/n stand for the volume ratio, mass ratio and molar ratio of MAETAC monomer to PEGMA monomer, respectively.

Hydrogel	Ratio of MAETAC to PEGMA			Elemental Analysis			Final Gel
Names	v/v	w/w	n/n	% C	% H	% N	Appearance
HS-1	9.00	6.77	11.74	40.93	9.10	4.55	Clear
HS-2	4.00	3.01	5.22	42.94	9.09	4.21	White
HS-3	2.33	1.76	3.04	44.15	8.96	3.74	White
HS-4	1.50	1.13	1.96	46.17	9.06	3.35	White
HS-5	1.00	0.75	1.30	48.65	9.11	3.00	White
HS-6	0.67	0.50	0.87	49.35	8.93	2.34	White
HS-7	0.43	0.32	0.56	49.64	8.86	1.74	White
HS-8	0.25	0.19	0.33	50.97	8.77	1.19	White
HS-9	0.11	0.08	0.14	52.79	8.51	0.63	Clear
HS-10	0.05	0.04	0.07	54.30	8.15	0.29	Clear
HS-11	0.01	0.01	0.01	54.39	8.16	<0.05	Clear

2.4 Results

2.4.1 Hydrogel Preparation and Characterization

Hydrogels were crosslinked by EGDMA using Irgacure 651 as a radical photoinitiator. Table 2.1 shows the chemical compositions of the MAETAC and PEGMA monomers used in the prepolymerization solution to make each hydrogel sample. Results from elemental analysis showed that the amount of MAETAC structure presented in the hydrogels corresponds to the feed ratio of the monomers: less MAETAC structure presented in the final gels when its concentration in the pre-polymerization solution is lower. Phase separation

occurred when PEGMA was added to a MAETAC aqueous solution (75.0%, v/v) in samples from HS-2 to HS-8, and those hydrogels were white in color. When an excess amount of MAETAC or PEGMA was present in the solution, this seemed not to be a problem: samples HS-1 and HS-9 to HS-11 all were transparent and clear gels. After the polymerization process, the prepared hydrogels were purified in a large amount of deionized water to remove unreacted monomers, and the gels were also fully swollen during this procedure.

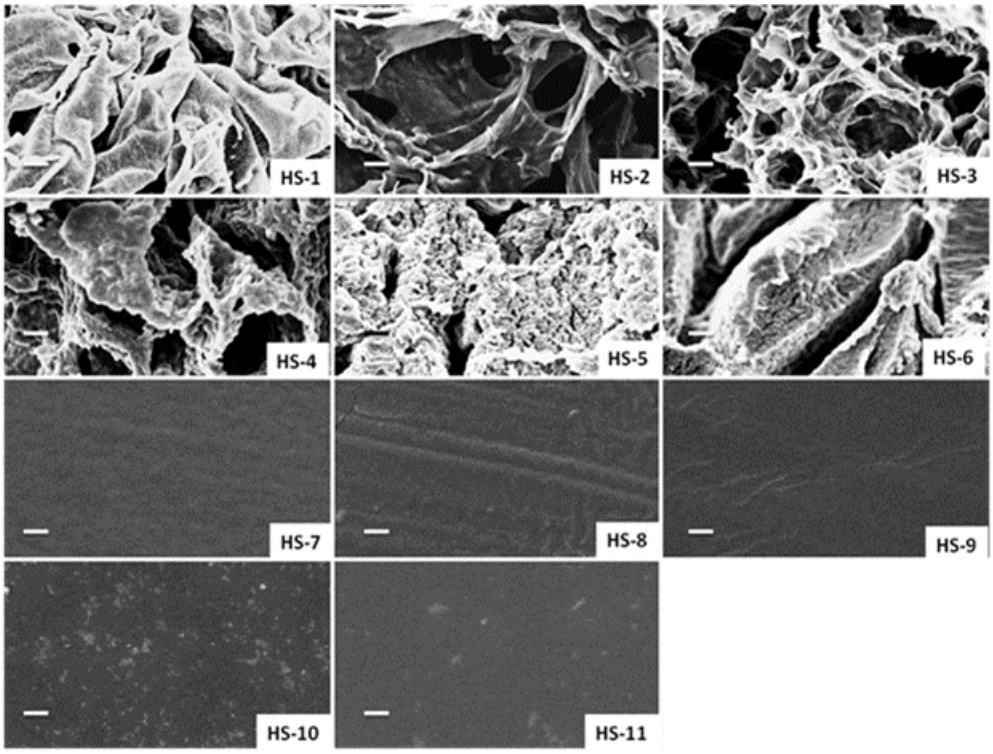

Figure 2.2: SEM images of hydrogel samples. Cross-section structures of the hydrogels under scanning electron microscopy (SEM) after freeze-drying (scale bar is 5 μm).

Purified hydrogels in deionized water were then freeze-dried to investigate the morphology by SEM. Figure 2.2 shows sample images of a cross-sectional view of the bulk structure of the dried hydrogels. HS-1 is mechanically soft and contains a large amount of water; the structure collapsed during the freeze-drying process. HS-2 and HS-3 showed large porous

structures, while due to the increased amount of PEGMA in the prepolymerized solutions; hydrogels HS-4 to HS-6 had interconnected pore morphology. From sample HS-7 to HS-11, analysis of the SEM micrographs showed no visible macrospores in the samples prepared using this method.

The equilibrium water content of the hydrogels decreased with the decreasing of the amount of MAETAC concentration in the monomer mixtures, which is in agreement with the SEM observation that the hydrogel porosity decreased with the increase of the PEGMA concentration of the polymerization solution (Figure 2.3). This might because of the presence of positively charged groups in the matrix contribute to an osmotic force leading to water absorption, as with increasing MAETAC content, the osmotic gradient increases therefore result in higher equilibrium water content or swelling ratio. For example, the water content for HS-1 (10.0% of PEGMA) was 99.1%, while in HS-9 (90.0% of PEGMA) it was 67.4%. The dramatic change of the swelling ratio from 108.64 to 1.64 with the increased amount of PEGMA from sample HS-1 to sample HS-11 further showed that pore volume largely decreased with the PEGMA concentration increased. Note that water comprises more than 95.0% the total weight of sample HS-1 and HS-2. They can be called superabsorbent [28], and might also hold other potential applications, such as in chromatography and water purification [29,30].

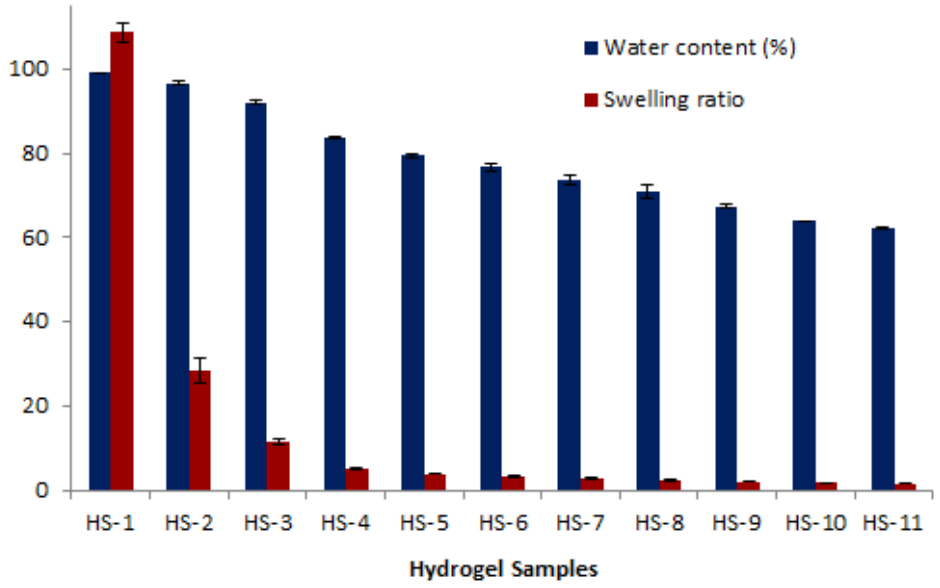

Figure 2.3: Equilibrium water contents and swelling ratio of hydrogels in deionized water (Means + SD, n=3).

The slopes of the linear portion of the compression stress-strain curves were used to compute mean values for the compression modulus. The compression modulus is directly related through the degree of swelling and hence the water content. Higher concentrations of PEGMA were expected to result in more tightly crosslinked hydrogels and a decrease in the ability of the network to absorb water. Therefore, in most cases the compression modulus of hydrogels increased with the increase in PEGMA concentration in the polymerization solution (Figure 2.4). HS-1 had a modulus of 17.7 kPa; with additional amounts of PEGMA, the compressive modulus of hydrogel HS-11 increased up to 128.9 kPa. Samples HS-10 and HS-11 were very brittle and had a lower modulus as compared to samples HS-8 and HS-9, probably because the gels were slightly cracked during the tests.

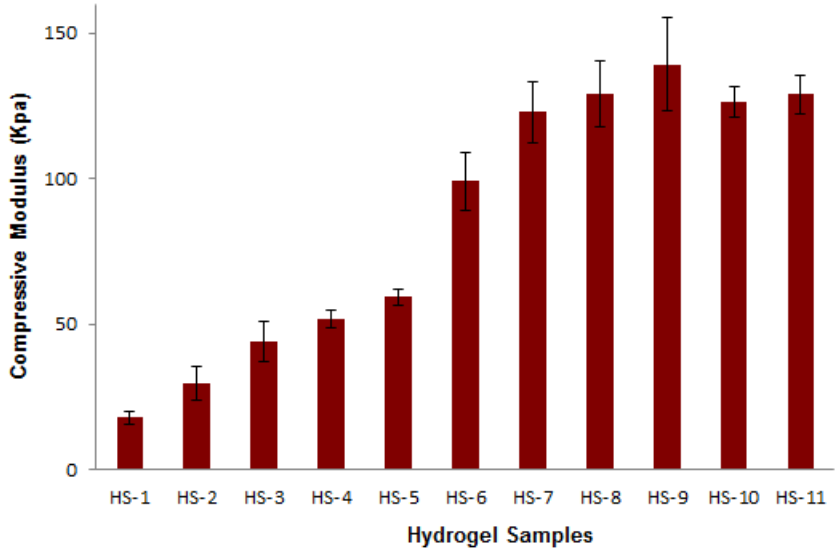

Figure 2.4: Compressive modulus of hydrogels **(**Means ± SD, n=3). The data was analyzed by calculating the linear region slopes of the stress-strain curves.

2.4.2 Attachment and Viability of Hippocampal Neuronal Cells on The Hydrogels

Dissociated mouse hippocampal neurons cells were plated on all hydrogel samples. After 3 days, cellular viability was assessed via the LIVE/DEAD cell viability/toxicity assay. Samples HS-1 to HS-5 showed strong cytotoxicity, with many dead cells on the surfaces, and no living cells was observed (data not shown). The other six samples, HS-6 to HS-11, had viable cells (Figure 2.5). HS-6 (0.7% viability, average 3.5 live cells/field) and HS-7 (2.0% viability, average 15.5 live cells/field) also exhibited a greater number of dead cells as compared to HS-8 (33.6% viability, average 224.3 live cells/field), and HS-9 (50.9% viability, average 201.6 live cells/field). As expected, with higher concentrations of PEGMA (greater than 90.0% v/v) in the hydrogels, the samples do not favor cell attachment, as PEG is normally neutral and non-adhesive to protein and cells [31]. Samples HS-10 and HS-11 have relatively fewer cells attached

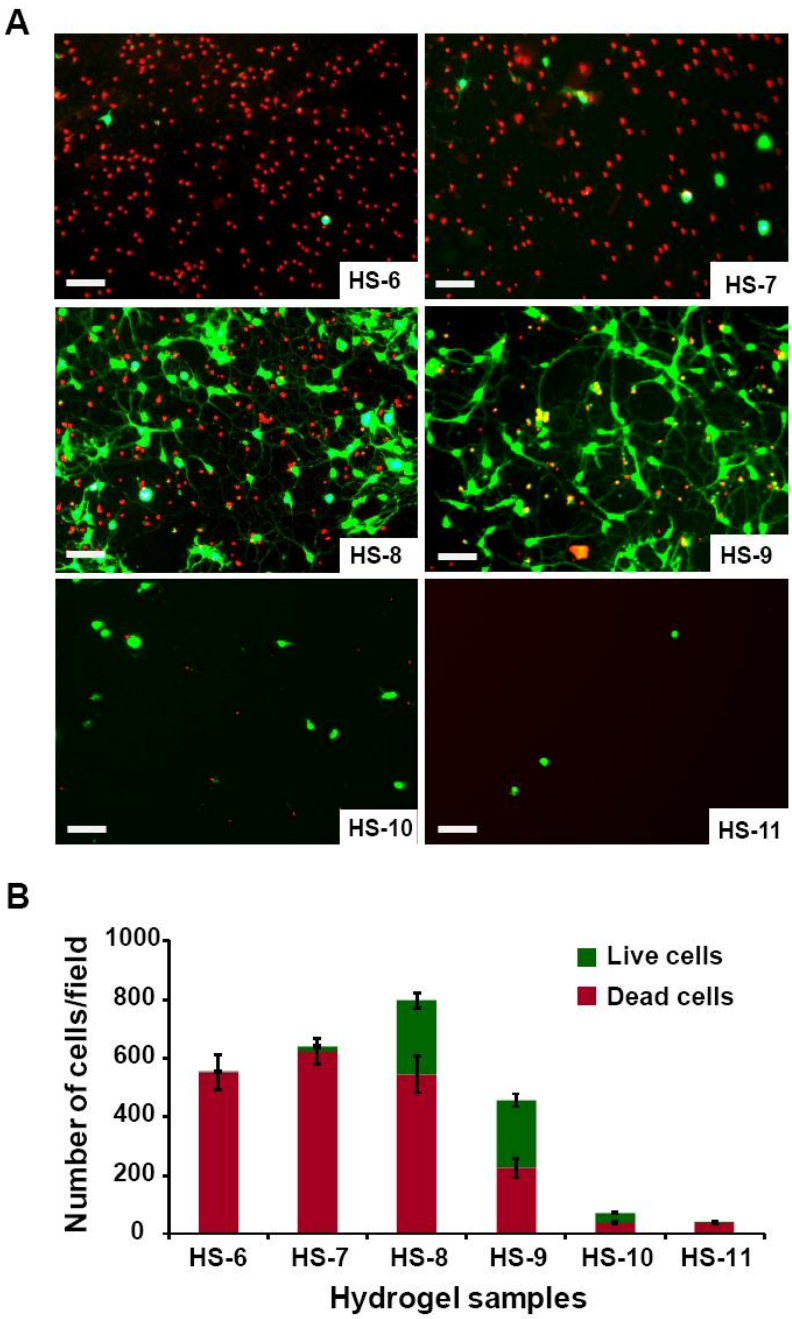

Figure 2.5: LIVE/DEAD assay of hippocampal cells on hydrogels**.** A) LIVE/DEAD viability/cytotoxicity assay of hippocampal cells on hydrogel samples (Scale bar is 50 µm). Cells on hydrogels were cultured for three days and then observed with fluorescent micrographs of live (calcein AM, green) and dead (ethidium homodimer-1, red). B) Analysis of LIVE/DEAD viability/cytotoxicity of hydrogel samples. Numbers of live (green columns) and dead (red columns) cells were counted manually in five random fields of each hydrogel sample, and each sample were repeated three times in the experiments to calculate the average number of cells on a random field.

to the gels as compared to sample HS-8 and HS-9 (average 35.8 and 1.7 cells/field, respectively), although the ratio of living cells are higher in these two sample (57.2% and 87.57%).

Results of double-label immunocytochemistry (Figure 2.6) showed that HS-6 hardly supported either neuronal (average 0.9 neuron/field) or astrocytic (average 5.3 astrocytes/field adhesion or survival), while HS-7 greatly favored astrocytic adhesion (average 0.7 neurons/field and 56.1 astrocytes/field). Cell attachment and growth were much higher on HS-8, with about an equal number of astrocytes and neurons, with an average of 104.7 neurons/field and 118.7 astrocytes/field. HS-9 had the highest cell attachment and neurite outgrowth, with an average of 160.1 neurons and 93.6 astrocytes on a random field. At higher concentrations of MAETAC, cellular attachment and growth decreased: sample HS-10 had 56.1 neurons and 15.9 astrocytes per random field, while sample HS-11 had very few cells attached (average 1.1 neurons/field and 0.2 astrocytes/field). Cell morphologies were different on the six samples, with sample HS-9 eliciting the longest process outgrowth from neurons (Figure 2.6A).

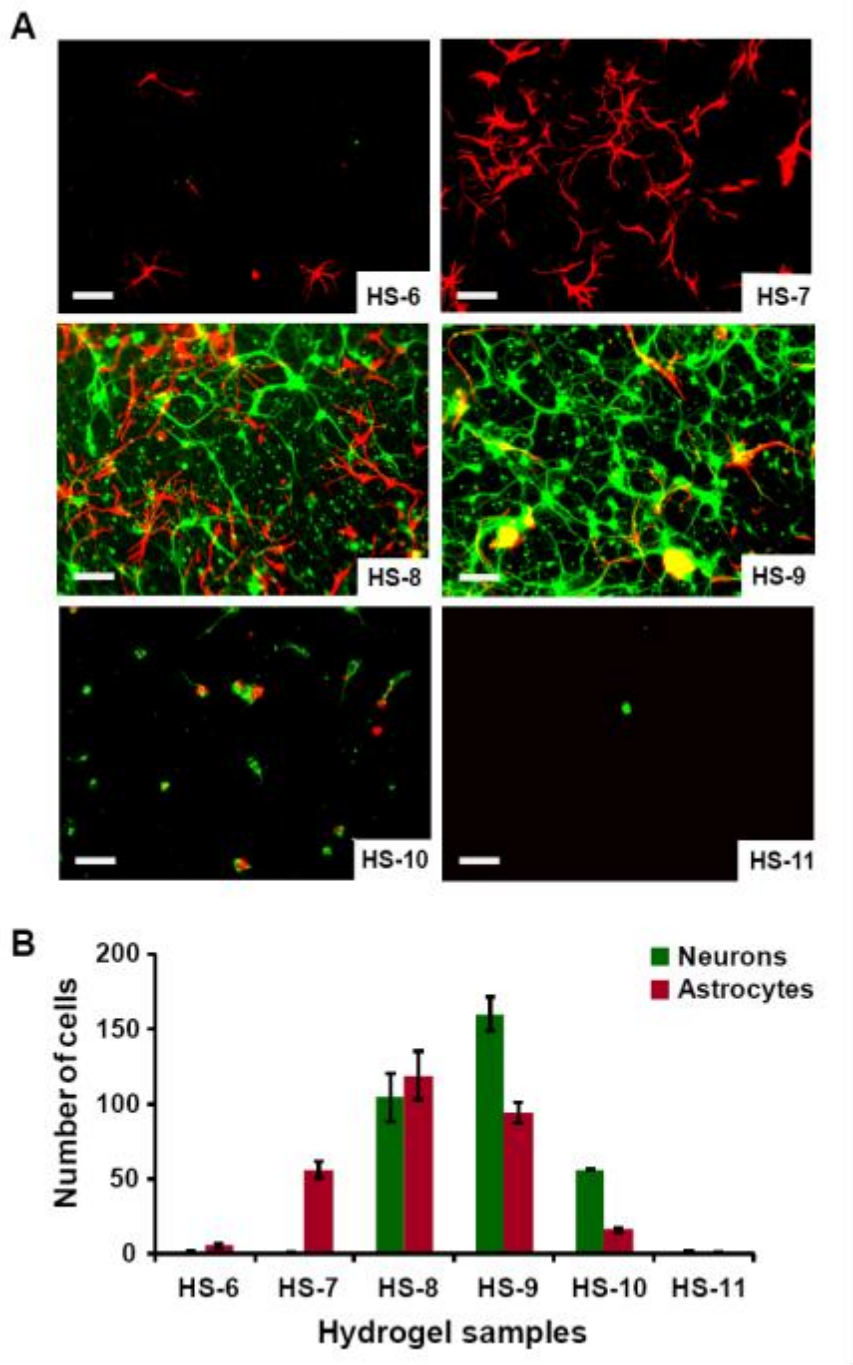

Figure 2.6: Immunocytochemistry of hydrogel samples**.** A) Immunocytochemistry performed on gel cultures demonstrates that these cells are composed of neurons (β-III-tubulin-positive cells, green) and astrocytes (GFAP-positive cells, red). Nuclei are counterstained with DAPI (blue). (Scale bar is 50 µm). B) Number of neurons (green columns) and astrocytes (red columns) grow on hydrogel samples. Cells were counted manually in five random fields of each hydrogel sample, and each sample was repeated three times in the experiments to calculate the average number of cells/field.

2.5 Discussion

In this study, using MAETAC monomers to emulate a tethered chemical structure of the neurotransmitter acetylcholine, we designed and synthesized a series of hydrogels by radical copolymerization of MAETAC and PEGMA monomers in the presence of the crosslinker EGDMA. The effects of the feed composition of monomers on physical properties of the hydrogels were systematically studied. In general, increasing the proportion of MAETAC monomers yielded increasing water content, swollen ratio and a corresponding decrease in compressive modulus in the gels. Modification of photo-crosslinkable PEGMA with MAETAC monomers improved mouse hippocampal neural cell attachment and growth in a concentration dependent manner, allowing identification of the critical concentration range of functional monomer MAETAC for brain neuronal cell survival and growth.

Most of the hydrogel samples prepared in this study are stiff, providing advantages over collagen gels or other naturally-derived soft gels. Nevertheless, the gels can easily be optimized to prepare softer gels by using different reaction systems (e.g., reduce the concentration of the monomers in the solution), or using different cross-linking methods (e.g., higher molecule weight of PEGDMA). Moreover, the results of this study have important implications for the recent interpretation that physical cues, such as substrate stiffness, are recognizable modifiers of cell behavior. Previous studies on polyacrylamide and polyethyleneglycol hydrogels have suggested that, within the same materials, softer gels greatly favored neurons, whereas harder gels promoted glial cultures [32]. Proliferation of encapsulated neural stem cells decreases with increase in the modulus of the alginate hydrogels [33], and primary neural stem cells differentiate into neurons on soft methacrylamide chitosan hydrogel [34]. Our results do not agree with those previously published reports which demonstrated that neurons favor soft rather

than stiff substrates, both neurons and astrocytes grow better on hard gels in this particular system. Although the exact mechanism of this behavior is not yet known, it is notable that the stiffnesses varied from 17 KPa to more than 120 KPa in those hydrogels, but only hard gels (HS-7 to HS-11, with similar stiffness, 122 KPa to 128 KPa) supported cellular attachment and neurite outgrowth. Each of these gels had similar porosities, swelling behaviors and mechanical properties, but with different concentrations of functional monomers. This suggests that, in these types of materials, cellular behavior is influenced to a higher degree by the chemical components than other properties of this system. While the gels are not suitable for brain implantation at this point, the gel system may find utility in other tissue engineering applications where gelation to produce stiff materials is desired, and also in cell encapsulation where cell seeding can be performed after gelation. In addition, softer hydrogel samples based on this system can be easily prepared for the application of brain implantation or cell encapsulation, and linear, soluble polymers can be prepared with the same components for substrate coating and *in vitro* cell culture studies.

While PEG based materials are normally neural and non-adhesive to protein and cells, they alone cannot provide an ideal environment to neuronal cell adhesion and growth. We demonstrate that diluting the concentration of MAETAC with non-toxic PEG based material can produce materials that have reduced cytotoxicity and even promote cell attachment and outgrowth. The results from this study also showed that hydrogels with relatively low concentration (less than 60.0% v/v or 66.2% n/n) of MAETAC have statistically reduced toxicity compared to the samples containing higher concentrations of MAETAC. Neurons grew significantly better on sample HS-9 (10.0% v/v or 12.7% n/n) among the eleven hydrogel samples prepared. It is noteworthy that cell viability increased almost 77 times just by varying

the concentration of MAETAC in the feed solution from 40.0% (v/v) to 10.0% (v/v), and these initial findings suggest that the presence of an optimal amount of MAETAC on the hydrogel surface is an important factor in the subsequent behavior of the cells that anchor on that surface and differentiate. This is in agreement with previous observations that cell attachment and survival are a function of MAETAC concentration [35]. Systematic changes in hydrogel monomer composition provide a valuable means for understanding the concentration-dependent pattern of cellular response on this type of materials. The results of the cellular studies suggested that this approach appeared to overcome the limited cell adhesion properties of PEG-based hydrogel systems.

Previous studies from other groups also showing that integrating acetylcholine-like functionalities (ALFs) in biocompatible polymers can induce specific neuronal responses, unfortunately, only few studies have been made on primary hippocampal neurons. Qin et al [36] prepared soluble biomimetic polymers with two initial monomers poly(ethylene glycol) monomethyl ether-glycidyl methacrylate (MePEG-GMA) and dimethylaminoethyl methacrylate (DMAEMA) at different ratios, the polymers were used to coat glass substrates and rat hippocampal neurons were plated onto the surfaces. The results showed that the ratio of the two initial monomers utilized for polymer synthesis significantly affects neuronal growth. The polymer surface prepared with 1:60 (mol/mol) of MePEG-GMA to DMAEMA induced neuronal growth response similar to that on poly-L-lysine. Christiane et al [37] have also incorporated ACh-like functionalities (ALFs) in a series of linear polymers based on diglycidylsebacate, leucine ethyl ester, and aminoethyl acetate. The polymers were also coated onto glass coverslips, and results showed that ALFs had a profound impact on sprouting and neurite extension of dorsal root ganglia (DRG) cells in a concentration-dependent manner, the polymer with 70%

ALF induced regenerative responses similar to laminin. Compared to these two previous studies, our results showed that the amount of MAETAC needed to promote neuronal cell attachment and growth is very low (~10% of MAETAC). This might be because, in both previous studies, ACh-like functionalities were derived from the tertiary amine group. At neural pH, only a fraction of these amine groups will be protonated which therefore offer a close mimicry of the acetylcholine structure, while the quaternary amine groups present in the acetylcholine structure and MAETAC are permanently charged. Also, since acetylcholine is an ester of acetic acid and choline, keeping the complete original chemical structure is essential for its functions. This may cause some major differences in cell behaviors on these polyelectrolytes.

Because each sample showed different numbers and types of cells, comparing neuronal morphology by using traditional statistical analysis methods, such as measuring the lengths of neurites, cannot be correctly applied among those samples. But the fluorescence micrographs illustrate some significant differences: neurons on HS-9 seemed much healthier and exhibited longer processes as compared to all the other samples. Also, since hydrogels provided bulky 3-D scaffolds as compared to thin monolayers of polymers coated on a substrate to encourage cell adhesion, it is difficult to directly compare the results in this work to standard neuron culture substrates, such as poly-lysine or laminin-coated glass coverslips. However, soluble polymer can easily be prepared using similar methods reported in this work without adding crosslinking EGDMA. Since MAETAC is permanently charged, which enhances the electrostatic interaction with glass surfaces, the soluble polymer can be used to coat glass coverslips simply by dipping method. Comparing hippocampal neuronal cell viability and morphologies on different coated substrates will be an area of interest for future work.

2.6 Conclusion

Systematic changes in hydrogel monomer composition provide a simple and valuable means for discovering bioactive materials. The hydrogels containing tethered acetylcholine-like functional structures described in this study represent promising clues for the future design of candidate scaffolds for neural tissue engineering and regenerative medicine applications. The critical concentration range of functional monomer MAETAC in the system was identified for brain neuronal cell culture, and this knowledge is critical to optimize the current system. For example, softer hydrogel samples based on this system can be easily prepared for the application of brain implantation or cell encapsulation, and linear, soluble polymers can be prepared with the same components for substrate coating and *in vitro* cell culture studies. Since sample HS-7 favored astrocytic attachment and growth while HS-9 and HS-10 favored neuron attachment and growth specifically, selectively culturing astrocytes or neurons is also possible by properly modifying physical and chemical properties of these types of hydrogels. Furthermore, because of the rich chemistry of the free hydroxyl groups present in the PEGMA monomer, those synthetic hydrogels can be readily modified with other functionalities, such as by linking nerve growth factor, covalently bonding extracellular matrix (ECM) proteins or peptides, etc., for applications such as tissue engineering, which is also a focus of future work.

Acknowledgments

We would like to acknowledge Dr. Ray Molloy and Professor Manfred Lindau for the initial cell studies. We would also like to acknowledge the use of the Microscopy and Imaging Facility at Cornell University and its facility manager, Carol Bayles, and the use of the electron microscope and the dynamic mechanical analyzer housed in the Cornell Center for Materials Research (CCMR), Shared Experimental Facilities, supported through the National Science Foundation Materials Research Science and Engineering Center Program (DMR-0520404) and the facility managers, John Hunt and Yuanming Zhang. We also acknowledge the assistance of the NHLBI DIR Light Microscopy Core Facility. This work was partially supported by NIH NSR01-044287 and by the Nanobiotechnology Centre (NBTC), an STC program of the National Science Foundation under agreement no. ECS-9876771, as well as the NHLBI Division of Intramural Research (P.Y. and H.M.G).

REFERENCES

[1] Nisbet DR, Crompton KE, Horne MK, Finkelstein DI, Forsythe JS. Neural tissue engineering of the CNS using hydrogels - a review. J Biomed Mater Res Part B Appl Biomater 2008;87:251-63.

[2] Constans A. Neural tissue engineering. Scientist 2004;18:40-2.

[3] Schmidt CE, Leach JB. Neural tissue engineering: strategies for repair and regeneration. Annu Rev Biomed Eng 2003;5:293-347.

[4] Subramanian A, Krishnan UM, Sethuraman S. Development of biomaterial scaffold for nerve tissue engineering: biomaterial mediated neural regeneration. J Biomed Sci 2009;16:108-19.

[5] Woerly S, Plant GW, Harvey AR. Neural tissue engineering: from polymer to biohybrid organs. Biomaterials 1996;17:301-10.

[6] Peppas NA, Sahlin JJ. Hydrogels as mucoadhesive and bioadhesive materials: a review. Biomaterials 1996;17:1553-61.

[7] Hejcl A, Lesny P, Pradny M, Michalek J, Jendelova P, Stulik J, et al. Biocompatible hydrogels in spinal cord injury repair. Physiol Res 2008;57:S121-S32.

[8] Zhong YH, Bellamkonda RV. Biomaterials for the central nervous system. J R Soc Interface 2008;5:957-75.

[9] Yu TT, Shoichet MS. Guided cell adhesion and outgrowth in peptide-modified channels for neural tissue engineering. Biomaterials 2005;26:1507-14.

[10] Geckil H, Xu F, Zhang XH, Moon S, Demirci U. Engineering hydrogels as extracellular matrix mimics. Nanomedicine 2010;5:469-84.

[11] Zhu JM. Bioactive modification of poly(ethylene glycol) hydrogels for tissue engineering. Biomaterials 2010;31:4639-56.

[12] Yu LMY, Leipzig ND, Shoichet MS. Promoting neuron adhesion and growth. Mater Today 2008;11:36-43.

[13] Snyder SH. Turning off neurotransmitters. Cell 2006;125:13-5.

[14] Stevens CF. Neurotransmitter release at central synapses. Neuron 2003;40:381-8.

[15] Gao J, Kim YM, Coe H, Zern B, Sheppard B, Wang YD. A neuroinductive biomaterial based on dopamine. Proc Natl Acad Sci USA 2006;103:16681-6.

[16] Saifuddin U, Vu TQ, Rezac M, Qian HH, Pepperberg DR, Desai TA. Assembly and characterization neurotransmitter-immobilized of biofunctional surfaces for interaction with postsynaptic membrane receptors. J Biomed Mater Res A 2003;66A:184-91.

[17] Vu TQ, Chowdhury S, Muni NJ, Qian HH, Standaert RF, Pepperberg DR. Activation of membrane receptors by a neurotransmitter conjugate designed for surface attachment. Biomaterials 2005;26:1895-903.

[18] Darr A, Calabro A. Synthesis and characterization of tyramine-based hyaluronan hydrogels. J Mater Sci Mater Med 2009;20:33-44.

[19] Bernardini N, Tomassy GS, Tata AM, Augusti-Tocco G, Biagioni S. Detection of basal and potassium-evoked acetylcholine release from embryonic DRG explants. J Neurochem 2004;88:1533-9.

[20] Whitteridge D. The role of acetylcholine in synaptic transmission - a critical review. J of Neurol Neurosurg Psychiatry 1948;11:134-40.

[21] Lecchi M, McIntosh JM, Bertrand S, Safran AB, Bertrand D. Functional properties of neuronal nicotinic acetylcholine receptors in the chick retina during development. Eur J Neurosci 2005;21:3182-8.

[22] Small DH, Reed G, Whitefield B, Nurcombe V. Cholinergic regulation of neurite outgrowth from isolated chick sympathetic neurons in culture. J Neurosci 1995;15:144-51.

[23] Tata AM, Cursi S, Biagioni S, Augusti-Tocco G. Cholinergic modulation of neurofilament expression and neurite outgrowth in chick sensory neurons. J Neurosci Res 2003;73:227-34.

[24] Kim SJ, Park SJ, Kim SI. Swelling behavior of interpenetrating polymer network hydrogels composed of poly(vinyl alcohol) and chitosan. React Funct Polym 2003;55:53-9.

[25] Park H, Guo X, Temenoff JS, Tabata Y, Caplan AI, Kasper FK, et al. Effect of swelling ratio of injectable hydrogel composites on chondrogenic differentiation of encapsulated rabbit marrow mesenchymal stem cells in vitro. Biomacromolecules 2009;10:541-6.

[26] Woerly S, Fort S, Pignot-Paintrand I, Cottet C, Carcenac C, Savasta M. Development of a sialic acid-containing hydrogel of poly[N-(2-hydroxypropyl) methacrylamide]: Characterization and implantation study. Biomacromolecules 2008;9:2329-37.

[27] Brewer GJ, Torricelli JR, Evege EK, Price PJ. Optimized survival of hippocampal-neurons in B27-supplemented neurobasal, a new serum-free medium combination. J Neurosci Res 1993;35:567-76.

[28] Zohuriaan-Mehr MJ, Kabiri K. Superabsorbent polymer materials: a review. Iran Polym J 2008;17:451-77.

[29] Dadhaniya PV, Patel MP, Patel RG. Swelling and dye adsorption study of novel superswelling [acrylamide/N-vinylpyrrolidone/3(2-hydroxyethyl carbamoyl) acrylic acid] hydrogels. Polym Bull 2006;57:21-31.

[30] Kioussis DR, Kofinas P. Characterization of anion diffusion in polymer hydrogels used for wastewater remediation. Polymer 2005;46:9342-7.

[31] Guarnieri D, De Capua A, Ventre M, Borzacchiello A, Pedone C, Marasco D, et al. Covalent immobilized RGD gradient on PEG hydrogel scaffold influences cell migration parameters. Acta Biomater 2010;6:2532-9.

[32] Saha K, Keung AJ, Irwin EF, Li Y, Little L, Schaffer DV, et al. Substrate modulus directs neural stem cell behavior. Biophys J 2008;95:4426-38.

[33] Banerjee A, Arha M, Choudhary S, Ashton RS, Bhatia SR, Schaffer DV, et al. The influence of hydrogel modulus on the proliferation and differentiation of encapsulated neural stem cells. Biomaterials 2009;30:4695-9.

[34] Leipzig ND, Shoichet MS. The effect of substrate stiffness on adult neural stem cell behavior. Biomaterials 2009;30:6867-78.

[35] Sosnik A, Sefton MV. Poloxamine hydrogels with a quaternary ammonium modification to improve cell attachment. J Biomed Mater Res A 2005;75A:295-307.

[36] Tu Q, Li L, Zhang YR, Wang JC, Liu R, Li ML, et al. The effect of acetylcholine-like biomimetic polymers on neuronal growth. Biomaterials 2011;32:3253-64.

[37] Gumera CB, Wang Y. Modulating neuronal responses by controlled integration of acetylcholine-like functionalities in biomimetic polymers. Adv Mater 2007;19:4404-9.

CHAPTER THREE

BIOMIMETIC POLYMER BRUSHES CONTAINING TETHERED ACETYLCHOLINE NEUROTRANSMITTERS FOR PROTEIN AND HIPPOCAMPAL NEURONAL CELL PATTERNING

ABSTRACT

This paper describes a method to control neuronal cell adhesion and differentiation with both chemical and topographic cues by using a spatially defined polymer brush pattern. First, biomimetic polymer brushes containing tethered neurotransmitter acetylcholine functionalities and free hydroxyl-terminated poly(ethylene glycol) (PEG) units were prepared using the "grown from" method through surface-initiated atom transfer radical polymerization (SI-ATRP) reactions. The surface properties of the resulting brushes were thoroughly characterized with various techniques and hippocampal neuronal cell culture on the brush surfaces exhibit cell viability and differentiation comparable to, or even better than, those on commonly used poly-L-lysine coated glass coverslips. The polymer brushes were then patterned *via* UV photolithography techniques to provide specially designed surface features with different sizes (varying from 2 μm to 200 μm) and orientations (horizontal and vertical). Protein absorption experiments and hippocampal neuronal cell culture tests on the brush patterns showed that both protein and neurons can adhere to the patterns and therefore be guided by such patterns. These results also indicate that, because of their unique chemical composition and well-defined nature, the developed polymer brushes may find many potential applications in cell-material interactions studies and neural tissue engineering.

Keywords: Polymer brushes, surface-initiated atom transfer radical polymerization, acetylcholine functionality, photolithography, neuronal cell patterning.

3.1 Introduction

In recent years, neural tissue engineering has rapidly emerged as a new field in central nervous system (CNS) therapeutics and has achieved much success [1]. It applies tissue engineering principles to therapy, and focuses on regulation of cell behavior and tissue progression through the implantation of foreign substances. The implanted materials have to meet certain criteria to be successfully integrated into the surrounding biological environments. First of all, they should provide appropriate chemical and physical properties that are analogous to the natural extracellular microenvironments to support neuronal cell adhesion and growth, such as proper biochemical factors, wettability, degradation rate, porosity, and mechanical strength. Synthetic polymers are attractive for this research area because many of their properties are controllable and they can also be further optimized for particular applications. To date, a wide variety of synthetic polymers with various chemical functionalities have been explored for CNS applications [2,3], some successful examples include PEG based materials, polyglycolic acid (PGA), and biomaterials containing functional bioactive components such as extracellular matrix (ECM) peptides and neurotrophic factors. Surface topography of the materials has been considered as another important factor that can directly influence neuron cellular behaviors, including adhesion, morphology, proliferation and differentiation [4,5]. Recently, there has been a surge of interest in creating patterned surfaces with techniques derived from microelectronics processes to provide well-defined surface architecture and geometry, thereby achieve a high-degree control over cell adhesion and induce formation of neuronal networks on material surfaces. For example, photolithographic techniques have been used for patterning neuronal cells at sub-cellular dimensions [6,7], and offer valuable new approaches for more fundamental studies of *in vitro* cell-surface and cell-cell interactions.

The application of micro-fabrication technology in neuronal tissue engineering has also stimulated interest and experiments in the development of a wide range of prosthetic and medical devices. However, many electrodes are limited in their long-term effectiveness due to their inability to effectively and chronically interface with host nervous tissue. Thus, research has been actively developing strategies to introduce thin films of synthetic polymers to tailor surface characteristics of those devices while maintaining their bulk properties. Polymer solution deposition, spin or spray coating, and self-assembled monolayers (SAM) are most commonly used methods to prepare polymer thin films [8]. Alternatively, polymer chains can be covalently attached to the substrate at one end to form polymer brushes [9]. The advantage of polymer brushes over other surface modification methods is their excellent mechanical and chemical robustness, at the same time offer unique physical properties to the substrates since the other end of the polymer chains may freely move in solution. They also provide a high degree of synthetic flexibility towards the introduction of a variety of functional groups. In particular, surface-initiated atom transfer radical polymerization polymerization (SI-ATRP) reactions can tolerate a wide range of functional monomers and be conducted under less stringent experimental conditions, they have become the most popular routes to control the functionality, density and thickness of the polymer brushes with near molecular precision [10]. Many specific material properties can be further amplified by this surface preparation method. For example, poly(PEGMA) brushes prepared by SI-ATRP method have been demonstrated to be "non-fouling" [11]. The brushes have been shown to be exceptionally resistant to the adsorption of adhesive proteins such as fibronection as well as protein complexes and concentrated protein mixtures such as fetal bovine serum (FBS), and to be able to prevent nonspecific cell adhesion for up to 30 days.

Another advantage of using polymer brushes over other coating methods is their compatibility with a wide range of micro- or nanofabrication techniques that can be used for cell patterning. The choice of chemical composition on the patterns is critical for both background (or off-pattern region) and foreground (or on-pattern regions) [4,7]. Non-adhesive materials, such as PEG based materials, were often used for the background filling to reduce nonspecific protein adsorption and cell adhesion. For the on-patterned region, rationally designed biomaterials with proper information contents and functionalities should be present in order to direct appropriate cellular activities, and one way to achieve such bioactivity is to integrate biomolecules into polymers. For example, surface-tethered neurotransmitters can activate the corresponding cellular receptors and induce specific neuronal responses [12-14]. In particular, acetylcholine (ACh, 2-Acetoxy-N,N,N-trimethylethanaminium) is one of the most important and interesting neurotransmitters in CNS, and has shown to regulate neuronal development and enhance neurite outgrowth *in vivo* [15]. Structural mimetics of acetylcholine, such as aminoethyl acetate and dimethylaminoethyl methacrylate (DMAEMA), have been used to prepare soluble polymers. Those tertiary amines can be protonated and become positively charged at neutral pH, therefore provide properties similar to acetylcholine and promote neurite sprouting and extension of dorsal root gnanglia (DRG) [14] or rat hippocampal neurons [16]. In other studies, permanently positively charged quaternary ammonium salts (QAS), such as (2-methacryloyloxy)ethyl-trimethylammonium chloride (MAETAC), have been used to provide chemical structures that more closely mimic that of acetylcholine [12,17], and to improve neuronal cell attachment on surfaces. The approaches of using MAETAC are better alternatives because they are pH-independent and can represent the entire functional structure of acetylcholine in a polymer system. However, those charged molecules have to be used at low concentration and combined

with more biocompatible components (e.g., polyethylene glycol fumarate, poloxamine, PHEMA or PEG) due to their acute cytotoxic effects [14,16,18-20]. In addition, in those previous studies, acetylcholine functionalities and their structural mimetics were either embedded in cross-linked hydrogels or incorporated in linear soluble polymers. Those polymers often lack flexibility and/or stability in CNS applications, especially when used as prosthetic device coatings. Unfortunately, to the best of our knowledge, there is currently no acetylcholine and PEG based copolymers were prepared in polymer brush forms for neuronal cell studies, despite many advantages that polymer brushes can offer in this area, such as stability, uniformity, well controlled structures, and readiness to be patterned using photolithography techniques.

In this study, to further explore the potential of biomimetic materials containing acetylcholine functionalities in neural tissue engineering, particularly the possibility of modulating the attachment and growth of primary hippocampal neurons on those synthetic materials, we prepared poly(PEGMA-*ran*-MAETAC) random copolymer brushes using SI-ATRP reactions on silicon substrates. The chemical structure of synthesized polymer brushes includes tethered "bio-active" acetylcholine segments (2-Acetoxy-N,N,N-trimethylethanaminium) to alter the "non-fouling" properties of poly(PEGMA) polymer brushes and to promote neuronal cell attachment, and the "bio-inert" poly(ethylene glycol) units in the polymer brushes were chosen to provide good biocompatibility and regulate nerve cell interaction with the surfaces. The aim of this study is to determine the effects of the acetylcholine functionalized PEG polymer brushes and their topography on neuronal cell behaviors, the knowledge gained from the study could provide us with a better understanding of cell-surface interactions on this specific type of material.

3.2 Materials and Methods

3.2.1 Materials

To prepare poly(PEGMA-*ran*-MAETAC) brushes from PEGMA and MAETAC monomers and pattern the brushes, allyl 2-bromo-2-methylpropionate, chlorodimethylhydrosilane, Pt on activated carbon (10 wt %), triethylamine, CuBr, $CuBr_2$, 2,2′-bipyridine, poly(ethylene glycol) methacrylate (PEGMA, Mw = 360) and a 75% w/v aqueous solution of 2-methacryloxyethyl trimethylammonium chloride (MAETAC) were purchased from Sigma-Aldrich. 2-methoxy(polyethylenoxy)propyltrichlorosilane (PEG-silane, $CH_3O(CH_2CH_2O)_{6\text{-}9}(CH_2)_3SiCl_3$, 90%) was purchased from Gelest, U.S.A. Silicon wafers were purchased from Platypus Technologies, U.S.A. For protein absorption tests, hippocampal neuronal culture and staining experiments, FITC-labelled BSA, poly-L-lysine (PLL), paraformaldehyde, phosphate buffered saline (PBS, pH 7.4), normal goat serum (NGS), 0.1% Triton-X100, mouse monoclonal anti-β-tubulin III antibodies were purchased from Sigma-Aldrich. Neurobasal-A, B27, trypsin were purchased from Gibco, U.S.A. LIVE/DEAD viability/cytotoxicity assay kit was from Invitrogen, U.S.A. Alexa Fluor® 488 goat anti-mouse IgG and Alexa Fluor® 568 goat anti-rabbit IgG, and DAPI were obtained from Molecular Probes, U.S.A. All solvents used were purchased from Sigma-Aldrich, and all the chemicals were used without further purification unless otherwise noted.

3.2.2 Preparation of Poly(PEGMA-*ran*-MAETAC) Brushes through SI-ATRP

ATRP initiator (3-(chlorodimethylsilyl)propyl 2-bromo-2-methylpropionate was synthesized and immobilized to substrates as previously reported [21]. To prepare polymer brushes, silicon wafers covered with initiator were cut into 1 × 2 cm pieces and placed in a dry

Schlenk tube. (57.4 mg, 0.4mmol), $CuBr_2$ (9.0 mg, 0.04mmol), and anhydrous 2,2′-bipyridine (156.8 mg, 1.0 mmol) were added to another dry Schlenk tube equipped with a magnetic stir bar. Both flasks were evacuated and purged with nitrogen three times, 10-15 min each time. PEGMA (3.6 mL, 11.0 mmol) and MAETAC (0.4 mL, 1.6 mmol) monomers were flowed through the inhibitor removal column (Aldrich Chemical Co.) before mixing with isopropanol (3.6 mL) and DI water (2.4 mL). The reaction mixtures were then bubbled with nitrogen gas for at least 30 min and transferred into the Schlenk tube with copper catalysts using a clean cannula. The mixture was stirred at room temperature under nitrogen for about 10 min before being transferred into the other Schlenk tube with initiator attached silicon substrates. Polymerization was carried out at room temperature for 5 h, after which the substrates were taken out of the solution, rinsed thoroughly with DI water and isopropanol, and blown dry with nitrogen gas.

3.2.3 Polymer Brush Surface Characterization

Water contact angles were measured using a contact angle goniometer (Ramé-Hart NRL C.A. model 100-00 115) at room temperature. Three measurements from different locations on the sample were recorded, and the data was reported as Mean $\pm$ SD. The thickness of polymer brushes was measured using an imaging ellipsometer (Nanofilm EP3) at a fixed angle of incidence (65 degrees) and wavelength (401-711 nm) mode. A Cauchy model/silicon oxide/silicon stack model was used to fit the data, in which the Cauchy parameter of poly(methyl methyacrylate) (PMMA) represented the polymer brush. Three different points were measured for each sample and the average and standard deviation were calculated. The topography of the polymer brush modified silicon surfaces was measured by atomic force microscopy (AFM) using a Dimension Icon AFM (Bruker Corporation, Karlsruhe, Germany). An area of 5 x 5 μm was

scanned using tapping mode, the drive frequency was 357.5 KHz, and the voltage was between 4.0 and 4.5 V. The drive amplitude was 64.1mV and the scan rate was 0.996 Hz. An arithmetic mean of the surface roughness (*Ra*) was calculated from the roughness profile determined by AFM.

Polymer brush-modified silicon wafers were also characterized by attenuated total reflectance Fourier transform infrared (ATR-FITR) spectroscopy using a VERTEX 80v and PIKE technologies VeeMAX II accessory equipped with a germanium crystal. A nitrogen cooled MCT detector was used and a ZnSe polarizer was set for parallel (p) polarization. Before collecting data, the system was left in vacuum for 10 min to minimize signal noise from air. The spectra were measured under reduced pressure (less than 3 hPa) and data was collected using 1024 scans with 4 cm^{-1} resolution. A spectrum from a freshly cleaned silicon wafer was used to determine the background signal.

X-ray photoelectron spectroscopy (XPS) measurements were performed using a Kratos Axis Ultra Spectrometer (Kratos Analytical, Manchester, UK) with a monochromatic Al Ka X-ray source (1486.6 eV) operating at 225 W under a vacuum of 1.0 - 10^8 Torr. The pass energy of the analyzer was set at 20 eV and the spectra were analyzed using Casa XPS v.2.3.14 software. The C-C peak at 285 eV was used as the reference for binding energy calibration. Near Edge X-Ray Absorption Fine Structure (NEXAFS) spectroscopy experiments were carried out on the U7A NIST/Dow materials characterization end station at the National Synchrotron Light Source at Brookhaven National Laboratory (BNL). The details of this experimental geometry and illustration of the setup have been reported previously [22]. The peak position of the lowest π^* phenyl resonance from polystyrene (285.5 eV) was used to calibrate the photon energy.

3.2.4 Patterning of Polymer Brushes by Photolithography

Poly(PEGMA-*ran*-MAETAC) brushes were patterned on silicon surface using photolithography as shown in Scheme 2. The silicon wafer was treated with freshly prepared piranha solution for 1 h and then cleaned with water, isopropanol and blown dry under nitrogen gas. Self-assembled monolayer of PEG silane was used as a non-adhesive backfill for the pattern. The clean wafer was immersed in a 1% (v/v) solution of the PEGylated silane in anhydrous toluene containing catalytic amounts of triethylamine overnight at room temperature, followed by rinsing with anhydrous ethanol and drying with nitrogen. After PEG-saline deposition, S1813 positive tone photoresist (Shipley) was spin-coated onto the PEG-functionalized silicon wafer at 3000 rpm for 60 sec, and soft baked at 115 °C for 1 min, resulting in a film about 1 μm thick. The wafer was then exposed to UV light (λ = 415 nm, 17 mW/cm^2) through patterned photo mask for 2 sec using an ABM contact aligner. After development in a tetramethylammonium hydroxide solution (AZ 300 MIF), the exposed PEG regions were etched using a Harrick oxygen plasma cleaner (PDC-32G) for 2 min.

The PEG backfilled substrate was immersed in a hexane solution of the ATRP initiator (5 mM) with catalyst amount of pyridine. The reaction was carried out at room temperature under the protection of nitrogen for 24 h. The remaining photoresist was stripped off using acetone. The initiator immobilized wafer was then cleaned with ethanol, water and acetone sequentially, and blown dried with nitrogen. The patterned surface with initiator was used immediately in the next step of surface-initiated polymerization to grow polymer brushes as described in the previous section (Sec. 2.2).

3.2.5 Protein Absorption on Patterned Polymer Brushes

Protein adsorption of the patterned surfaces was tested against FITC-labeled BSA (0.1 mg/ml in PBS buffer) at room temperature. After 2 hours the patterned silicon wafer was taken out of protein solution and rinsed with deionized water and immediately analyzed with a fluorescence microscope (BX51, Olympus, Japan). Images were recorded using a Cool Snap hx CCD camera (Roper Scientific) with an LMPlan FI 10x dry objective lens (excitation, 470 nm; emission, 525 nm). The fluorescence intensities were processed with Image-Pro Plus (Media Cybernetics, Inc., Bethesda, MD) software.

3.2.6 Primary Mouse Hippocampal Neuronal Cell Culture

Animal experiments were carried out according to the institutional animal care procedures. The polymer brush coated wafer samples were sterilized in 75% ethanol 5 h before use. Primary hippocampal neuronal cultures were prepared by Dr. Panpan Yu (NIH, Dr. Herbert M. Geller's lab) through enzymatic dissociation of hippocampi removed from postanatal day 0 mouse pups as previously described [18]. Briefly, hippocampi were dissected out, chopped into small pieces and digested with 0.125% trypsin. After digestion, a single cell suspension was prepared by trituration. The cells were plated at a density of 40,000 cells/mL onto the brush samples, and then cultured in Neurobasal-A medium supplemented with B27 and maintained for 3 days at 37°C before fixation. PLL coated glass slides were used as control in these experiments and followed the same cell culture procedure. All cell culture experiments were carried out in 24 well culture plates, and each experiment repeated 3 times.

3.2.7 Cell Viability, Immunostaining, and Statistical Analysis

Cell viability was measured using the standard LIVE/DEAD Viability/Cytotoxicity Assay Kit from Invitrogen. After 3 days of culture, each brush sample was placed in 1 mL growth media with 0.5 µL calcein and 2 µL ethidium homodimer, and incubated at 37°C for 20 min. Cell attachment and viability were visualized using an Eclipse 800 (Nikon Instruments Inc., Melville, NY) fluorescence microscope. Five random fields of each sample were imaged on both green and red channels and the number of live and dead cells was counted manually for each image. The number of live cells divided by the total number of live and dead cells was defined as the fractional viability.

All immunostaining experiments were carried out at room temperature. Cells on polymer brush samples and PLL coated glass cover slides were fixed after three days of culture with 4% paraformaldehyde in PBS buffer. The samples were then prepared for immunostaining by blocking and permeabilizing in 10% NGS and 0.1% Triton-X100 in PBS (v/v, PBS-T) for 1 h, followed by incubation with the primary antibodies of monoclonal mouse anti-β-tubulin III (1:1000) and polyclonal rabbit anti-GFAP (1:1000) (diluted in PBS-T buffer containing 2% NGS) for 2 h. The cells were then incubated for 1 h with secondary antibodies AlexaFluor®488-conjugated goat anti-mouse IgG (1:1000) and Alexa Fluor®568-conjugated goat anti-rabbit IgG (1:1000) diluted in PBS-T containing 2% NGS, followed by incubation with nuclear counterstain with DAPI (1:1000) in PBS buffer for 5 min at room temperature. After thoroughly rinsing with PBS buffer, cell culture samples were imaged using the fluoresence microscope. The number of cells was counted manually for each image using ImageJ to determine the number of neurons and astrocytes at each random field. Estimation of neurite outgrowth was determined by manually counting intersections of neurites with test lines of an unbiased

counting frame (horizontal lines, area per point of 0.5 inch^2), the resulting ratio of intersections of neurites to neuron cells was calculated as relative neurite length [23]. Each experiment was repeated three times. Statistical analyses were performed by one-way ANOVA followed by Turkey post hoc test. Results were considered statistically significant if $p<0.05$ and marked with asterisks.

3.3 Results

3.3.1 Preparation and Characterization of Poly(PEGMA-*ran*-MAETAC) Brushes

Poly(PEGMA-*ran*-MAETAC) brushes were synthesized on silicon substrates using the surface initiated atom transfer radical polymerization (SI-ATRP) method, and only small amount of MAETAC was used (10% v/v) to prepare the polymer brushes to avoid its cytotoxic effects [12,19]. The reaction was carried out in two steps (Figure 3.1A). In the first step, ATRP initiator was covalently attached to a clean silicon surface freshly treated in piranha solution to form a self-assembled monolayer (SAM). The modified surface became more hydrophobic compared to the bare silicon surface (static water contact angles are less than 10º), with the static water contact angles of 65º (SD $\pm$ 2º) after the reaction. In the second step, random copolymerization of PEGMA and MAETAC monomers was carried out under oxygen-free conditions at room temperature, and CuBr/bipyridine was used as a catalyst. After 5 hours of reaction at room temperature, the surfaces were cleaned with water and isopropanol. Static water contact angle measurements showed that the brush modified surfaces are more hydrophilic compared to the ATRP initiator modified surfaces in the first reaction step, with water contact angles of 47º (SD $\pm$ 3º). Ellipsometry measurement showed that the brush thickness was 21 $\pm$2 nm. An AFM microscope was used to investigate the surface topography and roughness (Figure 3.1B). The

polymer brushes gave a relatively smooth surface and the arithmetic average roughness (R_a) measured over an area of 5 × 5 µm was estimated to be ~ 3 ± 1.8 nm.

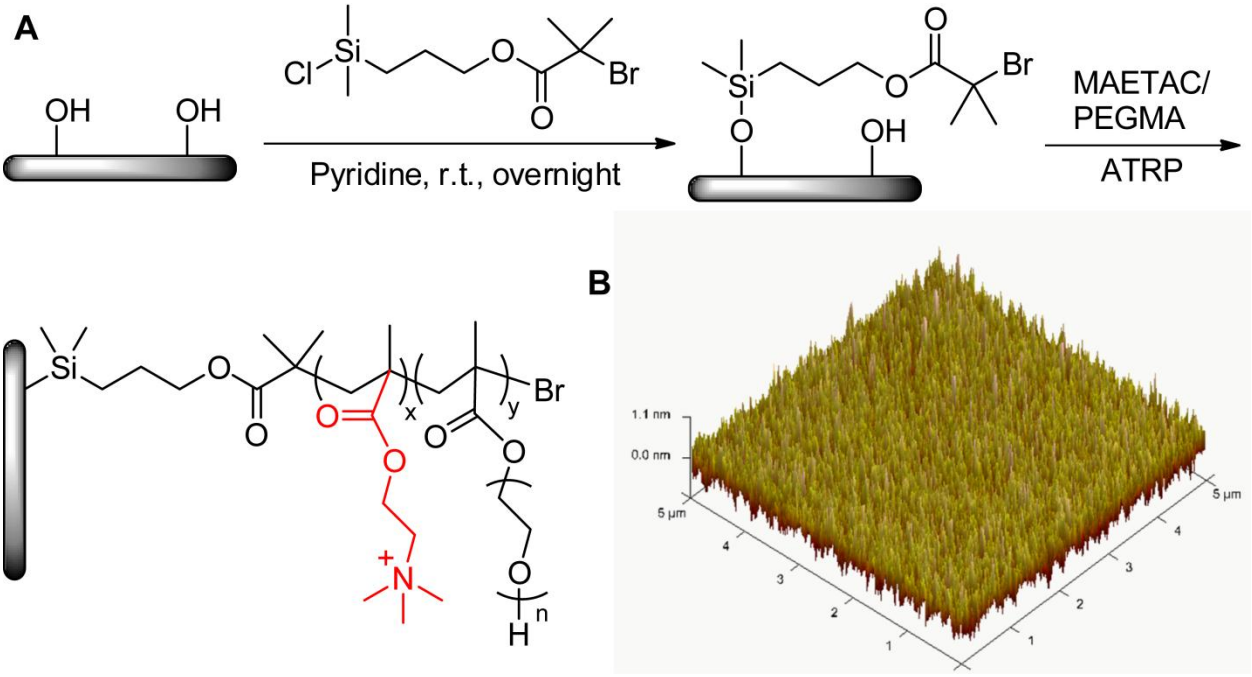

Figure 3.1: Synthesis and AFM image of polymer brushes. A) Schematic representation of initiator attachment to silicon surface and polymerization of monomers using a surface-initiated ATRP approach. Chemical structure of tethered acetylcholine was also highlighted (red) in the resulting polymer brushes. B) AFM image of poly(PEGMA-*ran*-MAETAC) brushes on silicon substrate (5 µm × 5 µm, *Ra* = 3±1.8 nm).

ATR-FTIR was used as an additional tool to characterize the substrate surface (Figure 3.2A). The presence of a strong absorption band at 1724 cm^{-1} is characteristic of a saturated ester carbonyl group stretching (–C=O), while the absorption region at 1121 cm^{-1} arises from the stretching of the C–O–C group in PEG units. The band at 2869 cm^{-1} is an aliphatic –C–H stretching vibration, and the broad absorption at 3200-3600 cm^{-1}corresponds to the –OH absorption on the PEG unit. Overall, the FTIR spectrum provided evidence that supports the formation of the target polymer brush on the silicon surface.

To fully characterize the surface chemistry of poly(PEGMA-*ran*-MAETAC) brushes, the presence of the brushes on the silicon surface was also evaluated by XPS analysis. An XPS wide scan examination and C1*s* core-level spectra of the brush surfaces are shown in Figure 2B. The C1*s* core-level spectrum (Fig. 3.2B, right) can be curve-fitted with three peak components having binding energies at 284.5, 286.2, and 288.5 eV, attributable to the C–C, C–O, and O=C–O species, respectively. The binding energy near 400.0 eV shown in the XPS wide scan (Figure 3.2B left) corresponds to quaternized nitrogen. In addition, NEXAFS has been described as a powerful tool to characterize a nitrogen containing compound [24]. Figure 3.2C shows the normalized carbon and nitrogen K edge NEXAFS spectra of the brush. The small resonance peak near 287.7 eV can be attributed to the C 1s$\rightarrow\pi^*_{C=O}$ signal. The characteristic signals at 291.4 eV is the C 1s$\rightarrow\sigma^*_{C-H}$, and a strong peak at 295.4 eV can be easily seen for this surface, they are indicative of the C 1s$\rightarrow\sigma^*_{C-O}$ resonances, demonstrating the PEG containing side chain groups dominating the surface [22,25]. The tall peak at 412.8 eV corresponds to the N 1s$\rightarrow\sigma^*_{C-N}$ transition in the nitrogen K edge. Spectra from four different angles (20°, 60°, 90°, 120°) were found to be identical and indicate that there is no specific orientation on this random polymer brush surface, in other words, the polymer brushes provide a surface with uniform chemical composition.

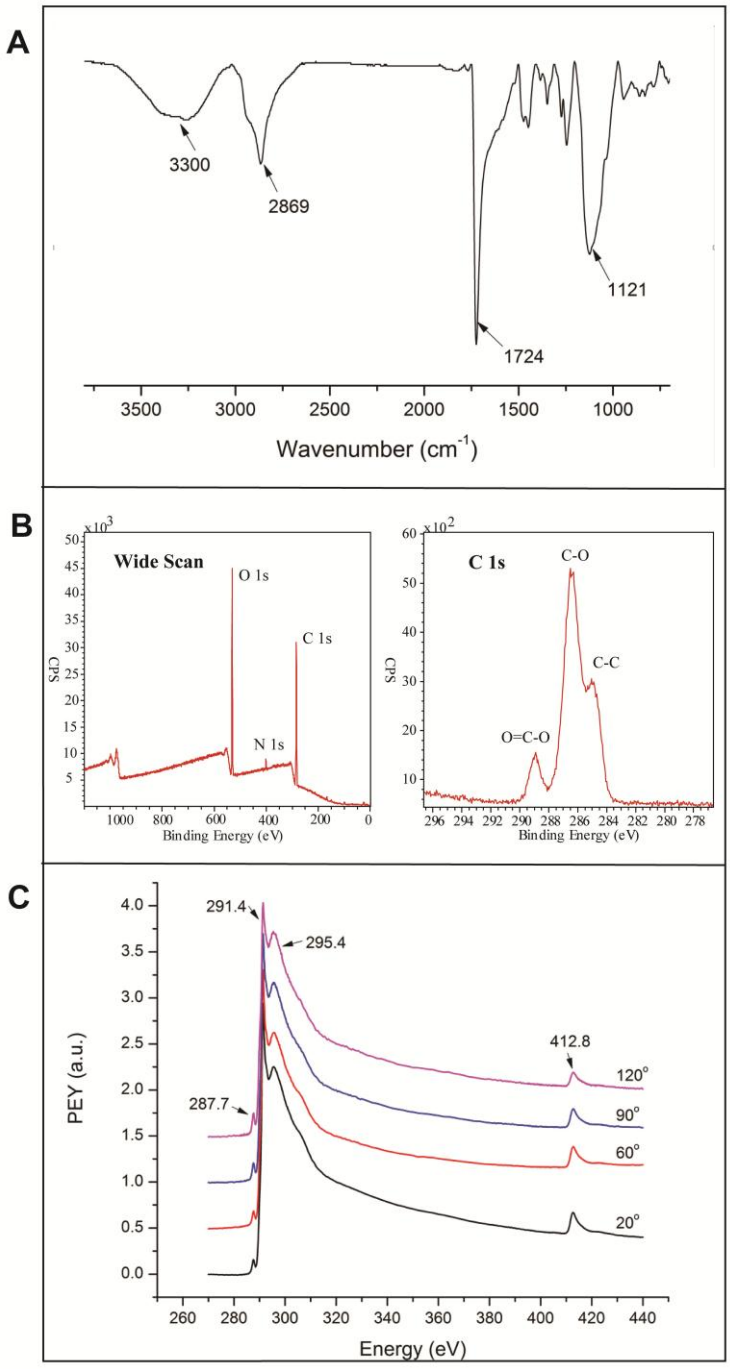

Figure 3.2: Physical characterization of polymer brushes**.** Characterization of poly(PEGMA-*ran*-MAETAC) brushes on silicon substrate. A) ATR-FTIR reflectance spectrum under nitrogen atmosphere. B) XPS wide scan (left) and C1s core level spectrum of the polymer brushes. C) NEXAFS spectra of brushes on silicon wafer at four different angles.

3.3.2 Polymer Brush Modified Silicon Surfaces for Hippocampal Neuron Cell Culture

Dissociated mouse hippocampal neurons were plated on the polymer brush surfaces. After 3 days of culture, cellular viability was assessed *via* the LIVE/DEAD cell viability/toxicity assay (Figure 3.3A and 3.3C). Neuronal cells maintain 75.6 % cell viability on the brush surface, which is also comparable to standard PLL coated glass coverslips under the same culture condition (77.6%). Results of double-label immunocytochemistry (Figure 3.3B and 3.3D) showed that the poly(PEGMA-*ran*-MAETAC) brushes favor the attachment and outgrowth of neurons over astrocytes, with 48.1 neurons and only 15.5 astrocytes per random field, giving an average of 3.1 times of more neurons than astrocytes in a random field. This is also comparable with neuronal cells on PLL coated glass surfaces cultured under the same conditions (average 4.3 neuron/astrocytes).

Morphometric analysis of neurite outgrowth on surfaces was described as a useful approach to investigate the mechanisms regulating differentiation of neurons and their connections. In this work, a simple procedure based on stereological principles was applied to morphometric analysis of cell culture on both polymer brushes and PLL modified surfaces [23]. Results of the analysis have showed that the hippocampal neurons cultured on the brush surfaces possessed the average mean neurite length per cell significantly longer than those cultured on the PLL modified control surfaces (Figure 3.3E), with average 2.98 intersections/cell on a polymer brush surfaces and 2.42 intersections/cell on a PLL coated surfaces, respectively.

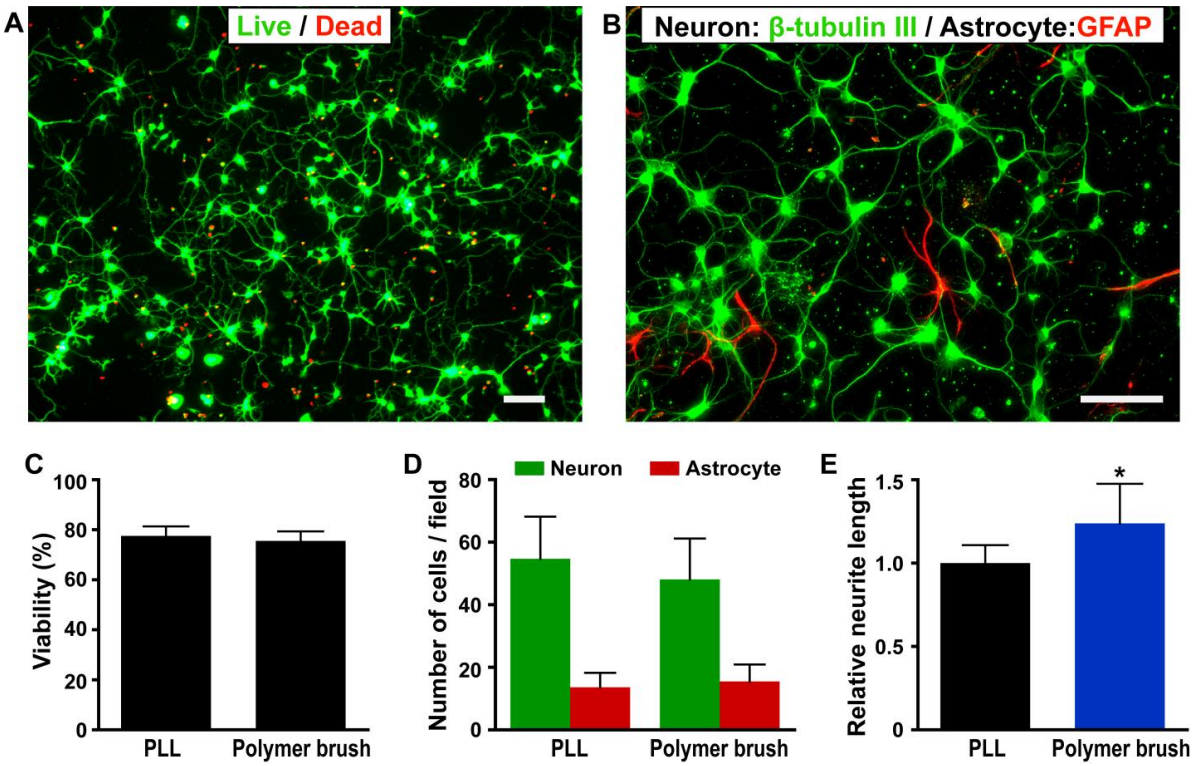

Figure 3.3: Neuronal cell culture on polymer brushes. Photographs of mouse hippocampal neuronal cells cultured on polymer brush modified silicon surfaces and data comparison with those on poly-L-lysine coated glass slides. A) LIVE/DEAD viability/cytotoxicity assay of hippocampal cells on polymer brushes (scale bar is 50 µm). Cells were cultured for three days and observed with fluorescent micrographs of live (calcein AM, green) and dead (ethidium homodimer-1, red). B) Immunocytochemistry demonstrates that neurons (β-III-tubulin-positive cells, green) outnumber astrocytes (GFAP-positive cells, red) on the surface. (Scale bar is 50 µm). C) Viability of cells on polymer brush is comparable to that of PLL coated glass slides. D) Similar number of neurons and astrocytes were observed on polymer brushes and the PLL control surfaces. E) Neurons on polymer brush surface exhibit longer processes compare to those on the PLL coated glass slides.

3.3.3 Protein Absorption and Neuronal Cell Patterning on Poly(MAETAC-*ran*-PEGMA) Brushes

Patterned polymer brushes have been successfully prepared using photolithography method (Figure 3.4A). The pattern was designed to present straight lines of different widths (2 µm to 200 µm) on the surface, and all the straight horizontal lines were also connected to each other at one end to provide curves and give another orientation (vertical). Figure 3.4B shows the

ellipsometry mapping picture of the patterned brushes. Incubating the patterned brush surface in FTIC-BSA solution demonstrated that protein can be nicely patterned on the substrate. Fluorescence imaging clearly shows that FTIC-BSA was absorbed on the brush patterns but not on the PEG SAM background (Figure 3.5A), indicating the difference between acetylcholine/PEG modified surfaces and PEG alone modified surfaces.

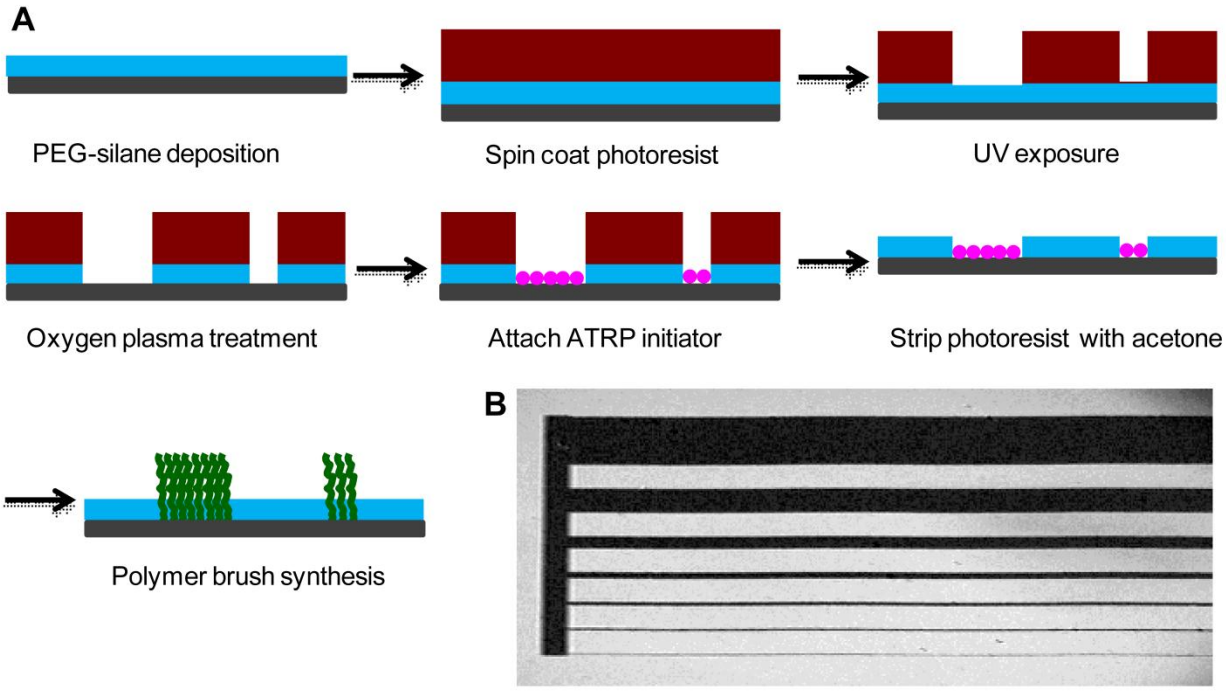

Figure 3.4: Patterning of polymer brushes *via* photolithography method. A) Surface modification steps used to create patterned polymer brushes via photolithographic techniques, and B) ellipsometry mapping photograph of patterned brushes on silicon wafer.

Hippocampal neurons can also be guided along the brush patterns. The images in Figure 5B provide evidence that geographic cues are also important factors in determining neuronal cell behaviors in this system. Neuronal growth is largely confined to poly(PEGMA-*ran*-MAETAC) brushes coated paths, while the degree of attachment and alignment of neurite outgrowth was dependent on pattern widths. There is a strong visual impression that 2 μm and 5 μm lines seem

too small to allow neuronal attachment (not shown, patterned lines cannot be identified under fluorescence microscope), as no specific attachment and alignment of neurons were observed on those lines. A few cells were attached to 12 µm lines, but they hardly formed any connection with other cells, neither have they developed long processes along the lines. However, cells seemed to prefer to attach to the lines wider than 12 µm. On 25 µm lines, neurite elongation was precisely oriented along the tracks of the brushes, and their processes intermingle with those of other neurons along the line. On lines with widths equal or great than 50 µm, more neurons attached to brushes, and neurites showed more significant outgrowth, and they form a meshwork within the lines. Networks become more complicated with the increase of the line widths. On 200 µm lines, cells grew in a manner similar to that of unpatterned brush surfaces, although cells are still strictly confined by the border of the pattern.

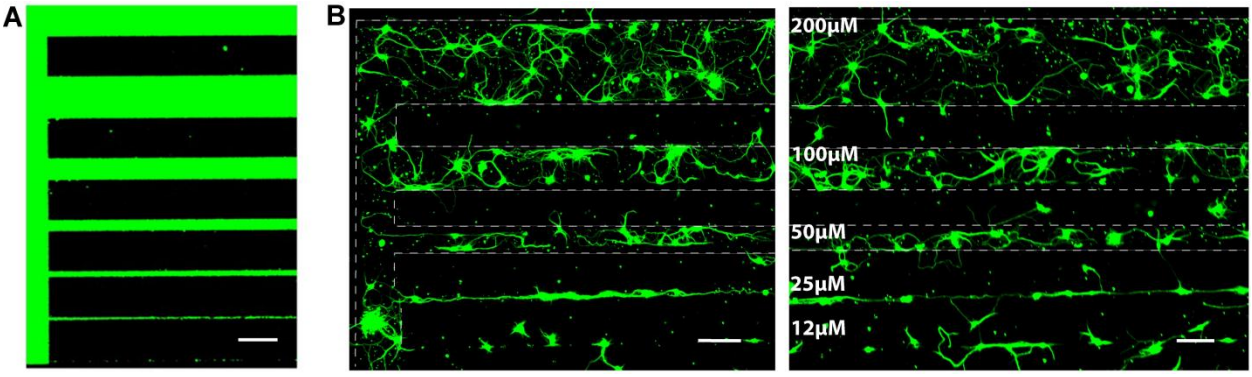

Figure 3.5: Protein and cell patterning on polymer brushes. A) Patterned FTIC-BSA and B) patterned mouse hippocampal neuronal cells on the poly(PEGMA-*ran*-MAETAC) brush surfaces (scale bar is 100 µm) . Dashed lines were added as visual guide for the patterned cells.

3.4 Discussion

3.4.1 Polymer Brush Preparation and Characterization.

In this study, biomimetic random copolymer brushes of neurotransmitter acetylcholine derivatives (MAETAC) and biocompatible PEG were prepared through SI-ATRP reaction. Before the polymerization reaction, a bromoester initiator was covalently linked to a silicon surface to form a self-assembled monolayer (SAM). This step of surface preparation provided a simple and reliable method to covalently tether the organic layer on the substrate. The silicon surface was used as a model substrate, but the technique can also be easily employed on other commonly used substrates such as glass, gold, silver, copper and platinum surfaces or silicon oxide based polymeric substrates [8,10]. The following polymerization of monomers was carried out in water/isopropanol solution to form polymer brushes on the surface. Related to this method, previous work [26] on SI-ATRP-polymerized poly(PEGMA) homopolymer brushes in water showed that chain growth from the surface was a controlled "living process", and the thickness of poly(PEGMA) brushes was a function of polymerization time. However, certain degrees of rapid chain termination on the surface in the early stage of polymerization were observed, and this phenomenon was followed by slow bimolecular coupling or disproportionate reactions that consume the active chains. Longer reaction times (more than 12 h) also introduced chain transfer from surface-active sites to the reaction solution. In another study, for "non-fouling" poly(OEGMA) polymer brushes prepared in water/methanol solvent mixtures [11], a linear relationship of brush thickness against reaction time was found for a reaction time less than 2 h. For a longer reaction time, a deviation from a linear fit to an exponential fit was observed, and after 5 h of reaction time, the thickness of the polymer brushes reached a value of roughly 50 nm. The authors explained this phenomenon could be caused by slow leakage of oxygen into the

reaction system and/or increased steric interference to chain growth for longer polymer brushes. In the same study, brush density was also varied to prepare a binary brush system of poly(OEGMA), and the thickness of the polymer brush reached a steady state value of 20 nm. Beyond this value no further increase in film thickness was observed. Furthermore, the homopolymer brushes of poly(MAETAC) [27] have also been prepared through ATRP reaction. The reaction was carried out in methanol, and it has been shown that transesterification of quaternary amine methacrylates can take place during methanolic ATRP. However, such transesterification can be avoided when methanol is replaced by isopropanol (IPA) because a secondary alcohol is less prone to ester interchange. In the present work, water/IPA was chosen as solvent to prepare polymer brushes containing both PEGMA and MAETAC units. The reaction was terminated after 5 h, and gave a uniform layer of brushes on the substrate surface. Polymer brush thickness with reaction time was not investigated in this study, since neuronal cells can respond to proper surface chemistry even at 1 nm thickness [28], and the effect of brush thickness on cell culture is not the focus of this study. The brushes are relatively thin (~ 21 nm), which is ideal for biomedical device coating applications, where the brushes can be used to optimize the surface chemical properties of the devices without dramatically changing the shape, size and mechanical properties of the devices.

The resulting poly(MAETAC-*ran*-PEGMA) brushes exhibited water contact angles (47º $\pm$ 3º) similar to the poly(PEGMA) brush prepared in water (44º) [26], and it may be concluded that including a small amount of acetylcholine functionality in the polymer brush does not significantly affect the hydrophobicity of the poly(PEGMA) surfaces. Maintaining the appropriate hydrophobicity in the polymer brush might be important to retain the biocompatibility/non-toxic properties of the poly(PEGMA) brush, since surface hydrophobicity

has consequently been widely cited as a key factor in determining protein and cell-surface interaction [29]. FT-IR, XPS and NEXAFS data have also confirmed the surface chemistry of the brushes, these results, together with AFM measurement of the surface, suggested that random copolymerization of PEGMA and MAETAC *via* SI-ATRP gave chemically uniform, well-defined polymer brushes on the silicon surface.

3.4.2 Mouse Hippocampal Neuronal Cell Attachment and Neurite Outgrowth on Polymer Brushes.

Previous studies have shown that pure PEG-based biomaterials can cause poor nerve cell survival due to its effect on cell adhesion, and the presence of MAETAC at high concentration may also lead to a large and acute loss of cell viability because of its cytotoxicity [18-20]. The polymer brushes reported here contain low concentration of MAETAC in order to maintain the biocompatibility of the polymer brushes, while providing tethered bioactive neurotransmitter components. The viability/toxicity assay of mouse hippocampal cells cultured on the polymer brush surfaces showed that, incorporating acetylcholine into poly(PEGMA) polymer brushes at this concentration can totally alter the "non-sticky" property of the poly(PEGMA) homopolymer brushes and dramatically improve neuronal cell attachment and survival (75.6 % viability)(Figure 3.3A and 3.3C), even though much of the material is PEG. Immunochemistry also showed that the brush surfaces permitted the growth of neurons and astrocytes comparable to that on PLL coated glass slides (Figure 3.3E). In addition, hippocampal neurons on the brush surfaces exhibited the healthy cellular growth morphology, possessing multiple dendrites and long axons. The relative length of neurites on a polymer brush surface is significantly longer than that on PLL coated glass substrates when the cells are cultured under the same conditions. The

mechanism of neuronal cell attachment and neurite outgrowth on the polymer brushes is currently unknown and it is an important topic that is worth future investigation. However, it is possible that acetylcholine functionalities in the polymer might mediate the effects of acetylcholine receptors of neurons [14]; alternatively, the positively charged polymer surfaces may lead to changes in the ion flux on the cell membrane [19]. This situation can be further complicated by protein adsorption to the surface prior to cell attachment, as described in the protein absorption test on polymer brushes (Sec. 3.3.). During experiments we also observed that neurons attached to the polymer brush surface are not as strongly attached as those on the PLL coated surfaces, so that cells were more easily washed away and the processes can also be broken during washing steps if it is not carefully handled. This is probably caused by the lower positive charge density on the surface and non-fouling properties of PEG units present in the brushes. In light of this evidence, we hypothesize that the weaker interaction between the surface and neuronal cells allows cells to differentiate easily, while high positive charge density leads to strong interaction which can retard neuronal cell attachment on the surfaces and hinder further differentiation and spreading. Comparing the effect of interaction forces to the neuronal cell growth and morphology on this type of synthetic materials is currently a focus of our research.

3.4.3 Protein and Neuronal Cell Patterning

In this work, a specifically designed pattern was introduced to the silicon substrate surface through UV photolithographic techniques. The pattern incorporates both surface chemical and topographic cues in one single visual field. Besides obvious reasons of time-saving and cost-effective character, the pattern provides a unique and convenient platform for cell-surface interaction studies. In detail, two different types of chemical signals were presented on

those patterns: the PEG polymer brushes with acetylcholine functionalities formed the on-pattern features, and PEG silane self-assembled monolayer (PEG-SAM) were used to backfill the patterns to provide non-adhesive off-pattern regions. The filled regions also served as negative control surfaces that highlight the differences between acetylcholine functionalized poly(PEGMA) brush surfaces and surfaces containing only PEG groups for neuronal cell adhesion and growth. The pattern also provides features different sizes (2 μm to 200 μm, 100 times difference) and directions (horizontal *vs.* vertical). To test the pattern, biomacromolecules such as BSA protein was used and Figure 5A showed that, compare to PEG-SAM background, BSA protein absorption is much higher on pattern features formed by polymer brushes. Protein absorption on the patterns could be explained by the positively charged nature of acetylcholine functionalities in the polymer brushes, since the pI of BSA is around 4.7, and in PBS solution BSA is negatively charged, which enhances the absorption of a protein on the positively charged brush surfaces. This is a significant change from poly(PEGMA) homopolymer brushes, as previously reported that poly(PEGMA) brushes resist non-specific binding and are exceptionally resistant to the adsorption of "sticky" proteins [11]. Protein absorption to the brush surface can also be the cause of improved "cell-surface" interactions on this type of materials, since in serum-containing culture medium, numerous species of protein molecules and albumin can be deposited and presumably dominate the surface characteristics, ultimately lead to improved conditions for cell adhesion and differentiation [8,30].

The designed pattern has also proven to be effective to study cell reactions to surface chemical and physical cues under exactly the same culture condition. Results of hippocampal neuronal cell culture on the pattern showed that neuronal cells can recognize the surface chemical signal and prefer to stay on lines of polymer brushes containing acetycholine

functionalities (Figure 5B). The size and the orientation of the patterns are also major factors to determine the cell attachment and interaction. At feature sizes smaller than 12 μm, neurons were not able to establish any connections, but they were tightly confined at 25 μm lines. More complicated interaction and networks were formed at larger feature sizes (50-200 μm). It is also seemed that, in this specific pattern, neurons tend to stay on horizontal lines than vertical lines at the same size scale (100 μm), probably because horizontal is the dominate direction in this case. In addition, growth of extending neurites is strongly influenced by the patterns, resulting in cells with very different morphologies. For example, at line widths of 100 μm, cells exhibited a star-shaped morphology, while at line width of 25 μm, cells were extended as line-shaped. Results of this study are in agreement with previous studies on the patterning of neuronal cells on the surfaces with other chemical components, such as micro-stamped PLL [28,31], phase mask interference lithography fabricated hydrogels [32], and microfabricated patterns of parylene-C [33], that the cell interaction and morphology of hippocampal neurons can be greatly affected by surface topographical cues. However, different from micro-stamped poly-lysine patterns [31], poly(PEGMA-*ran*-MAETAC) brush patterns need larger pattern sizes to allow neuronal attachment and growth ($\geq$ 25 μm *vs.* $\leq$ 10 μm). This can also be explained by the charge density on the patterns, since positively charged acetylcholine is largely shielded with "non-fouling" PEG units in the polymer brushes, therefore, such brushes might not be as effective at guiding neuronal cells at smaller scales.

3.5 Conclusion

It is of great importance to develop biocompatible polymeric materials for neuroprosthetic device coatings and to effectively control growth of neurites for regeneration in the central nervous system. This study demonstrated that poly(PEGMA-*ran*-MAETAC) brushes can provide a simple and reliable way to prepare a permissive surface for neuronal cell culture and patterning on the substrates. Cells maintained high viability during the 3 day period of culturing on the polymer brushes, and neurite outgrowth was comparable or even better than that on the standard poly-L-lysine coated surfaces. The brushes can also be easily patterned through standard photolithography techniques. Both BSA protein and hippocampal neurons can be localized and guided by such brush patterns, and the pattern sizes and orientation greatly affect neuronal cell morphology and interaction. Because of the positively charged nature of the acetylcholine functionalities and the biocompatibility characteristics of PEG units, the random copolymer brushes may also find potential application to pattern other biomacromolecules such as negatively charged DNA, RNA molecules [34], and to pattern other types of cells such as human endothelial cells [35]. The free hydroxyl terminal groups of the PEG units of the polymer brushes can also be readily modified into various functional groups including chloride, amine, and carboxylic acid groups [26], and covalently linked to other bioactive molecules for more specific neuronal engineering applications. In summary, with carefully designed patterns and introduction of functional specific bioactive molecules, the poly(PEGMA-*ran*-MAETAC) brushes may hold many potential in facilitating the study of neuronal physiologic processes where directed cell growth and migration is fundamental, and it may as well provide new solutions to problems involving cell - surface interactions and interfaces.

Acknowledgments

We thank Dr. Youyong Xu for help with polymer brush preparation, Prof. E. J. Kramer, Dr. Warren Taylor and Dr. Daniel A. Fisher for XPS and NEXAFS analysis. We would like to acknowledge the use of the Microscopy and Imaging Facility at Cornell University, the Cornell Center for Materials Research (CCMR), the Cornell NanoScale Science & Technology Facility (CNF), and the Nanobiotechnology Center (NBTC) at Cornell University. We also acknowledge the assistance of the NHLBI DIR Light Microscopy Core Facility. This work was partially supported through the National Science Foundation (DMR-1105253) and through ONR grant (N000141110330), NIH (NSR01-044287), as well as the NHLBI Division of Intramural Research (P.Y. and H.M.G).

REFERENCES

[1] Constans A. Neural tissue engineering. Scientist. 2004;18:40-42.

[2] Zhong YH, Bellamkonda RV. Biomaterials for the central nervous system. J R Soc Interface. 2008;5:957-75.

[3] Aurand ER, Lampe KJ, Bjugstad KB. Defining and designing polymers and hydrogels for neural tissue engineering. Neurosci Res. 2012;72:199-213.

[4] Khan S, Newaz G. A comprehensive review of surface modification for neural cell adhesion and patterning. J Biomed Mater Res A. 2010;93A:1209-24.

[5] Smeal RM, Rabbitt R, Biran R, Tresco PA. Substrate curvature influences the direction of nerve outgrowth. Ann Biomed Eng. 2005;33:376-82.

[6] Rohr S, Fluckiger-Labrada R, Kucera JP. Photolithographically defined deposition of attachment factors as a versatile method for patterning the growth of different cell types in culture. Pflug Arch Eur J Phy. 2003;446:125-32.

[7] Craighead HG, James CD, Turner AMP. Chemical and topographical patterning for directed cell attachment. Curr Opin Solid St M. 2001;5:177-84.

[8] Senaratne W, Andruzzi L, Ober CK. Self-assembled monolayers and polymer brushes in biotechnology: Current applications and future perspectives. Biomacromolecules. 2005;6:2427-48.

[9] Barbey R, Lavanant L, Paripovic D, Schuwer N, Sugnaux C, Tugulu S, et al. Polymer Brushes via Surface-Initiated Controlled Radical Polymerization: Synthesis, Characterization, Properties, and Applications. Chem Rev. 2009;109:5437-527.

[10] Edmondson S, Osborne VL, Huck WTS. Polymer brushes via surface-initiated polymerizations. Chem Soc Rev. 2004;33:14-22.

[11] Ma HW, Hyun JH, Stiller P, Chilkoti A. "Non-fouling" oligo(ethylene glycol)-functionalized polymer brushes synthesized by surface-initiated atom transfer radical polymerization. Adv Mater. 2004;16:338-41.

[12] Zhou Z, Yu P, Geller HM, Ober CK. The role of hydrogels with tethered acetylcholine functionality on the adhesion and viability of hippocampal neurons and glial cells.

[13] Saifuddin U, Vu TQ, Rezac M, Qian HH, Pepperberg DR, Desai TA. Assembly and characterization neurotransmitter-immobilized of biofunctional surfaces for interaction with postsynaptic membrane receptors. J Biomed Mater Res A. 2003;66A:184-91.

[14] Gumera CB, Wang Y. Modulating neuronal responses by controlled integration of acetylcholine-like functionalities in biomimetic polymers. Adv Mater. 2007;19:4404-+.

[15] Whitteridge D. The Role of Acetylcholine in Synaptic Transmission - a Critical Review. J Neurol Neurosur Ps. 1948;11:134-40.

[16] Tu Q, Li L, Zhang YR, Wang JC, Liu R, Li ML, et al. The effect of acetylcholine-like biomimetic polymers on neuronal growth. Biomaterials. 2011;32:3253-64.

[17] Sosnik A, Sefton MV. Poloxamine hydrogels with a quaternary ammonium modification to improve cell attachment. J Biomed Mater Res A. 2005;75A:295-307.

[18] Zhou Z, Yu P, Geller HM, Ober CK. The role of hydrogels with tethered acetylcholine functionality on the adhesion and viability of hippocampal neurons and glial cells. Biomaterials. 2012;33:2473-81.

[19] Dadsetan M, Knight AM, Lu LC, Windebank AJ, Yaszemski MJ. Stimulation of neurite outgrowth using positively charged hydrogels. Biomaterials. 2009;30:3874-81.

[20] Schneider GB, English A, Abraham M, Zaharias R, Stanford C, Keller J. The effect of hydrogel charge density on cell attachment. Biomaterials. 2004;25:3023-28.

[21] Dong R, Krishnan S, Baird BA, Lindau M, Ober CK. Patterned biofunctional poly(acrylic acid) brushes on silicon surfaces. Biomacromolecules. 2007;8:3082-92.

[22] Dimitriou MD, Zhou ZL, Yoo HS, Killops KL, Finlay JA, Cone G, et al. A General Approach to Controlling the Surface Composition of Poly(ethylene oxide)-Based Block Copolymers for Antifouling Coatings. Langmuir. 2011;27:13762-72.

[23] Ronn LCB, Ralets I, Hartz BP, Bech M, Berezin A, Berezin V, et al. A simple procedure for quantification of neurite outgrowth based on stereological principles. J Neurosci Meth. 2000;100:25-32.

[24] Shard AG, Whittle JD, Beck AJ, Brookes PN, Bullett NA, Talib RA, et al. A NEXAFS examination of unsaturation in plasma polymers of allylamine and propylamine. J Phys Chem B. 2004;108:12472-80.

[25] Epps TH, DeLongchamp DM, Fasolka MJ, Fischer DA, Jablonski EL. Substrate surface energy dependent morphology and dewetting in an ABC triblock copolymer film. Langmuir. 2007;23:3355-62.

[26] Xu D, Yu WH, Kang ET, Neoh KG. Functionalization of hydrogen-terminated silicon via surface-initiated atom-transfer radical polymerization and derivatization of the polymer brushes. J Colloid Interf Sci. 2004;279:78-87.

[27] Li YT, Armes SP, Jin XP, Zhu SP. Direct synthesis of well-defined quaternized homopolymers and diblock copolymers via ATRP in protic media. Macromolecules. 2003;36:8268-75.

[28] Ruiz A, Buzanska L, Gilliland D, Rauscher H, Sirghi L, Sobanski T, et al. Micro-stamped surfaces for the patterned growth of neural stem cells. Biomaterials. 2008;29:4766-74.

[29] Webb K, Hlady V, Tresco PA. Relative importance of surface wettability and charged functional groups on NIH 3T3 fibroblast attachment, spreading, and cytoskeletal organization. J Biomed Mater Res. 1998;41:422-30.

[30] Chen H, Yuan L, Song W, Wu ZK, Li D. Biocompatible polymer materials: Role of protein-surface interactions. Prog Polym Sci. 2008;33:1059-87.

[31] Branch DW, Wheeler BC, Brewer GJ, Leckband DE. Long-term maintenance of patterns of hippocampal pyramidal cells on substrates of polyethylene glycol and microstamped polylysine. Ieee T Bio-Med Eng. 2000;47:290-300.

[32] Jang JH, Jhaveri SJ, Rasin B, Koh C, Ober CK, Thomas EL. Three-dimensionally-patterned submicrometer-scale hydrogel/air networks that offer a new platform for biomedical applications. Nano Lett. 2008;8:1456-60.

[33] Delivopoulos E, Murray AF, MacLeod NK, Curtis JC. Guided growth of neurons and glia using microfabricated patterns of parylene-C on a SiO(2) background. Biomaterials. 2009;30:2048-58.

[34] Merdan T, Kopecek J, Kissel T. Prospects for cationic polymers in gene and oligonucleotide therapy against cancer. Adv Drug Deliver Rev. 2002;54:715-58.

[35] Vanwachem PB, Hogt AH, Beugeling T, Feijen J, Bantjes A, Detmers JP, et al. Adhesion of Cultured Human-Endothelial Cells onto Methacrylate Polymers with Varying Surface Wettability and Charge. Biomaterials. 1987;8:323-28.

CHAPTER FOUR

POLY(ETHYLENE GLYCOL)-PERFLUOROCARBON AMPHIPHILIC SIDE CHAIN-MODIFIED TRIBLOCK COPOLYMERS FOR MARINE ANTIFOULING AND FOULING RELEASE APPLICATIONS

ABSTRACT

The ideal marine antifouling/fouling release surface coatings should be non-toxic and non-leaching, while effectively resisting attachment of various marine organisms or reducing their attachment strength. Due to their dual function nature, polymeric materials containing amphiphilic structures may provide a promising solution to produce novel environmentally friendly antifouling/fouling release surface coatings for marine structures. In this work, we coupled poly(ethylene glycol) (PEG) of different molecular weight (M_w = 350, 550, 750) to a fixed length perfluorinated alkyl chain ($C_{10}H_4F_{16}$ or PF) to generate amphiphilic semifluorinated surfactants. The resulting macromolecules (PEG-PF) were then used as side chains to modify the pre-synthesized polystyrene$_{8K}$-*block*-poly(ethylene-*ran*-butylene)$_{25K}$-*block*-polyisoprene$_{10K}$ (abbreviated as PS-*b*-P(E/B)-*b*-PI or K3) triblock copolymer. The final modified block copolymers were confirmed with NMR and IR spectroscopies and elemental analysis, and were then applied on glass substrates through an established multilayer surface coating technique. Water contact angles and underwater bubble contact angles were used to characterize the surface properties of those polymer coatings. The coated surfaces were also examined against protein absorption and evaluated using biofouling assays against green alga *Ulva*. The results showed that those coatings can significantly reduce the protein absorption on the surfaces. Also, settlement of spores demonstrated that there were no signs of toxicity from those surfaces, sporelings grew normally on all coatings, but percentage removal of 7-day old sporelings from those coatings is higher than the controlled samples. Those initial tests indicated that the amphiphilic PEG-PF side chain modified triblock copolymers are promising antifouling/fouling release coating materials. However, the major challenge of the current approach is the low attachment yield of the semifluorinated amphiphilic side chains (PEG-PF) to the PS-*b*-P(E/B)-*b*-

PI polymer backbone. A more effective method needs to be identified to achieve higher attachment of those functional side chains in the future, and some of the possible strategies explored are discussed at the end of this work.

Keywords: Antifouling, fouling release, amphiphilic structures, triblock copolymers, semifluorinated surfactants.

4.1 Introduction

In the previous chapters of this thesis, we prepared biomaterials that can promote specific cell attachment and differentiation (mice hippocampal neuronal cells). However, cell adhesion on material surfaces is not always desirable. For example, marine biofouling on man-made structures such as ships and boats can cause numerous problems including an increase in frictional drag which leads to substantial energy penalties [1]. Historically, incorporation of toxic antifoulants such as lead, arsenic, mercury and their organic derivatives (e.g., organotin compounds) has been used as a method of controlling fouling; however, they are often harmful to non-target marine organisms as well as humans and pose environmental risks; therefore, most toxic biocides have been banned [2,3]. In past years, with increased legislation on toxicity requirements, more research has been focused on developing toxin-free, environmentally friendly alternative coating materials [4,5]. Polymeric materials are particularly popular as surface coatings, because they can meet a number of criteria simultaneously, such as low cost of production, controllable chemical and physical properties, and capability of incorporating a variety of functional groups. Polymer coatings used in this area can be divided into two major categories, antifouling coatings are able to resist fouling while the vessel is dockside and stable, and fouling release (FR) coatings degrade an organism's ability to form strong bonds with the surface, and the loosely attached organisms can be dislodged once the vessel is moving beyond a critical velocity [6]. Currently both hydrophobic and hydrophilic polymer systems have been demonstrated with antifouling or/and fouling release behaviours with some degree of success [4]. However, the antifouling/fouling release properties of those materials are largely dependent on the marine species that were used for the tests, because the adhesion biology of each species is different. Also, several other aspects can affect the successful usage of those coatings, including

surface wettability, surface energy, Young's modulus and surface roughness [7-9]. For example, it is now known that *Ulva* is more likely to adhere to hydrophilic surfaces, while settlement of diatoms are strongly promoted by hydrophobic coatings, including silicone based and fluorinated polymers [10,11], but the attachment strength is significantly weaker than those on hydrophilic substrates [12,13].

Therefore, a major challenge in marine antifouling/fouling release materials is to design a universal surface coating that can resist the settlement of a wide range of fouling organisms as well as the ability to readily release them at higher hydrodynamic forces. Polymer coatings with amphiphilic structures have been demonstrated to hold such potentials. Those types of polymers contain both hydrophobic and hydrophilic components; they commonly exist in cell membranes and biomacromolecules such as glycoproteins and hetero-polysaccharides in the extracellular polymeric substances; they are also widely used in detergents and have shown some unexpected and remarkable characteristics. It was hypothesized that such structures can undergo conformational change, thereby exposing different functionalities responding to the surrounding environments to create "ambiguous" surfaces that deter the settlement and adhesion of a range of organisms [14,15]. In recent years, several strategies have been developed to prepare polymers with amphiphilic structures for surface coatings. One of the strategies is to synthesize polymers with backbones that can provide either hydrophilic or hydrophobic character, and then covalently link side groups with the opposite character. For example, in the polystyrene-*block*-poly(ethylene oxide)-*stat*-(allyl glycidyl ether) polymer, poly(ethylene oxide) in the backbone provides hydrophilic character to the polymer, and allyl glycidyl ether units were able to be further functionalized with perfluorooctanethiol through thiol-ene "click" chemistry to introduce hydrophobic side chains. The resulting polymer has shown lower *Ulva* settlement and the

attachment strength was also significantly reduced [16]. Other research focused on functional modification of pre-synthesized polymers, where separated hydrophilic and hydrophobic side chains [17,18] or side chains containing both hydrophilic and hydrophobic segments were covalently linked to the pre-synthesized polymer backbones [19,20]. A schematic representation was listed to demonstrate and compare the differences of those major strategies in Figure 4.1.

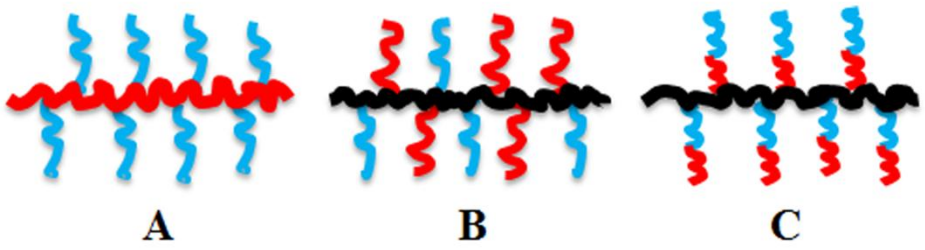

Figure 4.1: Schematic representation of different amphiphilic polymeric structures. A) synthesized polymers with backbones that can provide either hydrophilic or hydrophobic character, B) polymers with separate hydrophilic and hydrophobic side chains, and C) polymers with side chains containing both hydrophobic and hydrophilic segments. In this scheme, red and blue colors were used to represent hydrophobic and hydrophilic units respectively in the polymers, and black color was used to represent pre-synthesized polymers.

In order to prepare amphiphilic polymeric structures, both hydrophobic and hydrophilic components must be carefully selected. To provide hydrophobic character, saturated hydrocarbons, silicone- and perfluorocarbon-based materials can be used. In particular, perfluorocarbon materials offer a range of unique properties, and many facets of their behavior are still under active investigation. Compared to their hydrocarbon counterparts, perfluorocarbons show weak intermolecular attractive forces, exhibiting low boiling points [21] and small refractive indices [22]. Also, they have low surface tension and thus exhibit some valuable interfacial properties, for example, highly fluorinated organic molecules can generate a

separate phase usually referred to as a fluorous phase. As a result fluorocarbon coatings may exhibit repellence toward both water and oil. In addition, modifying fluorocarbons with hydrocarbons can bring new properties to this system. For instance, fluorinated surfactants are semi-fluorinated compounds characterized by a hydrocarbon portion and the highly hydrophobic perfluorocarbon region. They often show typical amphiphilic behaviors of the corresponding hydrogenated surfactants; however, because of the low polarizability and the large van der Waals volume of fluorine, they are not only more hydrophobic but also lipophobic. In addition, fluorinated surfactants have been shown to form highly stable perfluorocarbon/water emulsions with fluorinated compounds by significantly reducing the interfacial tension between the perfluorocarbon and water [23,24]. The combination of these unique characteristics of fluorinated surfactants enables many applications in materials science [25,26] and the biomedical field [27,28].

On the other hand, although many novel structures with hydrophilic properties have been explored to prepare amphiphilic polymers, such as proteins, oligopeptides, charged molecules, and polyalcohols [29-32], poly(ethylene glycol) macromolecules (PEGs) are still among the most commonly used materials to provide such hydrophilic properties. PEGs are uncharged, water-soluble molecules that exhibit many useful properties such as low toxicity and immunogenicity, and they can also effectively improve the biocompatibility of the materials [27,33,34]. Most importantly, PEG-containing surfaces exhibit non-adhesive properties with respect to various proteins and cells, mainly due to their superior ability to be hydrated with water molecules, coupled with their high surface mobility and steric stabilization effects [35-37]. Materials coatings containing PEG moieties have demonstrated resistance to settlement and the elevated release of marine fouling organisms in many studies [38-40], some interesting examples include

PEG monolayers [41,42], PEGylated hydrogels [43], and block copolymers with PEG as either side chain [17] or polymer backbone [16].

In this work, we are interested in preparing amphiphilic polymer systems containing both hydrophobic perfluorocarbons and hydrophilic PEG functional groups. Previous work has shown a higher release of diatoms from polymer coated surfaces with PEG side chains compared to those with semifluorinated side chains, while *Ulva* sporelings showed the opposite behavior [40]. However, the amphiphilic side chains containing both PEG and fluoroalkyl units resulted in low adhesion strength of both *Ulva* and *Navicula* [20]. In particular, Zonyl FSO-100 (or simplified as "Zonyl" here, DuPont^{TM}), a commercially available compound, has been studied for the preparation of this type of amphiphilic polymers and showed some interesting antifouling/fouling release properties. "Zonyl" is a water soluble surfactant with a free hydroxyl-terminated PEG segment covalently linked to a perfluorocarbon end group ($F(CF_2CF_2)_x(CH_2CH_2O)_yCH_2CH_2OH$, or abbreviated as PF-PEG-OH). It was used as a side chain to modify both comb-like poly(tert-butyl acrylate)-*block*-polystyrene polymer [20] and polystyrene-*block*-poly(ethylene-*ran*-butylene)-*block*-polyisoprene (PS_{8K}-*b*-$P(E/B)_{25K}$-*b*-PI_{10K}) ABC triblock copolymer [19]. The settlement and release assays of both *Navicula* diatoms and *Ulva* spores were comparable, and in some cases better, than traditional coatings such as PDMS-based coatings. It has been hypothesized that in those modified polymers, "Zonyl" side chains can undergo environmentally responsive dynamic surface reconstruction underwater, they can provide very low interfacial energy with water because of the PEG groups, and show non-adhesive nature due to the both perfluorocarbon and PEG groups. Those factors contribute good antifouling and fouling release properties to the final modified polymers.

However, the chemical structure of commercial "Zonyl" (PF-PEG-OH) has a broad

molecular weight distribution, according to its manufacturer provided molecular formula, $F(CF_2CF_2)_x(CH_2CH_2O)_yCH_2CH_2OH$, x = 0-15 and y = 1-7, respectively. Like many commercial materials, the content of perfluorocarbon and PEG in the structure is subject to changes in production from batch to batch, which limits its usage in systematic and fundamental studies. In addition, it is also well-known that perfluorinated compounds have lower solubility in organic solvents as the length of the perfluoroalkyl chain increased [44], and this may have a direct impact on the uniformity of the final modified amphiphilic polymer coatings. Furthermore, materials containing long fluorinated alkyl chains (more than 8 perfluorinated carbons) have been discovered to bio-accumulate in mammals and are currently subject to on-going toxicological scrutiny [45]. To overcome those issues and further investigate and understand the working mechanisms of this type of perfluorocarbon and PEG based amphiphilic structures for marine antifouling/fouling release applications, in the present work, we described the synthesis and characterization of perfluorocarbon and PEG based surfactants with a well-controlled "reversed Zonyl" structure (PEG-PF-OH). These molecules feature a short free hydroxyl-terminated fluorinated alkyl chain (PF-OH, eight carbons) terminated by monomethylated PEG groups with different lengths (Figure 4.2). In their chemical formulae, $CH_3O(CH_2CH_2O)_nCH_2(CF_2CF_2)_4CH_2OH$, n equals 7, 12, and 16 for PEG350-PF-OH, PEG550-PF-OH, and PEG750-PF-OH, respectively. The synthesized surfactants were then used as side groups to modify PS_{8K}-*b*-$P(E/B)_{25K}$-*b*-PI_{10K} triblock copolymer, thus to provide better controlled amphiphilic surface coatings for antifouling/fouling release studies. Moreover, in these polymer systems, short perfluorocarbons have low surface energy which drives a tendency to enrich the coating surfaces, and therefore they can help bring the whole side chain to the surface more effectively. Since PEGs are at the end of the side chains, the perfluorocarbons may also facilitate

the surface coverage of PEGs and thereby improve the non-adhesive effects. Another advantage of the system is that the effects of chain length of PEGs can be systematically compared. Previous studies have shown chain length and steric exclusion effects are critical factors in resisting protein and cell adhesion [46]. In summary, by using these new amphiphilic structures to modify the SEBI triblock copolymer and prepare anti-fouling surfaces, a better understanding of the surface behavior of those hydrofluorinated surfactants may be established, and the results can provide insights to design and optimize future generations of antifouling/fouling release materials.

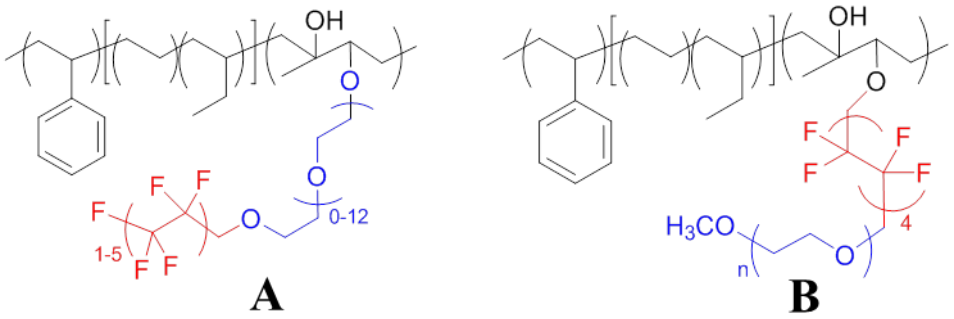

Figure 4.2: Structures of "Zonyl" and "Reversed Zonyl" modified triblock copolymers. A) "Zonyl" amphiphilic side chain and B) "Reversed Zonyl" amphiphilic side chain modified PS-*b*-P(E/B)-*b*-PI triblock copolymers as antifouling/fouling release surface coatings.

4.2 Materials and Methods

4.2.1 Materials

Monomethylated poly(ethylene glycol) (Mw = 350, 550, 750), methanesulfonyl chloride, 3-(Aminopropyl)trimethoxysilane, *m*-chloroperoxybenzoic acid (*m*CPBA), 9-borabicyclo [3.3.1] nonane (9-BBN), and sodium hydroxide (NaOH) were purchased from Sigma-Aldrich. 1H,1H,10H,10H-Perfluoro-1,10-decanediol was purchased from Exfluor research corporation.

Polystyrene$_{8k}$-*block*-poly(ethylene-*ran*-butylene)$_{25k}$-*block*-polyisoprene$_{20k}$ (PS-*b*-P(E/B)-*b*-PI, or K3) triblock copolymer, polystyrene-*block*-poly(ethylene-*ran*-butylene)-*block*-polystyrene (SEBS, MD6945) and SEBS grafted with maleic anhydride (MA-SEBS, FG1901X) were generously provided by Kraton Polymers. Anhydrous chloroform ($CHCl_3$), anhydrous tetrahydrofuran (THF), methylene chloride (CH_2Cl_2), methanol (CH_3OH), toluene, sulfuric acid (H_2SO_4), and 30 wt% hydrogen peroxide (H_2O_2) in water, anhydrous ethanol (CH_3CH_2OH), and all other chemicals were purchased from Sigma-Aldrich and used without further purification unless otherwise noted.

^1H, ^{13}C and ^{19}F NMR spectra were recorded on a Varian Gemini 300 MHz spectrometer with deuterated chloroform, chemical shifts (δ) were reported in parts per million (ppm) relative to trimethyl silane (TMS). FTIR spectrum of the polymer cast as a film from THF solution on a sodium chloride plate was collected using a mattson 2020 Galaxy series FTIR spectrometer. Elemental analysis for weight percentage of C, H, and N in the modified block copolymers was performed by Quantitative Technologies, Inc. (QTI).

4.2.2 Polymer Synthesis and Characterization

Synthesis of the target polymers was carried out into two parts, and depicted in figure 4.3 and 4.4: 1) synthesis of PEG-PE-OH amphiphilic side chains; 2) hydrogenation of polyisoprene block of the PS-*b*-P(E/B)-*b*-PI triblock copolymer, and covalently attach the amphiphilic side chains to triblock copolymer backbones. The details of each reaction and product characterization are described below.

General procedure for synthesis of monomethylated poly(ethylene glycol) mesylate (mPEG-Ms,

2 a-c). A dry 500 mL round bottom flask was charged with mPEG (10.0 g, 18.2 mmol) and anhydrous dichloromethane (250 mL), triethylamine (9.2 g, 90.9 mmol) and methanesulfonyl chloride (10.4 g, 90.9 mmol) were added and then the reaction mixtures were stirred overnight under nitrogen at room temperature. After the completion of the reactions, the precipitated triethylammonium hydrochloride salts were removed by vacuum filtration, and the filtrate was rotary evaporated to dryness, the filtrate was then dissolved in 200 mL distilled water. After extraction with dichloromethane, the dichloromethane layer was dried over anhydrous $MgSO_4$, and the concentration of the solution yielded the desired mPEG mesylates as pale yellow liquid.

PEG350-Ms (2a): ^{1}H NMR (300 MHz, $CDCl_3$, δ): 4.30 (m, 2H, -**CH**$_2$OSO$_2$-), 3.45-3.83 (m, -O**CH$_2$CH$_2$**O-), 3.35 (s, 3H, **CH$_3$**O-), 3.07 (s, 3H, **CH$_3$**SO$_3$-). ^{13}C NMR (300 MHz, $CDCl_3$, δ): 71.78, 70.34, 69.37, 68.38, 58.87, 37.56.

PEG550-Ms (2b): ^{1}H NMR (300 MHz, $CDCl_3$, δ): 4.34 (m, 2H, -**CH**$_2$OSO$_2$-), 3.50-3.73 (m, -O**CH$_2$CH$_2$**O-), 3.34 (s, 3H, **CH$_3$**O-), 3.05 (s, 3H, **CH$_3$**SO$_2$-). ^{13}C NMR (300 MHz, $CDCl_3$, δ): 71.88, 70.46, 69.43, 68.97, 58.97, 37.68.

PEG750-Ms (2c): ^{1}H NMR (300 MHz, $CDCl_3$, δ): 4.35 (m, 2H, -**CH**$_2$OSO$_2$-), 3.50-3.75 (m, -O**CH$_2$CH$_2$**O-), 3.35 (s, 3H, **CH$_3$**O-), 3.09 (s, 3H, **CH$_3$**SO$_3$-). ^{13}C NMR (300 MHz, $CDCl_3$, δ): 71.89,70.60, 70.53, 70.48, 69.28, 68.98, 59.01, 37.70.

*General procedure for synthesis of 1H, 1H-perfluoro-1-nonanyl-Poly(ethylene glycol) (PEG-PF-OH, **4 a-c**).* 5 g (0.8 mmol) of poly(ethylene glycol) methylate was dissolved in anhydrous THF, sodium hydride (1g, 42 mmol) and 1H, 1H-perfluoro-1-nonanol (3.6 g, 8 mmol). The reaction mixture was refluxed for 2 days and then quenched with water. The solvent was removed half via rotary evaporation, and the precipitated salts were removed by vacuum filtration. The filtrate

was then evaporated to dryness and taken up in CH_2Cl_2 and flowed through silica gel column with 10:1 CH_2Cl_2: methanol to remove any residual salts and unreacted reagents. The products were concentrated through rotary evaporation and the pure perfluoroalkyl block PEG was confirmed by ^{1}H, ^{13}C, and ^{19}F NMR.

PEG350-PF-OH (4a): ^{1}H NMR (300 MHz, $CDCl_3$, δ): 4.00 (t, 2H, -**CH**$_2$O-CF2CF2-), 3.45-3.83 (m, -O**CH$_2$CH$_2$**O-), 3.38 (s, 3H, **CH$_3$**O-). ^{19}F NMR (300 MHz, $CDCl_3$, δ) -119.89, -119.92,-122.10, -123.59. ^{13}C NMR (300 MHz, $CDCl_3$, δ): 71.88,70.59,70.55, 70.44, 70.38, 68, 18, 67.85, 58.89.

PEG550-PF-OH (4b): ^{1}H NMR (300 MHz, $CDCl_3$, δ): 3.99 (t, 2H, -**CH**$_2$O-CF2CF2-), 3.48-3.80 (m, -O**CH$_2$CH$_2$**O-), 3.38 (s, 3H, **CH$_3$**O-). ^{19}F NMR (300 MHz, $CDCl_3$, δ) -119.82, -119.86, -122.04,- -123.53. ^{13}C NMR (300 MHz, $CDCl_3$, δ): 72.25, 71.87, 70.66, 70.60, 70.51, 70.46, 68.16, 58.96.

PEG750-PF-OH (4c): ^{1}H NMR (300 MHz, $CDCl_3$, δ): 4.00 (t, 2H, -**CH**$_2$O-CF2CF2-), 3.55-3.77 (m, -O**CH$_2$CH$_2$**O-), 3.38 (s, 3H, **CH$_3$**O-). ^{19}F NMR (300 MHz, $CDCl_3$, δ) -119.78, -119.82,-121.99, -123.48. ^{13}C NMR (300 MHz, $CDCl_3$, δ): 72.30, 71.91, 70.70, 70.64, 70.54, 68.43, 68.33, 60.87 59.02.

*General procedure for synthesis of mesylate-perfluoro-1-nonanyl-Poly(ethylene glycol) (PEG-PF-Ms, **5 a-c**).* A dry 500 mL round bottom flask was charged with mPEG (10.0 g, 18.2 mmol) and anhydrous dichloromethane (250 mL), triethylamine (9.2g, 90.9 mmol) and methanesulfonyl chloride (10.4g, 90.9 mmol) were added and then the reactions were carried out using the same method as described in the preparation of *mPEG-Ms.*

PEG350-PF-Ms (5a): ^{1}H NMR (300 MHz, $CDCl_3$, δ): 4.05 (t, 2H, -**CH**$_2$O-CF2CF2-), 3.45-3.84

(m, -O**CH$_2$CH$_2$**O-), 3.28 (s, 3H, **CH$_3$**O-), 3.09 (s, 3H, **CH$_3$**SO$_3$-CH$_2$CF$_2$). ^{19}F NMR (300 MHz, $CDCl_3$, δ) -119.88, -119.91,-122.10, -123.58. ^{13}C NMR (300 MHz, $CDCl_3$, δ):72.18, 71.80, 70.59, 70.53, 70.44, 70.37, 68.14, 58.86, 31,50.

PEG550-PF-Ms (5b): ^{1}H NMR (300 MHz, $CDCl_3$, δ): 3.97 (t, 2H, -**CH$_2$**O-CF2CF2-), 3.39-3.72 (m, -O**CH$_2$CH$_2$**O-), 3.27 (s, 3H, **CH$_3$**O-), 3.06 (s, 3H, **CH$_3$**SO$_3$-CH$_2$CF$_2$). ^{19}F NMR (300 MHz, $CDCl_3$, δ): -119.61, -119.91, -119.88, -121.97, -122.04, -122.11, - 123.11, -123.58. ^{13}C NMR (300 MHz, $CDCl_3$, δ):72.17, 71.76, 70.55, 70.48, 70.39, 70.33, 68.11, 58.85, 31.51.

PEG750-PF-Ms (5c): ^{1}H NMR (300 MHz, $CDCl_3$, δ): 4.01 (t, 2H, -**CH$_2$**O-CF2CF2-), 3.36-3.79 (m, -O**CH$_2$CH$_2$**O-), 3.29 (s, 3H, **CH$_3$**O-), 3.08 (s, 3H, **CH$_3$**SO$_3$-CH$_2$CF$_2$). ^{19}F NMR (300 MHz, $CDCl_3$, δ) -119.87, -119.84,-122.06, -123.54. ^{13}C NMR (300 MHz, $CDCl_3$, δ): 72.22, 71.80, 70.59, 70.51, 70.42, 70.37, 68.43, 68.15, 58.91, 31.55.

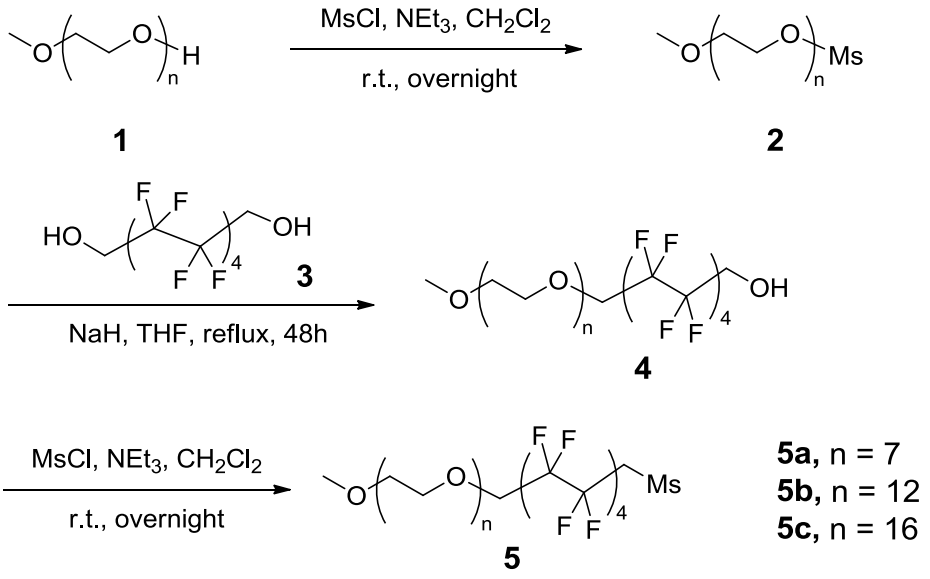

Figure 4.3: Synthesis of perfluorocarbon/PEG based (PEG-PF-Ms) surfactants**.**

*Synthesis of hydroxylated polystyrene$_{8k}$-block-poly(ethylene-ran-butylene)$_{25k}$-block-polyisoprene$_{20k}$ triblock copolymer through hydroboration/oxidation reaction (**7**, abbreviated as K3-OH).* All the apparatus was dried in an oven before the reaction, and the reaction was carried out using the same method as reported before with mild modification [47]. Briefly, dried PS-*b*-P(E/B)-*b*-PI was dissolved in anhydrous THF solvent and then cooled to -10 ºC. 9-BBN solution in anhydrous THF was then added into the solution and the reaction continue stirred at this temperature for 1-2 h to complete the reaction. To ensure no residual hydride in polymer solution, 1 mL of pure methanol was added to the reaction to react with any 9-BBN left after hydroboration. The reaction mixture was then stirred at room temperature 1 day before 6 N of NaOH solution was charged to the reaction flask under strong nitrogen flow. 30% H_2O_2 solution was also added to the solution slowly at low reaction temperature (-25 ºC). After the reaction mixture was continually stirred at -25 ºC for 1 h, the solution was gradually warmed to room temperature to ensure complete reaction. The hydroxylated polymer was precipitated from the THF solution with water, 1.0 M KOH water/methanol solution, 0.5 M KOH water/methanol solution to remove $NaB(OH)_4$, and then reprecipitated three times with water/methanol mixture. The white rubbery product was dried overnight in a vacuum oven at room temperature for 48 h to remove remaining solvent, and stored at room temperature until use. ^{1}H NMR (300 MHz, $CDCl_3$, δ): 6.3, 7.1 (5H, styrene), 3.31-3.75 (br, hydroxylated isoprene), 0.82, 1.23, 1,41, 1,65 (polymer backbone). Elemental analysis: C 82.51%, H 12.32%. IR (dry film): ν_{max} (cm^{-1}) 3350 (br, O-H stretching), 2923, 2855 (C-H stretching), 1494, 1465, 1382 (C-H bending), 1000-1100 (C-O stretching), 756, 700 (C-H bending, aromatic).

*General procedure for synthesis of semifluorinated PEG modified polystyrene$_{8k}$-block-poly(ethylene-ran-butylene)$_{25k}$-block-polyisoprene$_{20k.}$ **(8 a-c)*** Modified triblock copolymers were produced through a straightforward etherification reaction using PEG-PF-Ms and hydroxylated polymer. 1.5 g hydroxylated PS-*b*-P(E/B)-*b*-PI polymer was dissolved in anhydrous THF, 1g sodium hydride and mesylate-perfluoro-1-nonanyl-poly(ethylene glycol) (PEG-PF-Ms) was added to the solution and the reaction was refluxed for 2 days before quenched with water. The precipitated salts were removed by vacuum filtration, and washed with THF. 80% of the solvent was removed *via* rotary evaporation, and the modified polymer was precipitated in methanol. Finally, the reaction products were dried in vacuum oven for 48 h to remove residual solvent.

K3-PF-PEG350 (8a): ^{1}H NMR (300 MHz, $CDCl_3$, δ): 6.5, 7.1 (5H, styrene), 3.20-3.92 (br, -O**CH$_2$CH$_2$**O-), 0.82, 1.01, 1.25, 1.41, 1.84, 1.98 (polymer backbone). Elemental analysis: C 80.25%, H 11.44%. IR (dry film): ν_{max} (cm^{-1}) 3361 (br, O-H stretching), 2929, 2855 (C-H stretching), 1462, 1382 (C-H bending), 1138 (C-F strentching), 1000 (C-O stretching), 765, 703 (C-H bending, aromatic).

K3-PF-PEG550 (8b): ^{1}H NMR (300 MHz, $CDCl_3$, δ): 6.5, 7.1 (5H, styrene), 3.40-3.92 (br, -O**CH$_2$CH$_2$**O-), 0.82, 1.01, 1.25, 1.41, 1.93 (polymer backbone). Elemental analysis: C 79.50%, H 11.44%. IR (dry film): ν_{max} (cm^{-1}) 3380 (br, O-H stretching), 2923, 2858 (C-H stretching), 1459, 1379 (C-H bending), 1259, 1212, 1173, 1147 (C-F strentching), 910, 971, 1026 (C-O stretching), 765, 700 (C-H bending, aromatic).

K3-PF-PEG750 (8c): ^{1}H NMR (300 MHz, $CDCl_3$, δ): 6.5, 7.1 (5H, styrene), 3.30-4.01 (br, -O**CH$_2$CH$_2$**O-), 0.84, 1.08, 1.25, 1.85, 1.96, (polymer backbone). Elemental analysis: C 80.36%, H 11.55 %. IR (dry film): ν_{max} (cm^{-1}) 3350 (br, O-H stretching), 2926, 2858 (C-H stretching), 1497, 1382 (C-H bending), 1256, 1212, 1145 (C-F strentching), 1000-1200 (C-O stretching),

760, 706 (C-H bending, aromatic).

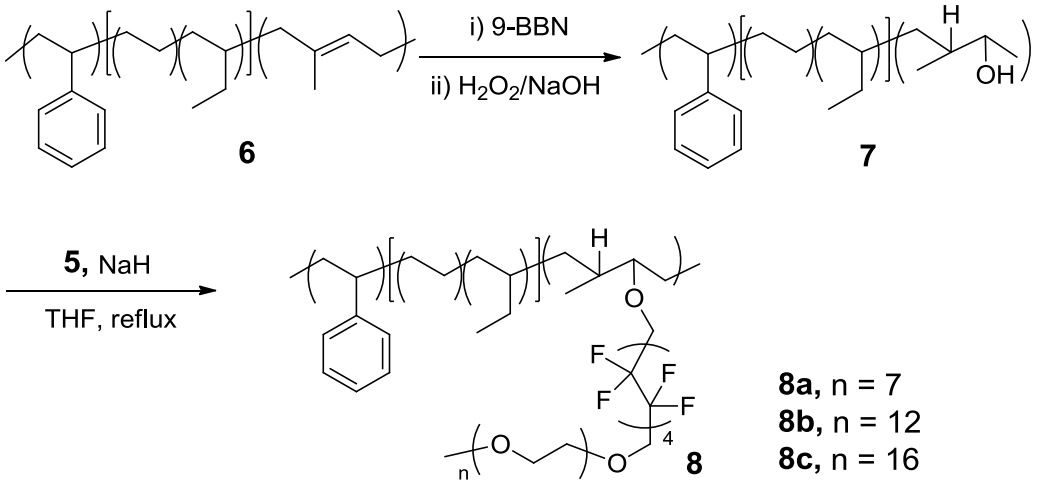

Figure 4.4: Covalent modification of K3 triblock copolymer with perfluorocarbon/PEG amphiphilic side chains.

4.2.3 Surface Preparation and Characterization

Surfaces with modified PS-*b*-P(E/B)-*b*-PI triblock copolymer were prepared for study using methods similar to those previously reported [17,19]. The procedures are also summarized here for completion (Figure 4.5). Briefly, standard microscope glass slides (3 in x 1 in.) were treated with freshly prepared piranhna solution (7:3 v/v, mixture of concentrated H_2SO_4 and 30 wt% H_2O_2 solution) overnight, and then immediately rinsed with distilled water, anhydrous ethanol and dried with nitrogen gas. The dried clean glass slides were then immersed in 3.5% (v/v, in anhydrous ethanol) 3-(aminopropyl)trimethoxysilane solution at room temperature overnight, followed by washing with water, anhydrous ethanol, and drying using nitrogen. The silane treated glass slides were cured by heating to 120 ºC in a vacuum oven at reduced pressure for 2 h before slowly cooled down to room temperature. The first layer coating were applied on

the silane treated glass slides by spinning coated with SEBS/MA-SEBS solution (2% w/v SEBS and 5% w/v MA-SEBS) in toluene (2500 rpm, 30 sec), followed by baking the glass slides at 120 ºC in a vacuum oven at reduced pressure for 12 h, allowing the maleic anhydride groups in the polymer backbone react with epoxy groups on the glass surfaces, therefore improving the bonding of the coating to the glass. The second layer was spin coated with SEBS solution (12 % w/v SEBS solution) three times (2500 rpm, 30 sec.), followed by further baking at 120 ºC in a vacuum oven at reduced pressure for 12 h to give a base layer thickness about 1 mm. The modified PS-*b*-P(E/B)-*b*-PI solutions (16 mg/mL, toluene) was finally spray coated on the surface using a Badger model 250 airbrush and 50 psi nitrogen gas, and annealed in a vacuum oven at reduced pressure at 60 ºC for 12 h, and then 120 ºC for 12 h to ensure the complete removal of the solvents.

Water contact angles were measured using an NRL contact angle goniometer (Rame-Hart model 100-00) at room temperature. Three measurements each for different locations on the sample were taken. The contact angle of an air bubble over the polymer surface immersed in water was determined using the captive bubble method [48,49]. In the measurement, an air bubble was snapped off the tip of a 22 gauge stainless steel syringe needle (0.7 mm o.d. and 0.4 mm i.d.), and then contacted by the surface immersed in water, followed by the measurement of angles between the surfaces and the air bubble.

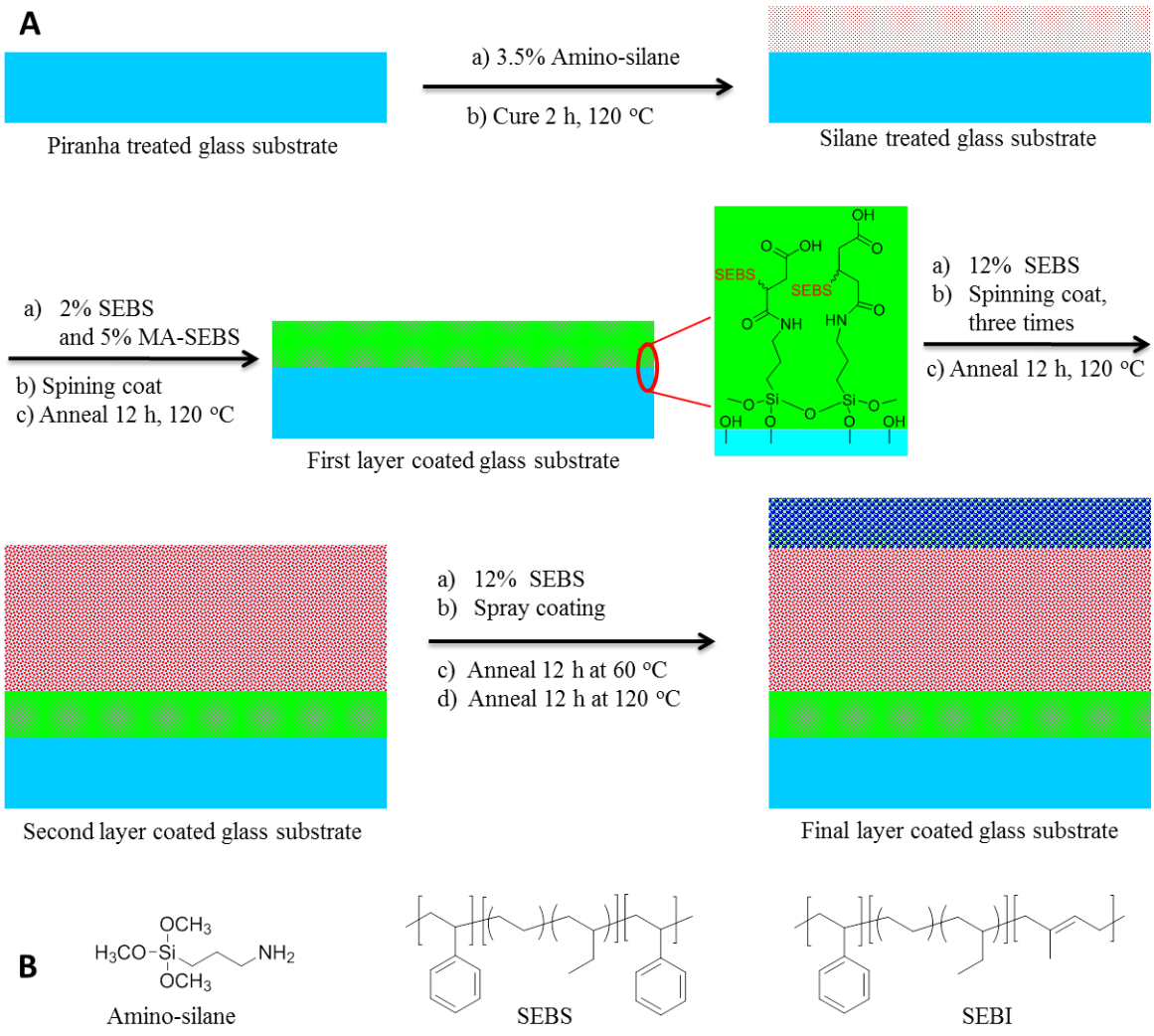

Figure 4.5: A) Schematic representation of multilayer coating process. B) Chemical structures of 3-(Aminopropyl)trimethoxysilane, Polystyrene-*block*-poly(ethylene-*ran*-butylene)-*block*-polystyrene (SEBS) and polystyrene$_{8k}$-*block*-poly(ethylene-*ran*-butylene)$_{25k}$-*block*-polyisoprene$_{20k}$ (SEBI or K3) triblock copolymer, respectively. They were used for multi-layer coating process described above.

4.2.4 Protein Absorption Tests

The polymer-coated glass slides were used for the protein adsorption experiments. The coated slides were immersed in isothiocyanate labelled bovine serum albumin (FITC-BSA, 0.1 mg/mL in PBS) solution for 2 h at room temperature, and then take out of the solution and

briefly rinsed with deionized water. The slides were then immediately imaged and analyzed with a fluorescent microscope. Fluorescence microscopy was performed using an Olympus BX51 upright microscope with a 406 UPlan Fluorite 10 × dry objective (N.A. 0.75). Fluorescein of FITC were observed with a 450 nm excitation and 550 nm emission filter set. Images were acquired using a Roper Cool Snap HQ CCD camera and analyzed using Image Pro image acquisition and processing software.

4.2.5 Biofouling Assay of Coated Glass Surfaces

All biofouling assays were performed by Dr. John A.Finlay in Prof. Maureen E. Callow's laboratory at the University of Birmingham, UK. All coatings were soaked in de-ionised water for 48 hours to reach equilibrium prior to testing. Following this, all coatings were immersed in 0.22 μm filtered artificial seawater for two hours before the start of the experiment. Zoospores were obtained from mature *Ulva* plants by the standard method, and 10 ml of zoospore suspension ($1.0x10^6$ spores ml^{-1}) were used in each individual dish in the dark at ~20 ^oC. Spores were then allowed to settle on the coatings for 45 minutes and washed gently with seawater to remove unsettled zoospores. The spores were cultured using supplemented seawater medium for 6 days to produce sporelings (young plants) on 6 replicate slides of each treatment. Sporeling growth medium was refreshed every 48 hours. Sporeling biomass was determined *in situ* by measuring the fluorescence of the chlorophyll contained within the sporelings in a Tecan fluorescence plate reader. Using this method the biomass was quantified in terms of relative fluorescent units (RFU). The RFU value for each slide is the mean of 70 point fluorescence readings taken from the central portion. The sporeling growth data are expressed as the mean RFU of 6 replicate slides; bars show SEM (standard error of the mean). Strength of attachment

of sporelings was assessed using the water jet apparatus with individual slides of each treatment being exposed to increasing water pressures. Biomass remaining was also assessed using the fluorescence plate reader. The percentage removal was calculated from readings taken before and after exposure to the water jet.

4.3 Results and Discussion

4.3.1 Polymer Synthesis and Characterization

The goal of this current work is to study PS-b-P(E/B)-b-PI triblock copolymer with new perfluorocarbon/PEG based amphiphilic structures for marine antifouling/fouling release applications. Synthesis of the target polymers was carried out into two parts, the ether linkages of each coupling step was chosen to induce resistance towards various forms of metabolism for long-term stable coatings, and the details of each step were depicted in figure 4.3 and 4.4. In the first part of the synthesis (Figure 4.3), the perfluoroalkyl-*block*-poly(ethylene glycol), abbreviated as PEG-PF-OH, is composed by a monodisperse, perfluroroalkane block attached to a PEG block through an ether linkage. PEG methyl ethers (compounds **1 a-c**, Mw = 350, 550, and 750) with one free hydroxyl end group were used as starting materials, the hydroxyl groups were then substituted with methanesulfonic acid functional groups (compounds **2 a-c**). Methanesulfonyl groups improve the neucleophilicity of the alcohol and provide better leaving group for the next step coupling reaction of PEG methyl ether and 1H,1H,10H,10H-Perfluoro-1,10-decanediol. The neucleophilic substitution of the diol on the methylate was carried out under strongly basic conditions and under reflux in anhydrous THF (compounds **3 a-c**). The reactions took place with high conversion, and mono-substituted products were isolated using column chromatography in good yields, with 98 %, 96% and 97% yield for PEG350-PF-OH,

PEG550-PF-OH, PEG750-PF-OH, respectively. Only one of the two hydroxyl groups on the starting 1H,1H,10H,10H-perfluoro-1,10-decanediol was reacted with the methanesulfonyl group

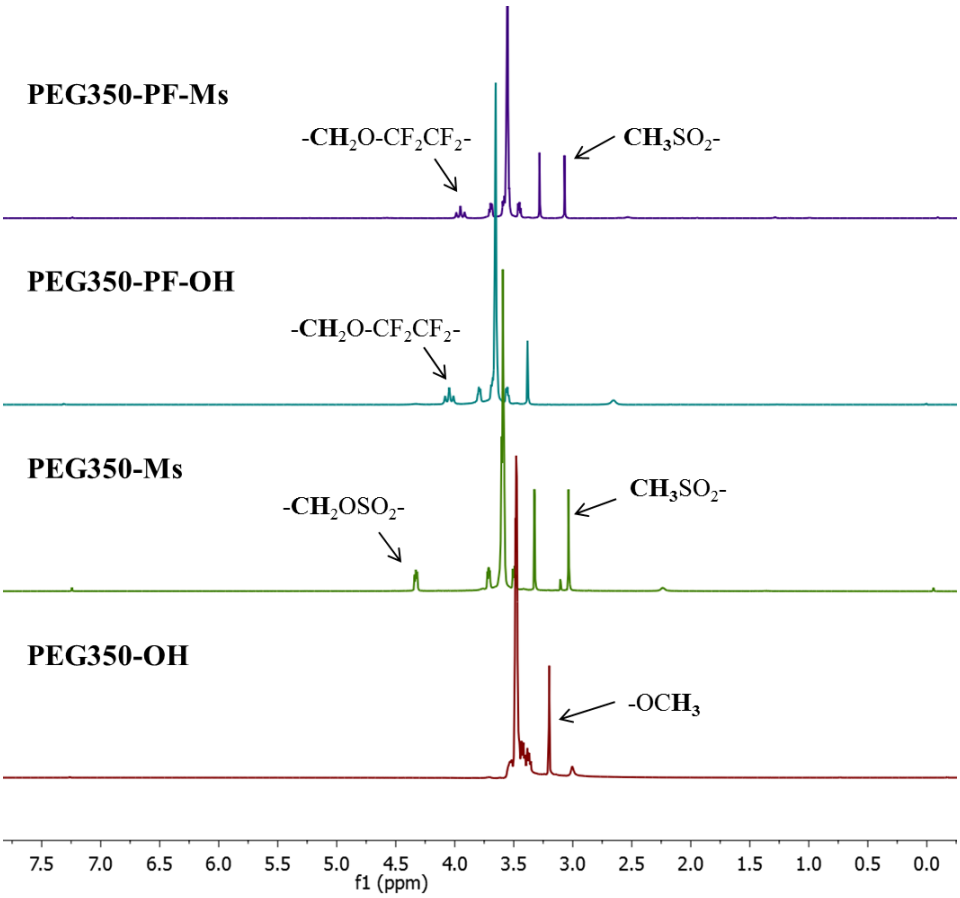

Figure 4.6: ^{1}H NMR spectra of each reaction product for preparing PEG350-PF-Ms amphiphilic side chain. Protons from a methanesulfonyl group (CH_3SO_2-) and PEG (-CH_2OSO_2-, -CH_2O-CF_2CF_2-) units can be used to trace the reaction progress. The same method can be used to monitor reactions for the preparation of PEG550-PF-Ms and PEG750-PF-Ms.

of the PEG chain, resulting the hydroxyl-terminated products. The free hydroxyl groups of the resulting PEG-PF-OH compounds were further substituted with methanesulfonyl groups in the same fashion as described in the preparation of PEG-Ms (compounds **4 a-c**), so they could be coupled with the PS-*b*-P(E/B)-*b*-PI triblock copolymer. ^{1}H, ^{13}C, and ^{19}F NMR were used to confirm the chemical structures of each reaction product, and the peak at 3.1 ppm in ^{1}H NMR is a clear indication of methyl group from methanesulfonyl functionalities (Figure 4.6), while the

chemical shifts of the protons from PEG changes when linked to different functional groups, showing 4.3 ppm when linked to methanesulfonyl and 4.0 ppm when linked to perfluorocarbons, respectively. It is worth noting that the resulting PEG-PF block copolymer showed dramatically improved solubility compare to the starting perfluorocarbon compounds, they can be dissolved in common organic solvents such as acetone, ethyl acetate, methanol and chloroform, and they are also water soluble. This is in agreement with previously reported results [50], that a long hydrophilic chain can overwhelm the hydrophobicity of the fluorinated chain and produce surfactants with good solubility in a broad range of solvents.

In the second stage of the polymer synthesis, hydroxylated PS-*b*-P(E/B)-*b*-PI was prepared through hydroboration/oxidation reaction of the polyisoprene block in the polymer (compound **7**). This reaction introduced free hydroxyl groups which can be further coupled with methylated perfluoroalkylated PEG molecules (PEG-PF-Ms) through neucleophilic substitution reactions. In the ^{1}H NMR spectra for PI block in $CDCl_3$, the chemical shifts at 5.01-5.71 ppm were assigned as protons on unsaturated C=C double bonds in polyisoprene block. After the hydroboration/oxidation reaction, the disappearance of peaks at 5.01-5.71 ppm indicated the completion of the reaction, and the appearance of a new broad peak at 3.5 ppm showed the presence of protons adjacent to the newly formed alcohol groups on the PI backbone. After the coupling reactions of amphiphilic side chains and the hydroxylated PS-*b*-P(E/B)-*b*-PI triblock copolymers, further analysis of the ^{1}H NMR spectra showed the appearance of new peaks at 3.4-3.8 ppm for the amphiphilic side chain functionalized samples. These new peaks in ^{1}H NMR also agree with peaks from PEG region in PEG550 linked PS-*b*-P(E/B)-*b*-PI triblock copolymer (K3-PEG550), and "Zonyl" modified PS-*b*-P(E/B)-*b*-PI triblock copolymer (K3-PEG-PF), demonstrating successful attachment of the PEG-PF side groups to the polymer backbones

(Figure 4.7).

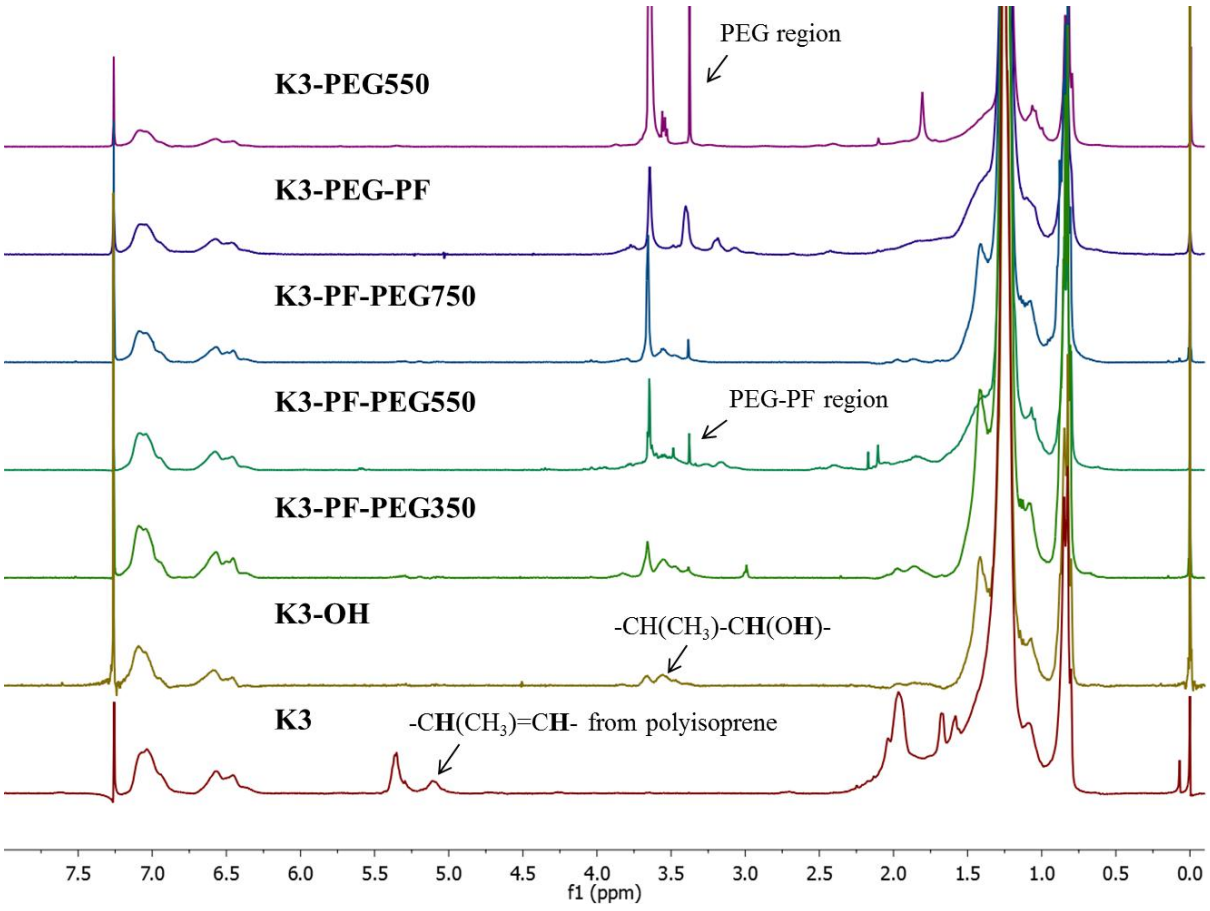

Figure 4.7: ^{1}H NMR spectra of starting polymer K3, hydroxylated K3 (K3-OH) and perfluorocarbon/PEG amphiphilic side chain modified K3 polymers (K3-PF-PEG). "Zonyl" modified K3 polymer (K3-PEG-PF) and PEG along modified K3 polymer (K3-PEG550) are also shown here as comparison.

IR spectroscopy (Figure 4.8) was also used to confirm the formation of amphiphilic side chain modified polymers. In the starting K3 material, the sharp absorption associated with unsaturated C=C at 960 cm^{-1} was quite distinct. After the hydroboration/oxidation reaction, this peak disappeared, while new broad bands around 1000-1200 cm^{-1} (C-O stretching) and 3300 cm^{-1} (O-H stretching) appeared. This indicated that all of the residual unsaturated alkene groups

were successfully converted to the hydroxylated form. Subsequently, the perfluorocarbon/PEG compound (PEG-PF) was convalently attached to hydroxylated triblock copolymer. The appearance of two strong peaks at ~ 1000 cm^{-1} (C-O-C stretching) and at 1145-1250 cm^{-1} (C-F stretching), suggesting the successful introduction of the semifluorinated amphiphilic side chain moieties in the polymer systems.

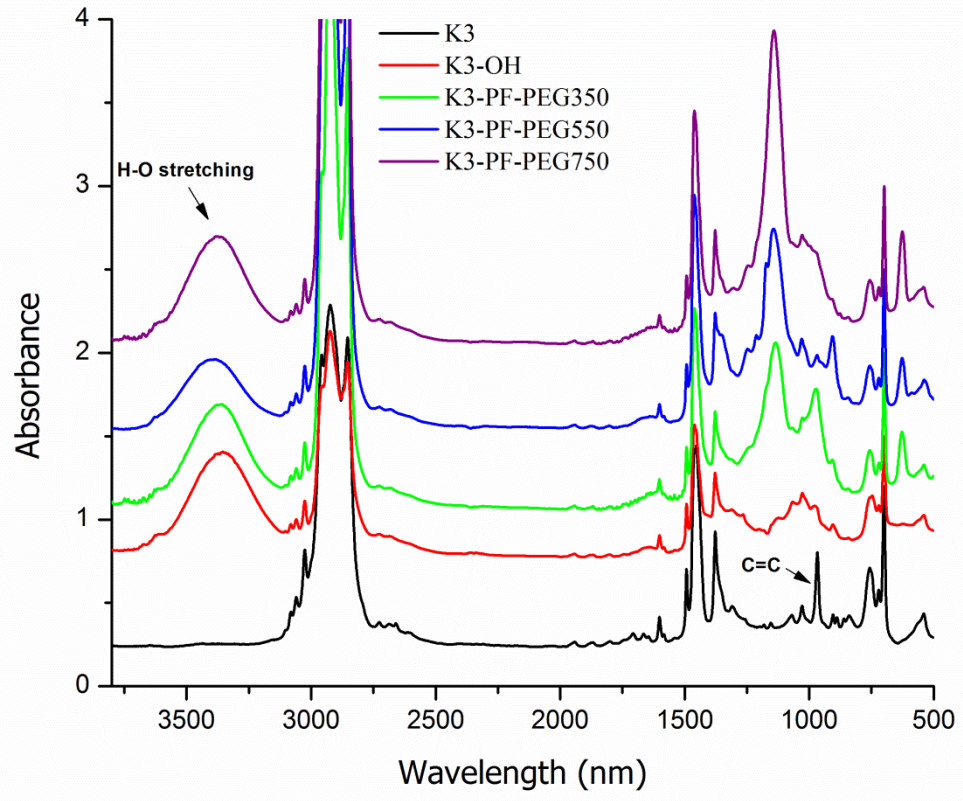

Figure 4.8: IR spectroscopy of perfluorocarbon/PEG amphiphilic side chain modified PS-*b*-P(E/B)-*b*-PI triblock copolymers.

Elemental analysis was also used to determine the chemical composition in the final polymers (Table 4.1), however, the results showed that the percentage attachment of the amphiphilic side chain (PEG-PF) was low and only less than 10% attachment was observed on all final polymers. Also, less attachment was observed for the PEG-PF side chains with larger

molecular weight or longer PEGs, probably due to the higher steric hindrance in the attachment reactions. The reactions have also been repeated several times using improved conditions, such as freshly dried solvents and reagents, excess side chain molecules (2-4 times), longer reaction time (3 days to one week), and different reaction groups (e.g., carbonyl chloride), each reaction gave very similar results. In addition, epoxidation of isoproprene blocks were also prepared to provide active functional groups for polymer backbone modification, and PEG-PF-OH molecules were used to open the epoxy-ring under acid catalyst [19,20]. Unfortunately, no improvement was observed. Another strategy we tried is to introduce two extra carbons from ethylene glycol (EG) to eliminate the difficulty of using perfluorocarbon alcohol; the improved molecules (PEG-PF-EG-OH) have hydroxyl groups further away from perfluorocarbon block and were used to open the epoxy-rings on polyisoproprene block. Still, only similar amounts of side chains can be attached to the polymer backbones. The difficulty of attaching amphiphilic side chains to the polymer backbones can be caused by unique chemical and physical properties of perfluorocarbon/PEG compounds, and the steric hindrance of their bulky structures may also deter the completion of the linkage reaction at high yield. As previously reported [51], PEGylated semifluorinated surfactants can self-assemble due to the amphiphilic character of this linear copolymer. In aqueous solution, this property is manifested by the formation of self-assembling nanoscopic micelle structures, the molecules generate self-assembled micelles having a fluorous phase-based inner core in aqueous solution. Therefore, the functional groups (-OH groups) are largely buried in the core and cannot be efficiently utilized in the reactions. A more careful study of micelle formation might provide some useful insights about how to improve its usage in nucleophilic substitution reactions in the future.

Table 4.1: Chemical composition of PEG-PF-OH side chains and elemental analysis of amphiphilic side chain modified PS-*b*-P(E/B)-*b*-PI triblock copolymers. Water contact angles of those polymers on glass substrates were also measured and compared in the table.

	Composition of Side Chains		Elemental Analysis			Water Contact Angle
Name	PEG (n)	PF (C)	C%	H%	N%	(mean ± SD)
K3	NA	NA	87.05	12.77	0.09	NA
K3-OH	NA	NA	82.51	12.32	0.08	81.8 ± 2.0
K3-PF-PEG350	7	8	80.25	11.44	0.05	89.8 ± 1.0
K3-PF-PEG550	12	8	79.50	11.44	0.09	87.0 ± 1.8
K3-PF-PEG750	16	8	80.36	11.55	0.05	86.8 ± 1.0

4.3.2 Surface Preparation and Characterization

Both settlement and adhesion of marine cells are affected by chemical [12,14], mechanical, topography [52,53], and biological [54] cues and can vary from one species to another. In the current work, an improved multilayer coating method was used to prepare the antifouling/fouling release surfaces with modified triblock copolymers (Figure 4.5). The modulus and the surface chemistry of the coatings can be controlled independently in this method, and a sufficiently thick polymer film can be applied on the surfaces without using excessive amounts of the polymers [55]. The lower Young's modulus of the coatings can be achieved by the use of a relatively thick bottom layer of the thermoplastic elastomer polystyrene-*block*-poly(ethylene-*ran*-butylene)-*block*-polystyrene (SEBS), since the release of sporelings has been shown to be related to the low modulus of PDMS [56], and the elastic modulus of SEBS (MD 6945) are very similar to that of PDMS [19]. Also, the application thickness of silicon coatings is typically 150 μm while it is 75 μm for fluoropolymers [57], thicker coating as seen with the silicone elastomers is more successful as it requires less energy to fracture the bond between the foulants and coating. By using the multilayer coating method, 1 mm thick of SEBS elastomer can be successfully applied to the glass substrates to provide proper mechanical

properties for the antifouling/fouling release applications. Finally, the modified amphiphilic polymers (16 mg/mL toluene solution) were spray coated on top of the SEBS base layers. The polystyrene block in the functionalized polymers was used to increase the compatibility of the modified polymer layer and SEBS base layer by entrapment in the cylindrical polystryrene domains at the SEBS surface, resulting in interlocked, non-leachable surface coatings with amphiphilic properties.

Water contact angle measurements are a simple and effective way to monitor the surface properties, where the higher water contact angles can be attributed to the presence of hydrophobic groups at the surface and the lower angles can be attributed to the presence of hydrophilic units. Compared to the SEBS base layer coated surfaces (water contact angle of 80.4° $\pm$ 0.8°), water contact angle analysis of the coated surface indicated the presence of low-surface-energy (Table 4.1), hydrophobic fluorinated moieties at the surface, with contact angles of 86.8°, 87.0°, and 89.8° for K3-PF-PEG750, K3-PF-PEG550, K3-PF-PEG350, respectively. Underwater bubble contact angles were also used to monitor the dynamic surface capability of facile reordering of the side chains (Figure 4.9). The angles were measured between the surfaces and the air bubble on the water side, thus, a low captive-bubble contact angle indicates a hydrophilic surface, while a higher angle indicates a more hydrophobic surface. The contact angle of the air bubble on the surface immersed in water decreased from 75° immediately after immersion to 50° after a day of immersion, and after 3 days to around 42° and reached an equilibrium value of 40° after one week, which indicated that the surface reconstruction occurred over a period of days. The decrease of the contact angle may be attributed to the molecular reorganization of the surface, which can occur by the migration of the polystyrene block and perfluorocarbon units away from the interface and/or the reorientation of the PEG segments to

the water-polymer interface, since surface-tethered PEGylated polymer brushes [58] have an equilibrium value of the captive-bubble contact angel of 31° in contact with water. The flipping of the side chains would facilitate the enthalpically favourable interaction of PEG with water while simultaneously minimizing the water contact of the hydrophobic fluoroalkyl segments. The equilibrium surface structures could minimize enthalpy and would be the one in which the polystyrene blocks and perfluorocarbon segments are largely buried under the PEG groups.

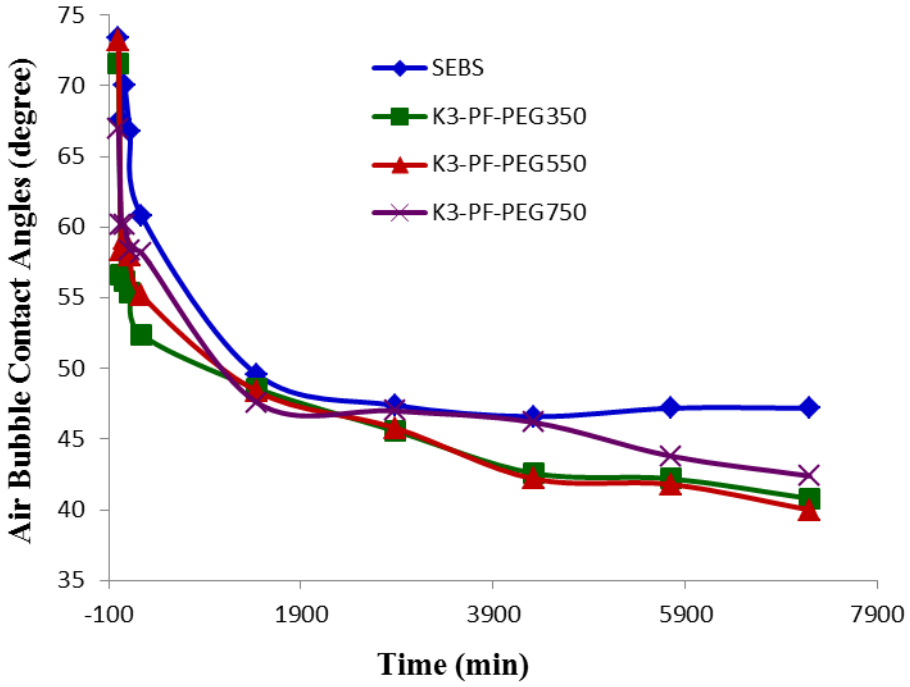

Figure 4.9: Captive air bubble contact angles of perfluorocarbon/PEG amphiphilic side chain modified PS-*b*-P(E/B)-*b*-PI on top of SEBS base layers. Underwater surface reconstruction took place slowly and took several days to reach equilibrium.

4.3.3 Protein Absorption on Polymer Coated Surfaces

Several key growth stages occur in the process of biological fouling, including the initial accumulation of absorbed organics, which frequently contain large proportions of proteins secreted by marine organisms [12,59,60], and the settlement and growth of pioneering bacteria creates a biofilm matrix, which is often a the first stage to subsequent fouling by macrofoulers [61]. Particularly, non-specific adsorption of proteins can take place on almost all artificial surfaces, and most of the time absorption is severe enough to reduce the desired surface properties of the substrates [62]. Different strategies have been employed to reduce unwanted non-specific adsorption of proteins, and materials using polyethylene glycol (PEG) or carbohydrate coatings are most common and most effective [63-65], partially because a high degree of hydration and conformational flexibility of those polymer surfaces minimizes the polymer-water interfacial energy, and lowers the driving force for adsorption of proteins at the surface [66]. In the present work, the polymer coated surfaces were exposed to a solution of fluorescently labeled protein (FITC-BSA) to test the polymers against non-specific protein absorption (Figure 4.10). The result showed that compared to the SEBS base-layer coatings, all the surfactant functionalized triblock copolymers are effective against FITC-BSA absorption, with K3-PF-PEG750 showed the lowest absorption among the three functional polymer samples. The test result is in agreement with the previous findings that the length of PEG unit is a major factor for its “non-adhesive” properties [36,65], and longer PEG chain length showed higher resistance against non-specific bindings towards proteins.

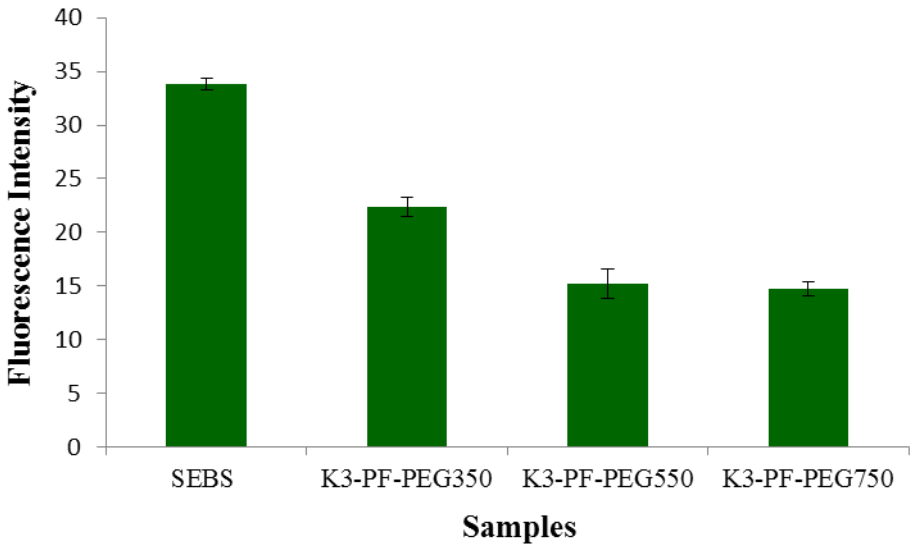

Figure 4.10: Comparison of relative fluorescence intensities of FITC-BSA adsorbed on perfluorocarbon/PEG amphiphilic side chain modified polymer coatings.

4.3.4 Settlement of Zoospores

Glass substrates coated with amphiphilic side chain functionalized triblock copolymers were evaluated against *Ulva* attachment (Figure 4.11). For all biofouling assays, clean glass microscope slides were included as standards, and glass slides coated with MD6945 SEBS base layers were also included as controls to highlight the differences in performance between the base layer alone and that with the amphiphilic multilayer coatings. The results showed that the settlement density of spores was broadly similar on amphiphilic polymer coated surfaces, and the settlement density on glass surfaces was higher. The spore settlement density was greatest on the sample with the highest molecular weight of PEG, K3-PF-PEG750. Sporeling growth was also similar on all surfaces, possibly because of similar molecular compositions at the polymer-water interface. There were no signs of toxicity from any of the surfaces. Sporelings grew normally on all coatings, and the green covering of sporelings was present on all test surfaces after 7 days of culture. The levels of biomass produced on each coating broadly followed the trend of spore

settlement density.

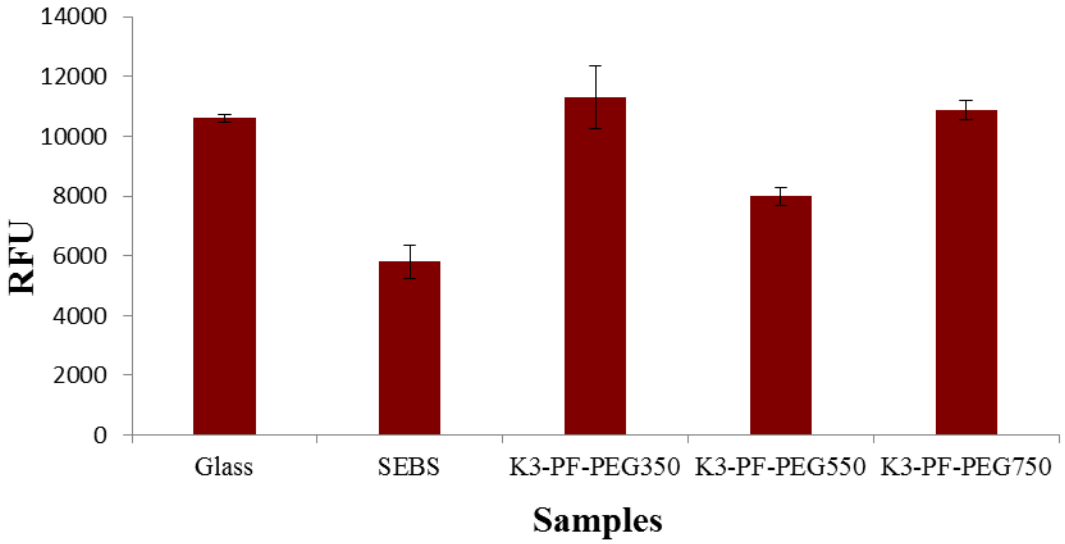

Figure 4.11: The biomass of *Ulva* sporelings on amphiphilic side chain linked triblock copolymer coatings after 7 days. Each point is the mean biomass from 6 replicate slides measured using a fluorescence plate reader (RFU; relative fluorescence unit). Bars show standard error of the mean.

The coated glass slide surfaces were also evaluated for sporeling release to see if additional information regarding the fouling release performance of these materials could be ascertained. The experiment was initially carried out using the water channel rather than the water jet. Despite using the maximum shear stress attainable (50 Pa) in the water channel there was no visual removal from any of the test coatings. The coatings were therefore re-tested with the water jet at a range of pressures. The results are shown in Figure 4.12. Compared to that of the glass control surfaces, the experimental results showed that adhesion strength of sporelings was lower on the amphiphilic surface coatings containing longer PEG segments (K3-PF-PEG550 and K3-PF-PEG750). Surfaces containing shorter PEG chains (K3-PF-PEG350) showed better performance than base layer SEBS coated surfaces alone, but were not sufficient enough to

outperform the control bare glass surfaces. Those results showed that proper chemical components in the amphiphilic polymer structures are essential for their biological performance, and polymers with longer PEG chains are promising candidate materials as fouling release surface coatings for this specific perfluorocarbon/PEG amphiphilic system.

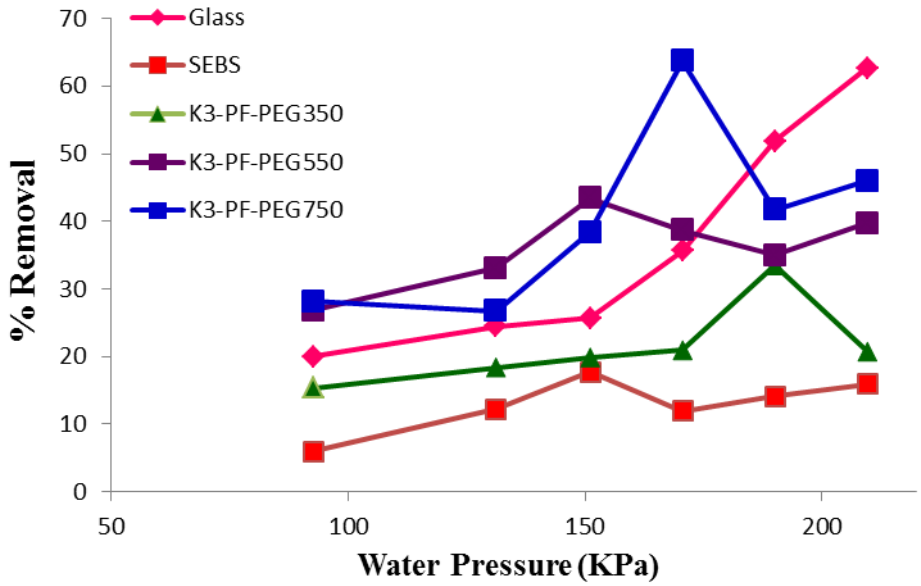

Figure 4.12: Percent removal of 7 day old sporelings from "reversed-Zonyl" modified block copolymer coatings plotted as a function of surface water pressure (kPa). Coatings were exposed to a range of different surface pressures from the water jet.

4.4 Conclusion

Generation of biomass on marine surfaces is highly undesirable, and preparation of environmentally-friendly, non-toxic polymeric surface coatings offer potential solutions for sustainable alternatives and provide a long-term mechanism to protect both the marine environment and human health. In this work, we synthesized perfluorocarbon/PEG based amphiphilic structures that present very good solubility in a broad range of organic or inorganic

solvents, and those macromolecules were further used to modify PS-*b*-P(E/B)-*b*-PI triblock copolymer to provide surface coatings for marine antifouling/fouling release applications. The resulting polymers were characterized using a combination of NMR, IR spectroscopy and elemental analysis to confirm their chemical structures. Those copolymers were then applied to the glass surfaces through a multilayer-coating technique. Water contact angles and underwater bubble contact angles suggested these surfaces could undergo reconstruction upon immersion in water, and are largely populated with PEG moieties after contact with water for more than two days. Those surfaces were also tested against FITC-BSA absorption, and the results showed that all the coatings provide significantly better resistance than the unmodified PS-*b*-P(E/B)-*b*-PI surfaces. Finally, those prepared surfaces were evaluated with *Ulva* and sporing. Lower settlement of *Ulva* spores was seen on coatings containing longer PEG side chains, and the % removal of 7 day old sporelings on those surfaces was better than the control SEBS samples, demonstrating their potential as antifouling/fouling release coatings. However, the current strategy suffered from low attachment yield of amphiphilic side chains on the precursor polymer backbones. In future a focus of our research on the mechanism of perfluorocarbon/PEG micelle formation or the development of different types of amphiphilic structures (e.g., hydrocarbon/PEG or silicon/PEG) will be needed to obtain better antifouling/fouling-release performance,

Acknowledgments

The authors would like to thank Dr. Warren Taylor, Dr. Edward J. Kramer for many insightful discussions and suggestions on this project, and also Dr. John A. Finlay, Dr. Maureen E. Callow, Dr. James A. Callow for help with *Ulva* tests. This work was supported by the US Department of Defense's Strategic Environmental Research and Development Program (SERDP), grant WP #1454 with additional support from the Office of Naval Research (ONR) through award #N00014-08-1-0010 (JAC and MEC), N00014-02-1-0170 (CKO and EJK) and Nanosurfaces Inc. (CKO and SHS). We also acknowledge partial support from the NSF Polymers Program (DMR-0704539) as well as the use of central facilities funded by the NSF-MRSEC program (UCSB MRL, DMR-0520415).

REFERENCES

[1] Chambers LD, Stokes KR, Walsh FC, Wood RJK. Modern approaches to marine antifouling coatings. Surf Coat Tech. 2006;201:3642-52.

[2] Champ MA. A review of organotin regulatory strategies, pending actions, related costs and benefits. Sci Total Environ. 2000;258:21-71.

[3] Terlizzi A, Fraschetti S, Gianguzza P, Faimali M, Boero F. Environmental impact of antifouling technologies: state of the art and perspectives. Aquat Conserv. 2001;11:311-17.

[4] Krishnan S, Weinman CJ, Ober CK. Advances in polymers for anti-biofouling surfaces. J Mater Chem. 2008;18:3405-13.

[5] Webster DC, Chisholm BJ, Stafslien SJ. Mini-review: Combinatorial approaches for the design of novel coating systems. Biofouling. 2007;23:179-92.

[6] Brady RF, Singer IL. Mechanical factors favoring release from fouling release coatings. Biofouling. 2000;15:73-81.

[7] Kim J, Chisholm BJ, Bahr J. Adhesion study of silicone coatings: the interaction of thickness, modulus and shear rate on adhesion force. Biofouling. 2007;23:113-20.

[8] Beigbeder A, Degee P, Conlan SL, Mutton RJ, Clare AS, Pettitt ME, et al. Preparation and characterisation of silicone-based coatings filled with carbon nanotubes and natural sepiolite and their application as marine fouling-release coatings. Biofouling. 2008;24:291-302.

[9] Kim J, Nyren-Erickson E, Stafslien S, Daniels J, Bahr J, Chisholm BJ. Release characteristics of reattached barnacles to non-toxic silicone coatings. Biofouling. 2008;24:313-19.

[10] Holland R, Dugdale TM, Wetherbee R, Brennan AB, Finlay JA, Callow JA, et al. Adhesion and motility of fouling diatoms on a silicone elastomer. Biofouling. 2004;20:323-29.

[11] Casse F, Stafslien SJ, Bahr JA, Daniels J, Finlay JA, Callow JA, et al. Combinatorial

materials research applied to the development of new surface coatings V. Application of a spinning water-jet for the semi-high throughput assessment of the attachment strength of marine fouling algae. Biofouling. 2007;23:121-30.

[12] Finlay JA, Callow ME, Ista LK, Lopez GP, Callow JA. The influence of surface wettability on the adhesion strength of settled spores of the green alga Enteromorpha and the diatom Amphora. Integr Comp Biol. 2002;42:1116-22.

[13] Finlay JA, Callow ME, Schultz MP, Swain GW, Callow JA. Adhesion strength of settled spores of the green alga Enteromorpha. Biofouling. 2002;18:251-56.

[14] Callow JA, Callow ME, Ista LK, Lopez G, Chaudhury MK. The influence of surface energy on the wetting behaviour of the spore adhesive of the marine alga Ulva linza (synonym Enteromorpha linza). J Roy Soc Interface. 2005;2:319-25.

[15] Gudipati CS, Finlay JA, Callow JA, Callow ME, Wooley KL. The antifouling and fouling-release perfomance of hyperbranched fluoropolymer (HBFP)-poly(ethylene glycol) (PEG) composite coatings evaluated by adsorption of biomacromolecules and the green fouling alga Ulva. Langmuir. 2005;21:3044-53.

[16] Dimitriou MD, Zhou ZL, Yoo HS, Killops KL, Finlay JA, Cone G, et al. A General Approach to Controlling the Surface Composition of Poly(ethylene oxide)-Based Block Copolymers for Antifouling Coatings. Langmuir. 2011;27:13762-72.

[17] Park D, Weinman CJ, Finlay JA, Fletcher BR, Paik MY, Sundaram HS, et al. Amphiphilic Surface Active Triblock Copolymers with Mixed Hydrophobic and Hydrophilic Side Chains for Tuned Marine Fouling-Release Properties. Langmuir. 2010;26:9772-81.

[18] Sundaram HS, Cho YJ, Dimitriou MD, Weinman CJ, Finlay JA, Cone G, et al. Fluorine-free mixed amphiphilic polymers based on PDMS and PEG side chains for fouling release applications. Biofouling. 2011;27:589-601.

[19] Weinman CJ, Finlay JA, Park D, Paik MY, Krishnan S, Sundaram HS, et al. ABC Triblock Surface Active Block Copolymer with Grafted Ethoxylated Fluoroalkyl Amphiphilic Side Chains for Marine Antifouling/Fouling-Release Applications. Langmuir. 2009;25:12266-74.

[20] Krishnan S, Ayothi R, Hexemer A, Finlay JA, Sohn KE, Perry R, et al. Anti-biofouling properties of comblike block copolymers with amphiphilic side chains. Langmuir. 2006;22:5075-86.

[21] Drummond CJ, Georgaklis G, Chan DYC. Fluorocarbons: Surface free energies and van der Waals interaction. Langmuir. 1996;12:2617-21.

[22] Huyskens PL. Differences in the Structures of Highly Polar and Hydrogen-Bonded Liquids. J Mol Struct. 1989;198:123-33.

[23] Riess JG. Highly Fluorinated Systems for Oxygen-Transport, Diagnosis and Drug-Delivery. Colloid Surface A. 1994;84:33-48.

[24] Krafft MP. Fluorocarbons and fluorinated amphiphiles in drug delivery and biomedical research. Adv Drug Deliver Rev. 2001;47:209-28.

[25] Yi T, Haag R, Brenn R, Delto R, Weickman H, Thomann R, et al. PMMA gradient materials and in situ nanocoating via self-assembly of semifluorinated hyperbranched amphiphiles. Macromol Chem Physic. 2005;206:135-41.

[26] Bleta R, Blin JL, Stebe MJ. Solubilization of various fluorocarbons in a fluorinated surfactant/water system: Relation with the design of porous materials. J Phys Chem B. 2006;110:23547-56.

[27] Park HD, Bae JW, Park KD, Ooya T, Yui N, Jang JH, et al. Surface modification of polyurethane using sulfonated PEG grafted polyrotaxane for improved biocompatibility. Macromol Res. 2006;14:73-80.

[28] Krafft MP, Riess JG. Perfluorocarbons: Life sciences and biomedical uses - Dedicated to the memory of Professor Guy Ourisson, a true RENAISSANCE man. J Polym Sci Pol Chem. 2007;45:1185-98.

[29] Marie E, Rotureau E, Dellacherie E, Durand A. From polymeric surfactants to colloidal systems 4. Neutral and anionic amphiphilic polysaccharides for miniemulsion stabilization and polymerization. Colloid Surface A. 2007;308:25-32.

[30] Ogawa S, Osanai S. Inhibition effect of sugar-based amphiphiles on eutectic formation in the freezing-thawing process of aqueous NaCl solution. Cryobiology. 2007;54:173-80.

[31] van Hell AJ, Costa CICA, Flesch FM, Sutter M, Jiskoot W, Crommelin DJA, et al. Self-assembly of recombinant amphiphilic oligopeptides into vesicles. Biomacromolecules. 2007;8:2753-61.

[32] Le Droumaguet B, Mantovani G, Haddleton DM, Velonia K. Formation of giant amphiphiles by post-functionalization of hydrophilic protein-polymer conjugates. J Mater Chem. 2007;17:1916-22.

[33] Loret S, Gilson P, Barakat I, Grandfils C, Dandrifosse G. Biocompatibility of polyethylene glycols (PEG): An approach using bovine serum albumin (BSA) as a protein model. Pflug Arch Eur J Phy. 2000;440:R233-R33.

[34] Zhang M, Li XH, Gong YD, Zhao NM, Zhang XF. Properties and biocompatibility of chitosan films modified by blending with PEG. Biomaterials. 2002;23:2641-48.

[35] Unsworth LD, Sheardown H, Brash JL. Polyethylene oxide surfaces of variable chain density by chemisorption of PEO-thiol on gold: Adsorption of proteins from plasma studied by radiolabelling and immunoblotting. Biomaterials. 2005;26:5927-33.

[36] Unsworth LD, Sheardown H, Brash JL. Protein resistance of surfaces prepared by sorption of end-thiolated poly(ethylene glycol) to gold: Effect of surface chain density. Langmuir. 2005;21:1036-41.

[37] Luk YY, Kato M, Mrksich M. Self-assembled monolayers of alkanethiolates presenting mannitol groups are inert to protein adsorption and cell attachment. Langmuir. 2000;16:9604-08.

[38] Youngblood JP, Andruzzi L, Ober CK, Hexemer A, Kramer EJ, Callow JA, et al. Coatings based on side-chain ether-linked poly(ethylene glycol) and fluorocarbon polymers for the control of marine biofouling. Biofouling. 2003;19:91-98.

[39] Youngblood JP, Andruzzi L, Senaratne W, Ober CK, Callow ME, Callow JA, et al. New materials for marine biofouling resistance and release: Semi-fluorinated and pegylated block copolymer bilayer coatings. Abstr Pap Am Chem S. 2003;225:U713-U14.

[40] Krishnan S, Wang N, Ober CK, Finlay JA, Callow ME, Callow JA, et al. Comparison of the fouling release properties of hydrophobic fluorinated and hydrophilic PEGylated block copolymer surfaces: Attachment strength of the diatom Navicula and the green alga Ulva. Biomacromolecules. 2006;7:1449-62.

[41] Finlay JA, Krishnan S, Callow ME, Callow JA, Dong R, Asgill N, et al. Settlement of Ulva zoospores on patterned fluorinated and PEGylated monolayer surfaces. Langmuir. 2008;24:503-10.

[42] Schilp S, Rosenhahn A, Pettitt ME, Bowen J, Callow ME, Callow JA, et al. Physicochemical Properties of (Ethylene Glycol)-Containing Self-Assembled Monolayers Relevant for Protein and Algal Cell Resistance. Langmuir. 2009;25:10077-82.

[43] Ekblad T, Bergstroem G, Ederth T, Conlan SL, Mutton R, Clare AS, et al. Poly(ethylene glycol)-Containing Hydrogel Surfaces for Antifouling Applications in Marine and Freshwater Environments. Biomacromolecules. 2008;9:2775-83.

[44] de Wolf E, van Koten G, Deelman BJ. Fluorous phase separation techniques in catalysis. Chem Soc Rev. 1999;28:37-41.

[45] Lau C, Anitole K, Hodes C, Lai D, Pfahles-Hutchens A, Seed J. Perfluoroalkyl acids: A review of monitoring and toxicological findings. Toxicol Sci. 2007;99:366-94.

[46] Zhu B, Eurell T, Gunawan R, Leckband D. Chain-length dependence of the protein and cell resistance of oligo(ethylene glycol)-terminated self-assembled monolayers on gold. J Biomed Mater Res. 2001;56:406-16.

[47] Teertstra SJ, Lin WY, Gauthier M, Ingratta M, Duhamel J. Comparison of the long range polymer chain dynamics of polystyrene and cis-polyisoprene using polymers randomly labeled with pyrene. Polymer. 2009;50:5456-66.

[48] Andrade JD, King RN, Gregonis DE, Coleman DL. Surface Characterization of Poly(Hydroxyethyl Methacrylate) and Related Polymers .1. Contact-Angle Methods in Water. J Polym Sci Pol Sym. 1979:313-36.

[49] Andrade JD, Ma SM, King RN, Gregonis DE. Contact Angles at the Solid-Water Interface. J Colloid Interf Sci. 1979;72:488-94.

[50] Gentilini C, Boccalon M, Pasquato L. Straightforward synthesis of fluorinated amphiphilic thiols. Eur J Org Chem. 2008:3308-13.

[51] Hoang KC, Mecozzi S. Aqueous solubilization of highly fluorinated molecules by semifluorinated surfactants. Langmuir. 2004;20:7347-50.

[52] Callow ME, Jennings AR, Brennan AB, Seegert CE, Gibson A, Wilson L, et al. Microtopographic cues for settlement of zoospores of the green fouling alga Enteromorpha. Biofouling. 2002;18:237-45.

[53] Hoipkemeier-Wilson L, Schumacher J, Carman M, Gibson A, Feinberg A, Callow M, et al. Antifouling potential of lubricious, micro-engineered, PDMS elastomers against zoospores of the green fouling alga Ulva (Enteromorpha). Biofouling. 2004;20:53-63.

[54] Tait K, Joint I, Daykin M, Milton DL, Williams P, Camara M. Disruption of quorum sensing in seawater abolishes attraction of zoospores of the green alga Ulva to bacterial biofilms. Environ Microbiol. 2005;7:229-40.

[55] Hexemer A, Sivaniah E, Kramer EJ, Xiang M, Li X, Fischer A, et al. Managing polymer surface structure using surface active block copolymers in block copolymer mixtures. J Polym Sci Pol Phys. 2004;42:411-20.

[56] Chaudhury MK, Finlay JA, Chung JY, Callow ME, Callow JA. The influence of elastic modulus and thickness on the release of the soft-fouling green alga Ulva linza (syn. Enteromorpha linza) from poly(dimethylsiloxane) (PDMS) model networks. Biofouling. 2005;21:41-48.

[57] Brady RF. A fracture mechanical analysis of fouling release from nontoxic antifouling coatings. Prog Org Coat. 2001;43:188-92.

[58] Andruzzi L, Senaratne W, Hexemer A, Sheets ED, Ilic B, Kramer EJ, et al. Oligo(ethylene glycol) containing polymer brushes as bioselective surfaces. Langmuir. 2005;21:2495-504.

[59] Yamamoto H, Sakai Y, Ohkawa K. Synthesis and wettability characteristics of model adhesive protein sequences inspired by a marine mussel. Biomacromolecules. 2000;1:543-51.

[60] Aldred N, Clare AS. The adhesive strategies of cyprids and development of barnacle-resistant marine coatings. Biofouling. 2008;24:351-63.

[61] Costerton JW. Introduction to biofilm. Int J Antimicrob Ag. 1999;11:217-21.

[62] Mrksich M. Model substrates for studying and controlling cell adhesion. Abstr Pap Am Chem S. 2000;219:U572-U72.

[63] Prime KL, Whitesides GM. Self-Assembled Organic Monolayers - Model Systems for Studying Adsorption of Proteins at Surfaces. Science. 1991;252:1164-67.

[64] Holland NB, Qiu YX, Ruegsegger M, Marchant RE. Biomimetic engineering of non-adhesive glycocalyx-like surfaces using oligosaccharide surfactant polymers. Nature. 1998;392:799-801.

[65] Snellings GMBF, Vansteenkiste SO, Corneillie SI, Davies MC, Schacht EH. Protein adhesion at poly(ethylene glycol) modified surface. Adv Mater. 2000;12:1959-+.

[66] Vaidya A, Chaudhury MK. Synthesis and surface properties of environmentally responsive segmented polyurethanes. J Colloid Interf Sci. 2002;249:235-45.

CHAPTER FIVE

FUNCTIONAL TRIBLOCK COPOLYMERS CONTAINING QUATERNARY AMMONIUM SALTS AS NON-LEACHING ANTIMICROBIAL SURFACE COATING MATERIALS

ABSTRACT

Polymers with antimicrobial properties have played a significant role in healthcare and many industrial environments. In particular, those with antimicrobial agents covalently attached onto the polymer backbones offer good stability and high antimicrobial effectiveness due to the distinct properties of the polymers. In this work we report two different strategies to prepare antimicrobial polymeric materials based on polystyrene-*block*-poly(ethylene-*ran*-butylene)-*block*-polyisoprene (PS-*b*-P(E/B)-*b*-PI or K3) triblock copolymers. In the first strategy, antimicrobial quaternary ammonium salts (QAS) were covalently linked to the polymer backbone to provide bioactive polymers. In the second approach, we incorporated both bioactive moieties (QAS) and non-adhesive biopassive moieties (PEG) in the polymer to provide dual functional antimicrobial polymers. Both functional polymers were synthesized through multi-step organic synthesis and their chemical structures were confirmed by NMR, IR spectroscopy and elemental analysis. The resulting polymers were then further coated on aminosilane treated glass substrates using spray coating techniques to prepare permanent, non-leaching surfaces, and the surfaces were characterized using water contact angle measurements and FTIC-BSA protein adsorption measurements. Incubating the coated glass substrates with gram-positive bacteria (*S. aureus*), gram-negative bacteria (*E. coli*) and marine bacteria (*C. marina*) species demonstrated that the coated surfaces are distinctly different in their working mechanisms. Unlike bioactive antimicrobial polymers with QAS functionalities alone, dual functional antimicrobial polymer coatings with both QAS and PEG segments can significantly reduce the number of both live and dead bacteria on the surfaces, without killing the cells in the culture media. These polymers offer opportunities for further modification and they may hold potential applications as antimicrobial coatings for biomedical devices and industrial instruments where bacterial adhesion is problematic.

Keywords: non-leaching surfaces, bioactive and biopassive surface coatings, triblock copolymer, antimicrobial coatings, marine antifouling

5.1 Introduction

Microbial infection is a major concern for healthcare and industrial environments, and materials with antifouling and antimicrobial properties are useful in many domains such as food manufacturing, hospitals, building materials, water purification, or marine applications (antifouling paints). Quaternary ammonium salts (QAS) are able to kill microorganisms such as bacteria and fungi by interacting with the cell membrane, allowing release the intracellular contents of organisms [1]. They are now widely used as cationic disinfectants or biocidal coatings to prevent the growth of microorganisms on material surfaces [2]. Small QAS molecules achieve protection by leaching from coatings, but these molecules are often short-lived in the systems and also cause negative environmental impact due to their highly toxic nature. To overcome these problems, anchoring the QAS antimicrobial compounds to a polymer backbone by a covalent non-hydrolysable bond provides a promising approach to develop polymeric materials which not only show high antibacterial activity, but also offer long term stability and uniformity. Currently, such polymeric products containing QAS antibacterial components are commercially available and have found remarkable utility in hygiene and in biomedical applications [3]. Compared to small molecules with the same functional groups, functional polymers containing QAS also have potential advantages because their characteristic properties mainly depend on the extraordinarily large size of the polymer molecules. The interaction of polycations with the negatively charged cell surface can also take place to a greater degree than that of monomeric cations due to the high charge density carried by the polymers.

Microbial growth and biofilm formation is also problematic in the marine environment. It is believed that adhesion and aggregation of thin layer of organic matter and microbes on surfaces help to form biofilms [4,5], and bacteria are usually dominant components of biofilms

owing to their high abundance in sea water. Biofilms are instrumental to habitat selection and settlement of many sessile marine organisms, such as invertebrate larvae and microalgae spores, and in turn can modify and manipulate surface chemical and physical conditions and leads to more serious fouling. Ultimately, they can pose a serious threat to the safe and efficient operation of marine vessels and equipment, and consequently lead to excessive consumption of energy and enormous economic losses for maritime industries [6]. Recently, materials with non-leaching, chemically bound antimicrobial moieties for the control of marine biofouling have been explored and it is a subject of much interest and extensive research. Synthetic polymers have become particularly popular in this area because their chemical and physical properties, such as length scales, surface chemistries, architectures, and mechanical strength, which can be tailored for specific usages. Various synthetic routes have been developed for covalent bonding of antimicrobial functional groups to the polymeric materials for surface preparation, resulting in materials that can be used in either biopassive or bioactive surface preparations [7]. Biopassive surfaces reduce the adsorption of proteins and thus reduce the adhesion of microorganisms, while bioactive surfaces kill microorganisms on contact. In recent years, new platforms have also been developed to overcome the issue of biofouling by incorporating the active moiety into a biopassive background, thereby providing the surface with both biopassive and bioactive functionalities. It could be proposed that a combination of these two different mechanisms of antibacterial action should result in a very effective antibacterial coating. A successful example of this type of dual function coatings is one in which the antimicrobial agent vancomycin is attached to the surface through a poly(ethylene glycol) or PEG linker [8]; the PEG linker prevents protein adsorption and thus maintains the efficacy of the antimicrobial agent. It also allowed the detachment of dead cells and cell material by a simple rinsing step, while the

immobilized vancomycin leads to reduced numbers of live bacteria and increased numbers of dead bacteria on the surface.

In the present study, we aim to prepare non-leachable polymer coatings with probable antimicrobial and/or antifouling activities based on modification of polystyrene$_{8k}$-*block*-poly(ethylene-*ran*-butylene)$_{25k}$-*block*-polyisoprene$_{20k}$ (abbreviated as PS-*b*-P(E/B)-*b*-PI or K3) triblock copolymer. The PS-*b*-P(E/B)-*b*-PI triblock copolymer has been previously used by us for marine antifouling/fouling release applications [9,10], it is specifically designed to optimize the surface segregation of side chain functional moieties. In the PS-*b*-P(E/B)-*b*-PI triblock copolymer, the polystyrene block was used to mechanically tether a thin layer of the functionalized triblock copolymer and deliver chemical functionality to the surface, and the poly(ethylene-*ran*-butylene) block serves as a "molecular spacer" that gives the functionalized isoprene block a greater ability to explore its conformational space and segregate to the surface. The polyisoprene block has double bonds which can be chemically modified to provide desired functional groups and deliver those functional groups on the surfaces. Previously, Park et al. [11] have prepared semifluorinated-quaternized PS-*b*-P(E/B)-*b*-PI triblock copolymer by using the quaternization reaction of semifluorinated hexylbromide with aminated PS-*b*-P(E/B)-*b*-PI polymer, and antibacterial experiments showed that the polymer surfaces were highly antibacterial against airborne *S. aureus* with > 99% inhibition. However, antibacterial activity against gram-negative bacteria *C. marina* on the surfaces only showed moderate results, and these materials did not exhibit good antifouling/fouling release properties for marine algae, probably because the high density of the positively charged N^+ sites promoted strong electrostatic attraction between the surfaces and algal cells. Unfortunately, no bacteria in liquid media was used for testing in this study; it is difficult to establish the relationship between

airborne antibacterial activities with under water antifouling activities on those surfaces, since polymers containing perfluocarbons have been shown to be surface active and can undergo surface reconstruction when the environments change from air to water [10]. In addition, although a few cationic polymers possessing perfluoroalkyl groups were reported as antibacterial materials [12-14], those structures are not naturally presented in cell membranes and they can bio-accumulate and therefore pose safety concerns [15]. Many unique properties of perfluorocarbons, such as low solubility, weak intermolecular attractive forces, and low surface tension, may also strongly influence their biological activities [16,17]. In contrast, non-fluorinated polymers are more environmentally friendly, and quaternary ammonium compounds containing long hydrocarbon terminal chains have been proven to be highly effective towards a broad range of microbials [2,18-20], including both gram-positive and gram-negative bacterial species.

To further explore the potential of PS-*b*-P(E/B)-*b*-PI triblock copolymers as stable, non-leaching surface coatings to provide long term protection against bacterial infection and colonization, in this work, we report two different strategies to modify the triblock copolymer with quaternary ammonium groups containing long alkyl chains. In the first strategy, antimicrobial quaternary ammonium salts (QAS) were attached to the polymer backbones to provide bioactive polymers (K3-QA100-HC) whose quaternary ammonium units were intended to kill bacterial cells. In the second approach, we incorporated both the bioactive moieties (QAS) and the non-adhesive bio-passive moieties (PEG) in the polymer to provide dual function polymers (Figure 5.1). PEG was chosen as bio-passive side chains because it has been extensively studied to reduce the protein absorption on biomaterial surfaces, and it also discourages the adhesion of bacteria by reducing the contact between the bacteria and the surface

without killing them [21,22]. More importantly, PEGs have been widely used in biomedical applications, and have shown excellent biocompatibility. Alternatively, quaternary ammonium compounds may serve as bacterial repellents in the polymer system, since bacterial cells tend to avoid toxic materials, and the surface tethered QAS can also actively kill the bacteria that has attached to the surfaces. In both approaches, all the functional moieties were covalently linked to the PS-*b*-P(E/B)-*b*-PI polymer backbone through non-hydrolysable amine bonds. The resulting polymers were applied on glass surfaces and incubated with several predominant infecting organisms (gram-positive *S. aureus*, gram-negative *E. coli* and marine bacteria *C. marina*) in culture media for a sufficient period of time to test their antimicrobial activities in aqueous environments. The ultimate goal of this study was to provide two different types of antimicrobial polymers based on different working mechanisms (killing vs. repelling), and use them as environmentally friendly, non-leachable surface coatings. We were also interested in testing a simple and effective model system to monitor the behavior of bacterial cells both in the culture media and on the functional polymer coated surfaces, and use it to compare the abilities of different coatings against biofilm formation, without using the elaborate flow chamber devices [23]. The resulting polymers may provide insight for designing future highly effective antimicrobial polymeric materials, and may also hold many potential applications such as biomedical device coatings and other coatings for industrial instruments, especially where different types of antimicrobial coatings are needed for each specific working environment.

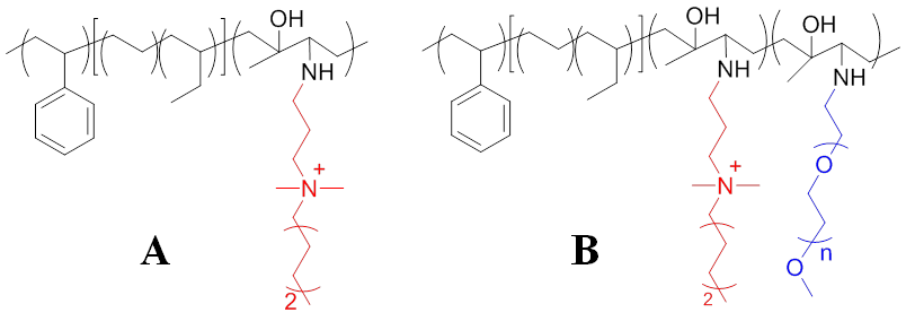

Figure 5.1: Chemical structures of QAS/PEG modified polymers. A) bioactive quaternary ammonium salts (QAS, red) modified and B) both bioactive QAS and biopassive poly(ethylene glycol) (blue) modified PS-b-P(E/B)-b-PI triblock copolymers.

5.2 Materials and Methods

5.2.1 Materials

Monomethylated poly(ethylene glycol), M_w = 550 (mPEG 550), N,N-dimethylformamide (DMF), 1-methyl-2- pyrrolidinone (NMP), tetrahydrofuran (THF), methylene chloride, 3-(dimethylamino)-1-propylamine (DMAPA), sodium azide (NaN_3), and 1-bromohexane ($C_6H_{13}Br$) were purchased from Aldrich and used as received. Methanesulfonyl chloride, Triphenylphosphine (TPP), potassium carbonate, and *m*-chloroperoxybenzoic acid (*m*CPBA) were purchased from Sigma-Aldrich. The polystyrene$_{8k}$-*block*-poly(ethylene-ran-butylene)$_{25k}$-*block*-polyisoprene$_{20k}$, (PS-*b*-P(E/B)-*b*-PI) triblock copolymer was produced using anionic polymerization and subsequent catalytic hydrogenation by Kraton Polymers. Polystyrene-*block*-poly(ethylene-*ran*-butylene)-*block*-polystyrene (SEBS) triblock thermoplastic elastomers (Kraton MD6945) and SEBS grafted with maleic anhydride (MA-SEBS, Kraton FG1901X) were also provided by Kraton Polymers. All other chemicals were purchased from Sigma-Aldrich and used without further purification.

5.2.2 Material and Surface Characterizations.

The elemental analyses for C, H, N of polymers were performed by Quantitative Technologies, Inc. (QTI). The polymer films for IR spectra of polymers were formed on sodium chloride salt plates and the spectra were obtained using a Mattson 2020 Galaxy Series FTIR spectrometer. Static water contact angles on various quaternary amine coatings were measured at room temperature using a contact angle goniometer from KSV Instruments Ltd. The contact angles were measured after the water droplet was placed on the samples at times of 0, 30, 60, 120, and 180 s. Every data point is the averaged angle measured at three random spots on each sample.

5.2.3 Polymer Synthesis and Characterization

Various molar ratios of PEG and QAS were used to prepare dual functional polymers (feeding ratio at 30:70, 50:50, 70:30 mol/mol), however, initial bacterial studies have shown that all of the dual functional polymer coated surfaces have similar antimicrobial properties, although more dead cells were observed on the surfaces with a QAS/PEG ratio of 70:30. Polymer coatings with a QAS/ PEG ratio of 30:70 gave the best cell repelling results. Therefore, only this polymer sample was used to carry out all the testing experiments and was reported here, and it was also used to compare with bioactive QAS modified triblock copolymers (K3-QA100-HC).

Synthesis of Poly(ethylene glycol) mesylate (mPEG550 methylate). In a dry 500 mL round bottom flask, mPEG (10.0 g, 18.2 mmol) was dissolved in anhydrous dichloromethane (250 mL), triethylamine (9.2g, 90.9 mmol) and methanesulfonyl chloride (10.4g, 90.9 mmol) were added to the solution and then the reaction mixture was stirred overnight under nitrogen at room

temperature. The precipitated triethylammonium hydrochloride salts were removed by vacuum filtration, and the filtrate was rotary evaporated to dryness, the filtrate was then dissolved in 200 mL distilled water. After extraction with dichloromethane, the dichloromethane layer was dried over anhydrous $MgSO_4$, and the concentration of the solution yielded the desired mPEG mesylate in 95% as pale yellow liquid. ^{1}H NMR (300 MHz, $CDCl_3$, δ): 4.38 (m, 2H, -**CH**$_2$OSO$_2$-), 3.45-3.83 (m, -O**CH$_2$CH$_2$**O-), 3.38 (s, 3H, **CH$_3$**O-), 3.09 (s, 3H, **CH$_3$**SO$_3$-). ^{13}C NMR (300 MHz, $CDCl_3$, δ): 71.88, 70.59, 69.34, 68.97, 58.97, 37.80.

Synthesis of Poly(ethylene glycol) Methyl Ether Amine (mPEG 550 amine). mPEG mesylate (7.0 g, 11.1 mmol) was added drop wise to the suspension of NaN_3 (1.1g, 16.9 mmol) in 350 mL of DMAC over a period of 30 min, the reaction mixture was then stirred overnight at 100 ^{o}C with aluminium foil coating the reaction flask to protect the material from light. After the reaction, DMAC was reduced under vacuum before 100 mL of dichloromethane was added. A solid precipitate was removed with vacuum filtration and the dichloromethane was then removed with vacuum to yield intermediate azide. The conversion was confirmed by the appearance of a sharp azide stratch at 2100 cm^{-1} in the IR spectrum [24]. The dried azide sample was dissolved in 300 mL anhydrous tetrahydrofurane (THF), and triphenylphosphone (8.73 g, 33.3 mmol) was added. The solution was stirred at room temperature for 4 h before adding 4 mL of water and stirring overnight. THF was removed in *vacuo* after the reaction, and 200 mL water was added, the white precipitate was removed by vacuum filtration and the filtrate washed with toluene (3 x 100 mL). The water was removed in *vacuo* to yield the product as light yellow oil. ^{1}H NMR (300 MHz, $CDCl_3$, δ): 3.48-3.65 (m,-O**CH$_2$CH$_2$**O-), 3.37 (s, 3H, **CH$_3$**O-), 2.95(s, 2H, -**CH$_2$**NH$_2$), 1.93 (s, 2H, -CH$_2$**NH$_2$**). ^{13}C NMR (300 MHz, $CDCl_3$, δ): 73.32, 71.77, 70.82, 58.73, 41.52.

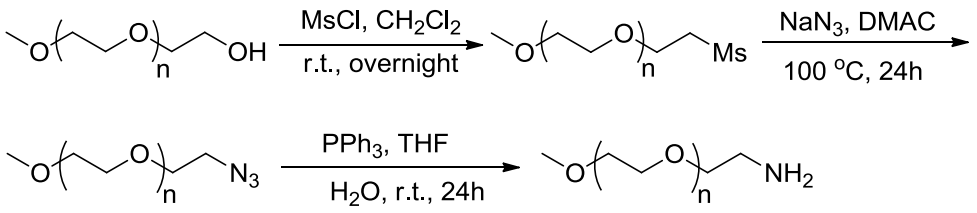

Figure 5.2: Synthesis of poly(ethylene glycol) methyl ether amine (mPEG-NH_2)**.**

Epoxidation of PS-b-P(E/B)-B-PI. In a typical epoxidation reaction, the PS_{8K}-*b*-$P(E/B)_{25K}$-*b*-PI_{10K} triblock copolymer (5.0 g, 14.5 mmol of reactive isoprene sites) was dissolved in cyclohexane (4 % w/v) in a round-bottomed flask. 3-meta-Chloroperoxybenzoic acid (*m*CPBA, 3.9 g, 17.4 mmol) was added to the mixture, and the solution was stirred vigorously for 6 h at room temperature. Subsequently, the polymer was precipitated in 500 mL methanol, collected by filtration, and re-precipitated to remove residual *m*CPBA and its respective byproducts. The white rubbery product was dried at room temperature under reduced pressure for 48 h to remove remaining solvent. ^{1}H NMR for epoxidized PS_{8K}-*b*-$P(E/B)_{25K}$-*b*-PI_{10K} (300 MHz, $CDCl_3$, δ): 6.58, 7.07, (5H, styrene), 2.65 (br s, 1H, epoxidized isoprene, -CH_2C**H**$(O)C(CH_3)CH_2$-), 0.80, 0.85, 1.25, 1.48, 1.87 (backbone). IR (dry film) υ_{max} (cm^{-1}): 2926, 2855 (C-H stretching); 1465, 1380 (C-H bending); 906 (C-O-C asymmetric stretching); 700 (C-H bending, aromatic).

Amination of Epoxidized PS-b-P(E/B)-B-PI. Epoxidized PS-*b*-P(E/B)-*b*-PI (2.1 g, 5.8 mmol of epoxy) was dissolved in 50 mL of NMP in a 300 mL round bottom flask at 90 °C, DMAPA and mPEG amine at ratio of 3:7 (mol/mol) and TPP (0.4 g, 1.6 mmol) were added to the solution, the amination reaction was performed for 48 h at 160 °C under reflux. The aminated block

copolymer (with tertiary ammonium salts or abbreviated as TA) was precipitated in excess hot distilled water, filtered, dissolved in 50 mL of NMP, re-precipitated in excess distilled water, filtered, and dried under reduced pressure at room temperature for 48 h.

K3-TA100-HC: ^{1}H NMR (300 MHz, CDCl3, δ): 6.58, 7.21, (br, styrene), 3.19 (s, -NHC**H**$_2$CH$_2$-), 2.67 (br s, 1H, epoxidized isoprene, -CH2C**H**(O)C(CH3)CH2-), 2.33 (m, -CH$_2$-C**H$_2$**-N(CH$_3$)$_2$), 2.21 (s, -CH$_2$-N(C**H$_3$**)$_2$), 1.85 (m, -NHCH$_2$C**H$_2$**CH$_2$-),0.82, 1.25, 1.47, 1.61 (backbone). IR (dry film) υ_{max} (cm^{-1}): 3400 (br, O-H stretching, N-H stretching), 2926, 2855 (C-H stretching); 1603 (N-H bending), 1465, 1379 (C-H bending); 900-1260 (C-N stretching), 700 (C-H bending, aromatic).

K3-TA30-PEG70: ^{1}H NMR (300 MHz, CDCl3, δ): 6.58, 7.21, (br, styrene), 3.44-3.68 (m, -O**CH$_2$CH$_2$**O-), 3.38 (t, C**H$_3$**O- and –NH**CH$_2$**-), 3.18 (s, -NHC**H**$_2$CH$_2$-), 2.65 (br s, 1H, epoxidized isoprene, -CH2C**H**(O)C(CH3)CH2-), 2.38 (m, -CH$_2$-C**H$_2$**-N(CH$_3$)$_2$), 2.23 (s, -CH$_2$-N(C**H$_3$**)$_2$), 2.02 (m, -NHCH$_2$C**H$_2$**CH$_2$-),0.82, 1.25, 1.84(backbone). IR (dry film) υ_{max} (cm^{-1}): 3400 (br, O-H stretching, N-H stretching), 2926, 2855 (C-H stretching); 1600 (N-H bending), 1465, 1380 (C-H bending); 1100-1200 (C-N stretching), 1070 (C-O stretching), 700 (C-H bending, aromatic).

Quaternization of Aminated PS-b-P(E/B)-b-PI. Aminated PS-*b*-P(E/B)-*b*-PI (2.1 g) was dissolved in 20 mL of DMF in a 100 mL round bottom flask at 90 °C. Excess amount of hexyl bromide compound (7.0 g, 42.4 mmol) and potassium carbonate (1.6 g, 11.6 mmol) were added to the reaction mixture. The quaternization reaction was performed for 48 h at 90 °C under a nitrogen atmosphere. Following completion of the reaction, most of DMF was removed using a rotary evaporator. The resulting quaternary amines were precipitated in excess diethyl ether,

filtered, dissolved in 5 mL of DMF, re-precipitated in excess diethyl ether. The final products were filtered and dried under reduced pressure at room temperature for 48 h.

K3-QA100-HC: ^{1}H NMR (300 MHz, CDCl3, δ): 6.58, 7.21, (br, styrene), 3.42-3.56 (m, -O**CH_2CH_2**O-), 3.38 (t,–NH**CH_2-**), 2.62 (m, -CH_2-C**H_2**-N(CH_3)$_2$), 2.38 (s, -C**H_2**-N^+(C**H_3**)$_2$-), 1.72 (m, -NHCH_2C**H_2**CH_2-), 0.75, 0.85, 1.26, 1.35 (backbone and saturated hydrocarbons). IR (dry film) υ_{max} (cm-1): 3400 (br, O-H stretching, N-H stretching), 2926, 2855 (C-H stretching); 1617 (N-H bending), 1465, 1380 (C-H bending); 1000-1200 (C-O stretching, C-N stretching), 970 (quaternary nitrogen), 700 (C-H bending, aromatic). Elemental analysis: C (54.29%), O (10.57%), and N (3.94%).

K3-QA30-PEG70: ^{1}H NMR (300 MHz, CDCl3, δ): 6.58, 7.21, (br, styrene), 3.44-3.75 (m, -O**CH_2CH_2**O-), 3.38 (t, C**H_3**O- and –NH**CH_2-**), 3.20 (s, -N^+(CH_3)$_2$C**H_2**CH_2-), 2.82 (s, -C**H**(CH_2)$_2$NH-), 2.56 (m, -CH_2-C**H_2**-N(CH_3)$_2$), 2.36 (s, -C**H_2**-N^+(C**H_3**)$_2$-), 2.02 (m, -NHCH_2C**H_2**CH_2-), 0.82, 1.25, 1.84 (backbone and saturated hydrocarbons). IR (dry film) υ_{max} (cm-1): 3400 (br, O-H stretching, N-H stretching), 2926, 2855 (C-H stretching); 1600 (N-H bending), 1465, 1380 (C-H bending); 1100-1260 (C-O stretching, C-N stretching), 1070 (C-O stretching), 970 (quaternary nitrogen), 700 (C-H bending, aromatic). Elemental analysis: C (75.14%), O (10.99%), and N (0.41%).

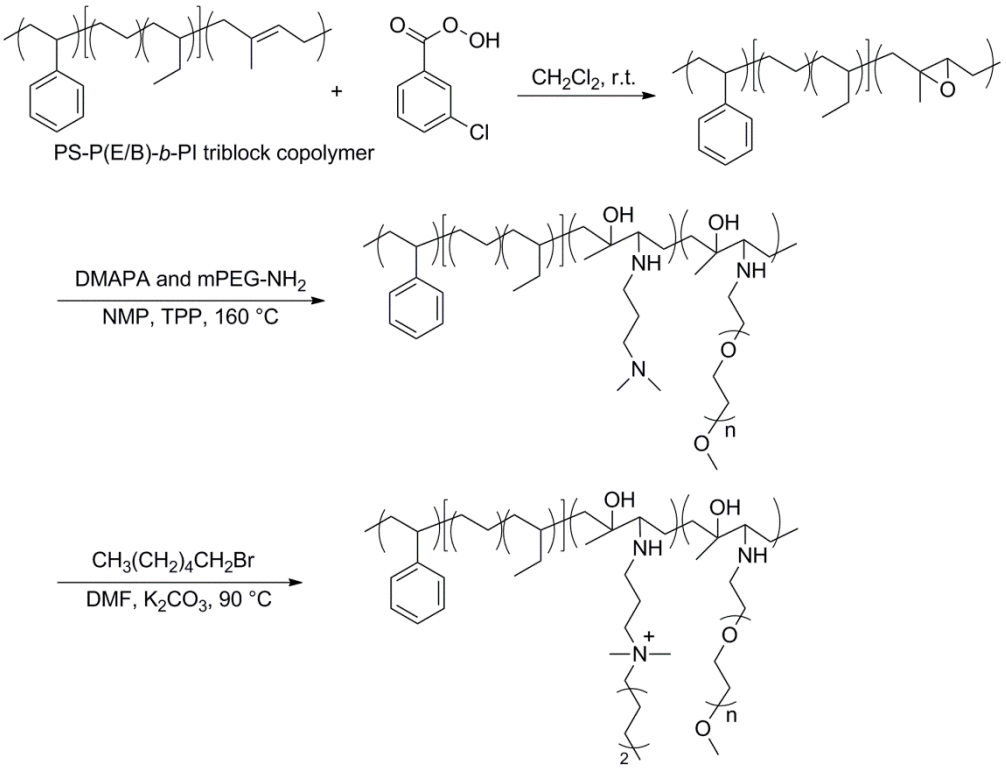

Figure 5.3: Synthesis of QAS/PEG modified triblock polymers**.** Synthesis of dual functional quaternary amine salt (QAS) and poly(ethylene glycol) (PEG) modified PS-b-P(E/B)-b-PI (also abbreviated as K3) triblock copolymers. The bioactive QAS modified triblock copolymer (K3-QA100-HC) was prepared in the same fashion without using mPEG-NH2 side chains.

5.2.4 Surface Preparation with Functionalized Polymers

To prepare surfaces with modified PS-*b*-P(E/B)-*b*-PI triblock copolymers for antimicrobial and biofouling assays, polymers were coated on glass slides through multilayer coating techniques using similar procedures as previously reported [25] with mild modification. First the standard microscope glass slides were sequentially treated with freshly prepared piranha solution and (3-Aminopropyl)trimethoxysilane solution (2.5 g/mL in ethanol). The clean and dried glass slides were then spin coated with polystyrene-*b*-poly(ethylene-*ran*-butylene)-*b*-polystyrene (SEBS, 2% in toluene) triblock thermoplastic elastomers and SEBS grafted MA-SEBS (5% in toluene) base layer, followed by annealing at 120 °C for 12 h in vacuum oven. For

antimicrobial assay, the solutions of polymers in chloroform (1.5 %, w/v) were spray-coated on the prepared base layer coated glass slides using a Badger 250 airbrush. The coated surfaces were annealed under a vacuum at 60 °C for 12 h, followed by an additional 12 h at 120 °C, and stored in dark at room temperature until use (Figure 5.4).

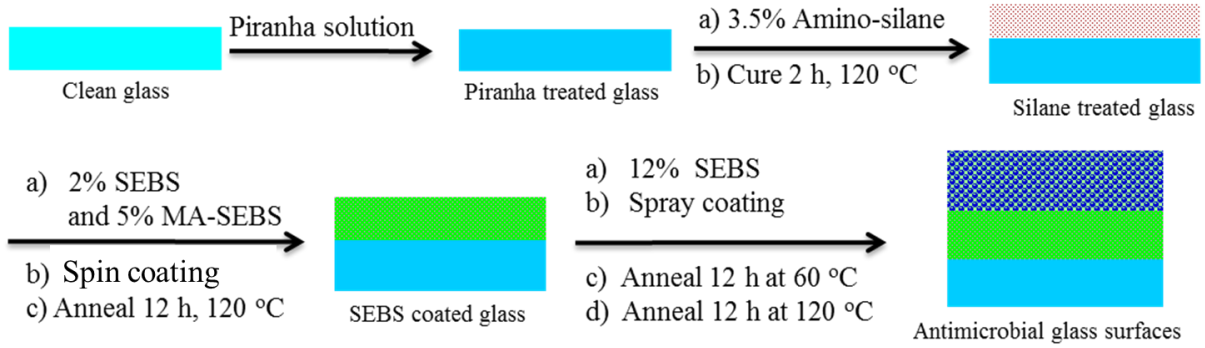

Figure 5.4: Surface preparation of antimicrobial triblock copolymers on glass substrates. Surface preparation of functional triblock copolymers on glass substrates for antimicrobial applications.

5.2.5 Protein Absorption Tests

Protein adsorption of the surfaces was tested toward FITC-labeled BSA (Sigma, 0.1 mg/ml in PBS buffer) at room temperature. The coated glass slides with polymer films were soaked in the protein solution for 2 hours before taken out of the solution and rinsed with deionized water. The dried slides were then immediately analyzed with a fluorescent microscope. The average fluorescence intensity was assumed to be directly proportional to the amount of adsorbed proteins. Fluorescence images were recorded on an Olympus fluorescence microscope (upright BX51, Olympus, Roper Cool Snap hx CCD camera, Japan) using a 10x objective (excitation, 470 nm; emission, 525 nm), and the fluorescence intensities were measured using ImageProPlus software. Each sample was measured three times and reported as mean $\pm$ SD.

5.2.6 Measurement of Antimicrobial Activity

All bacteria cell cultures were prepared by Dr. David Miller in Prof. Ester R. Angert's laboratory (Cornell University). Samples of bacteria (*S. aureus*, *E. coli*, or *C. marina*) were grown overnight with the growth medium in a sterilized 50 mL conical tube. Trypticase Soy Broth (TSB, 5 mL; per liter: 3 g of soy meal peptone, 17 g of casein peptone, 2.5 g of glucose, 5 g of NaCl, and 2.5 g of dipotassium hydrogen phosphate) was used for *S. aureus* and *E. coli* at 37 ^{o}C, and marine broth was used for *C. marina* culture at 30 ^{o}C. In the next day, fresh medium was inoculated with bacteria and the culture was allowed to grow for 2 hours or more to ensure bacteria were in exponential growth, and this culture was further used to inoculate 50 mL sterile Sarstedt tubes. 10 µL of the fresh culture was added to 25 mL of the appropriate growth medium, and the coated glass slides were also placed in the culture tubes. The tubes were put on a rocking platform so that the coated surface was facing up and parallel to the liquid surface, and ensuring the slide surfaces were covered with culture liquid at all times while they were on the rocker. The tubes were allowed to incubate for 48 h at room temperature. After 48 h of incubation, 1 mL of each cell culture was taken from the culture tube, and was used to measure OD_{600} immediately, and sterile clean culture medium was used to blank the spectrophotometer. For the samples with OD_{600} readings greater than 1.0, they were also diluted appropriately with fresh culture medium to obtain more accurate readings. Each sample was measured three times and reported as an average.

After 2 days of incubation, the coated slides were taken out of the solution and rinsed three times with distilled water. The viability of the cells was tested using LIVE/DEAD BacLight bacterial viability kit (Molecular Probes.). Equal volumes (1.5 µL) of SYTO 9 and propidium iodide were mixed thoroughly in a micro-centrifuge tube with 0.5 mL of sterilized DI

water. 5 μL of the staining solution was added to each glass slide surface, and the surfaces were immediately covered with thin clear glass coverslips, followed by incubating in the dark for 10 min at room temperature. Phase-contrast and fluorescence microscopy were performed using an Olympus BX61 epifluorescence microscope with a 100× UPlanApo (N.A.135) objective. The microscope was equipped with filter cubes for viewing SYTO 9 and propidium iodide fluorescence. Clean glass microscope slides were used as controls. Three separate trials were carried out in triplicate for each assay trial, and the values reported are the average of the three trials.

5.3 Results and Discussion

5.3.1 Polymer Synthesis and Characterization

In this work, we use quaternary ammonium salts to modify pre-synthesized PS-*b*-P(E/B)-*b*-PI (abbreviated as K3) triblock copolymer to prepare non-leaching antimicrobial/antifouling surfaces. Two strategies were reported to prepare the final functionalized polymers. In the first strategy, quaternary ammonium salts (QAS) alone were used as side chains to modify the K3 polymer backbones to prepare bioactive surfaces (K3-QA100-HC). In the second strategy, both quaternary ammonium salts and PEG units were included as side chains to prepare dual functional polymers for surface coatings (K3-QA30-PEG70), where long PEG chains provide non-adhesive backgrounds and QAS chains further repel/kill the bacterial cells. Three-step reactions were carried out to synthesize each functionalized copolymers from starting polymer K3 (Figure 5.3), although for functionalized triblock copolymers with both QAS and PEG, several extra steps have to be taken to prepare mPEG-amine (Figure 5.2), because purchase of amine functional poly(ethylene glycol) methyl ether is highly cost prohibitive. For polymer

modification reactions, the backbone triblock copolymer PS-*b*-P(E/B)-*b*-PI was first epoxidized to introduce epoxy functional rings for the next step amination attachment reaction (Figure 5.3). The epoxidization reaction was carried out in a mild reaction condition and the reaction product was obtained at high yield (95%). In the next step, the synthesized mPEG-amine was mixed with DMAPA at different molar ratios (100:0, 30:70), and then reacted with PS-*b*-P(E/B)-*b*-PI backbone triblock polymer. The amination reactions with epoxidized PS-*b*-P(E/B)-*b*-PI was relatively difficult, reactions were run at 160 °C for 48 h, the reaction products were purified by precipitation method and were followed by quaternization reaction. Excess 1-bromohexane was used in the final reaction step under basic conditions, and the reaction was performed for 48 h at 90 °C. Elemental analysis (Table 5.1) was used to confirm the chemical composition of the final modified PS-b-P(E/B)-b-PI (or K3) triblock copolymer, incorporation of PEG (70% mol/mol) in the polymer reduces the content of nitrogen (N%) in the final products from 3.94% to 0.41%.

Table 5.1. Feed ratios of QAS and PEG during amination reaction of triblock copolymers and elemental analysis results of final polymers. The starting material K3 was also listed for comparison.

	Feeding Ratio (n/n)		Elemental Analysis		
Name	**QAS**	**PEG**	**C%**	**H%**	**N%**
K3	NA	NA	86.26	13.56	<0.05
K3-QA100-HC	100.00	0.00	54.29	10.57	3.94
K3-QA30-PEG70	30.00	70.00	75.14	10.99	0.41

The completion of each reaction steps can be easily identified from ^{1}H NMR spectra (Figure 5.5). Epoxidation reaction of the starting materials showed that there was no longer evidence of any alkene protons (5.0-5.5 ppm), and a significant peak at 2.65 ppm appeared indicating the presence of protons adjacent to the newly formed oxirane rings on the

polyisoprene block of the polymer backbone. After amination reaction, ^{1}H NMR spectra showed

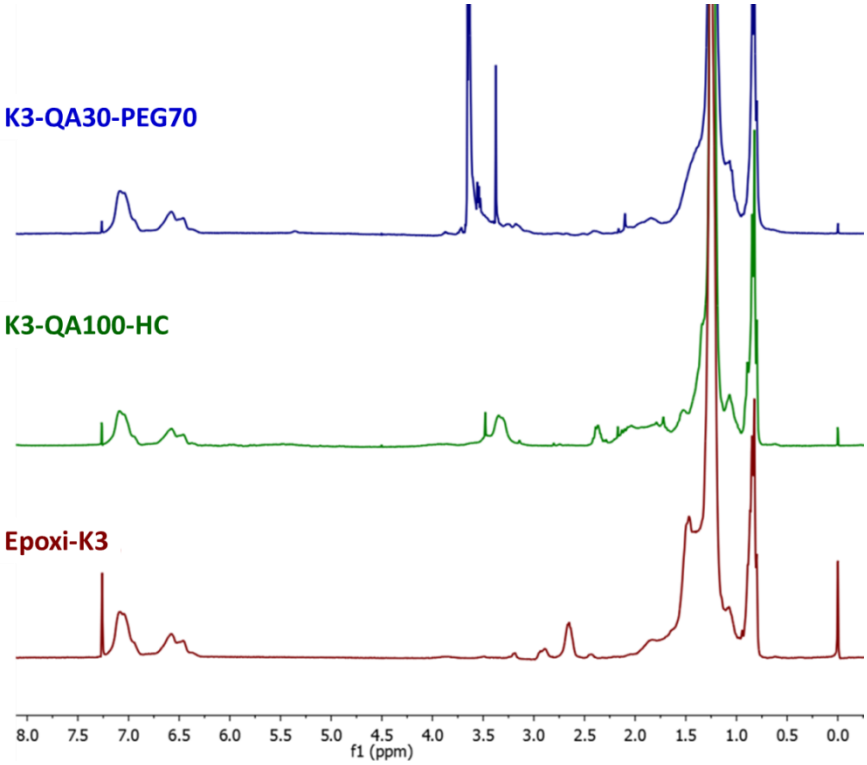

Figure 5.5: ^{1}H NMR spectrum of QAS/PEG modified triblock copolymers**.** ^{1}H NMR comparison of epoxidized K3, K3-QA100-HC and K3-QA30-PEG70 polymers.

the disappearance of epoxy rings in the backbone polymer (2.65 ppm) and appearance of new peaks (3.1-3.7 ppm for PEG, and 1.7-3.0 ppm for DMAPA). Quaternization of the tertiary amine was also confirmed by ^{1}H NMR spectroscopy, 3.80-3.20 ppm hold multiple broad peaks corresponding to -CH_2CH_2O- of PEG side chain, -$N^+(CH_3)_2CH_2(CH_2)_4CH_3$ and -OCH_3 chain end of PEG. 2.70-1.70 ppm indicates -CH_3 of the polymer backbone and –$N^+(CH_3)_2CH_2(CH_2)_4CH_3$ of the side chain. Peaks around 1.7-0.7 ppm are from the polymer backbone and –$N^+(CH_3)_2CH_2(CH_2)_4CH_3$ of the side chain, a significant increase in the number of hydrogen atom signals in this region also indicated the completion of quaternization reactions. Peaks at 3.50

ppm in ^{1}H NMR spectra also confirmed the presence of the quaternary amines in the polymers. In addition, the difference of K3-QA100-HC and K3-QA30-PEG70 can also be distinguished by NMR spectra, where PEG has significant signals from 3.4-3.8 ppm, and $–OCH_3$ has a sharp peak at 3.38 ppm.

Infrared spectroscopy (IR) is a useful tool to characterize polymeric materials. In this study, the polymers were dissolved in chloroform and carefully cast on the sodium chloride salt plate to form a thin film. The characteristic absorption of the starting polymer PS-*b*-P(E/B)-*b*-PI can be found at 2926, 2855 cm^{-1} (-C-H stretching), 1463, 1385 cm^{-1} (-C-H bending), 965 cm^{-1} (=C-H bending), and 700 cm^{-1} (aromatic –C-H bending). After the epoxidation reaction, the sharp double bond peak at 965 cm^{-1} disappeared, and new absorption peaks appeared around 906 cm^{-1} and 1050 cm^{-1} corresponding to the epoxidized isoprene (-C-O-C- stretching) in the epoxidized PS-*b*-P(E/B)-*b*-PI triblock copolymer (Figure 5.6). The amination reactions introduced new bands at 1600 cm^{-1} (-N-H bending), 1100-1200 cm^{-1} (C-N stretching), and -N-H stretches at 3300 cm^{-1}, indicating the existence of new functional groups from DMAPA and PEG in the polymers. The changes in the IR spectrum after quaternary ammonium salt formation were minimal, a small band at 968 cm^{-1} can be assigned to quaternary nitrogen. In K3-QA100-HC spectrum, the 1463, 1385 cm^{-1} (-C-H bending) peaks were particularly stronger compare to K3 and Epoxi-K3, because high amount of saturated carbon terminal groups were introduced to the system. The strong, broad peak at 1000-1200 cm^{-1} in K3-QA30-PEG70 also proves the existence of PEG functionalities (-C-O-C- stretching). In general, IR spectra support the view that the QAS and PEG units have been successfully introduced into each functional polymer system.

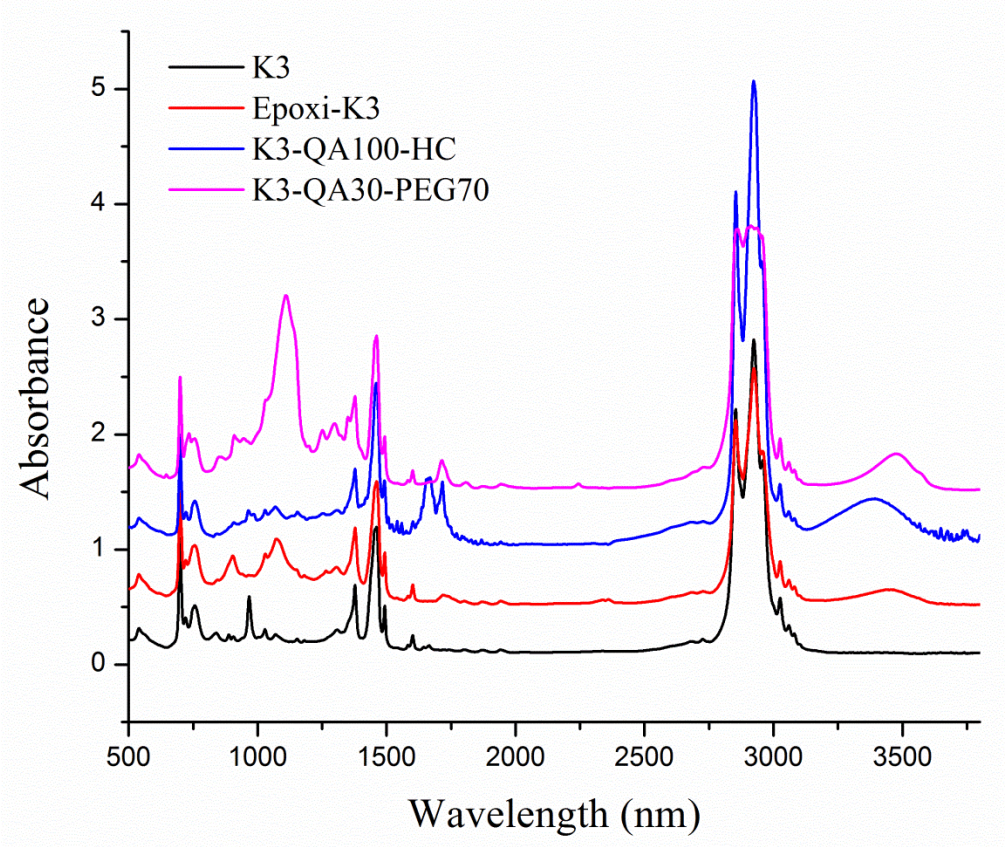

Figure 5.6: IR spectra of QAS functionalized polymers compared with unmodified PS-*b*-P(E/B)-*b*-PI (K3) and epoxidized PS-*b*-P(E/B)-*b*-PI (epoxy-K3) triblock copolymers.

5.3.2 Surface Characterization Of Polymer Coated Glass Substrates

Static water contact angle measurements (Figure 5.7) suggest that the surfaces of quaternary ammonium salt modified polymer samples become more hydrophilic after contacting with water in just a few minutes, while the control sample (K3) showed very small changes during the tests. PS-*b*-P(E/B)-*b*-PI polymer linked with only quaternary ammonium salts (K3-QA100-HC) coated surfaces exhibited the lowest starting contact angle (33.5°) among all the samples tested, and the angles reduced to 23.3° after only 3 min in contact with water. We also tested water contact angles of previously published semifluorinated-quaternized PS-*b*-P(E/B)-*b*-PI triblock copolymer coated surface, and the angles went down from 85.3° to 19.7° during the

same period of time. The contact angle changes in both polymer systems might be caused by the dynamic surface reconstruction in water/air interface. In air, low surface energy saturated hydrocarbon or perfluorocarbon chains are most likely to segregate to the surface, giving higher water contact angles, but while in contact with water, quaternary ammonium salts quickly absorbed water and resulted in reduced contact angles. Similar phenomena were also observed on the K3-QA30-PEG70 coated surfaces, the contact angles changed from 87.3° to 77.0° within three minutes after contact with water, due to highly hydrophilic QAS components and long PEG chains. Although in general, the contact angles of K3-QA30-PEG70 polymer surfaces are much higher than QAS modified surfaces alone, probably because there is much less of the highly hydrophilic, charged QAS moieties in the polymer system (30% *vs.* 100%). In addition, the long PEG chains also provide more steric hindrance which can make the active surface reconstruction under water more difficult, so it might take much longer time for the low surface energy saturated hydrocarbon chains to move away from the surfaces, therefore, the surfaces showed higher water contact angles or more hydrophobic characteristics. In summary, contact angle measurements in this study suggested the functional polymer coated surfaces can exhibit different hydrophobicity in air and under water. Since hydrophobicity of the material surfaces is one of the most important factors which govern the mechanism of bacterial adhesion [26], the results indicated the importance of conducting experiments in aqueous environments for *in vitro* and *in vivo* biomedical or marine antimicrobial/antifouling applications, although it is also very useful to study the antibacterial effectiveness of the surfaces for airborne bacteria as described in a previous study [11].

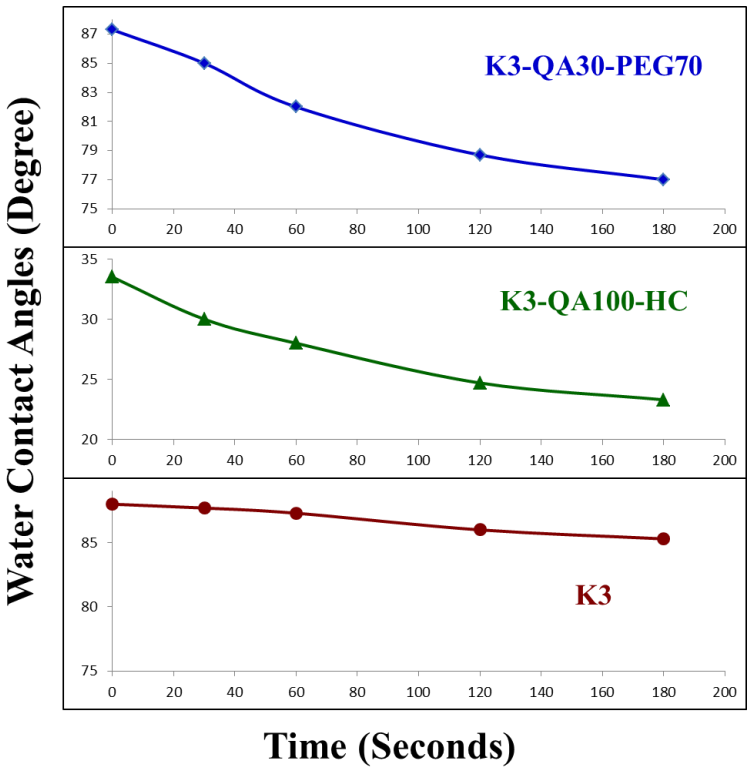

Figure 5.7: Water contact angles of surfaces coated with starting material K3 and quaternary ammonium salt modified triblock copolymers (K3-QA100-HC and K3-QA30-PEG70).

5.3.3 Protein Absorption Tests And Evaluation Of Antimicrobial Activities

Serum or tissue proteins, such as albumin, fibronectin, laminin, and denaturized collagen, can promote or inhibit bacterial adhesion by either binding to the substrate, or binding to the bacterial surface or by just being present in the liquid medium during the adhesion process [27]. In particular, albumin is one of the most abundant proteins present in nature, and albumin absorption is often used to evaluate the antifouling characteristics of possible materials [28]. It has been reported that albumin adsorbed on the material surface prevents binding of microorganisms [29], and the absorption process can happen as fast as seconds after the protein contacts the surface [30]. In this study, polymer coated glass slides were exposed to bovine serum albumin solution (FTIC-BSA, 0.1 mg/mL in PBS buffer) for 2 h at room temperature to

ensure the sufficient interaction between protein and the surfaces (Figure 5.8). The florescence intensity was recorded and compared among the samples. As expected, K3-QA100-HC coated samples exhibited the highest amount of protein absorption, and incorporated PEG segments in the polymer system can dramatically reduce the absorption. This trend can be explained by the charge density on those surfaces, since BSA protein is negatively charged at neutral condition (pI = 4.6), it can be easily adsorbed on positively charged surfaces through electrostatic interaction, and more QAS on the surfaces will result more BSA deposition on the surfaces. On the other hand, PEG has been reported to be non-adhesive to proteins, large amount of PEG in the system can help reduce the protein deposition on the surfaces, as we showed in this work (Figure 5.8).

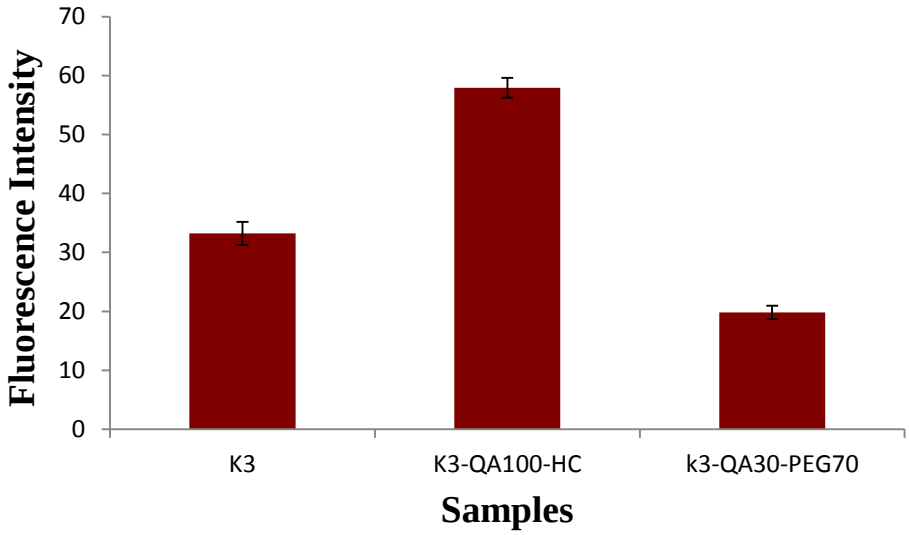

Figure 5.8: Results of protein absorption tests on functional polymer coated glass surfaces compared to unmodified polymer (K3) coated surfaces.

Antimicrobial activities of the coated surfaces were measured by incubating the coated surfaces with the bacteria containing media for 2 days to ensure sufficient contact between the surfaces and the cells. The experiments were carried out with moderate shaking on a rocker table

to provide quasi-linear medium flow over the surfaces of the samples, mimicking the interaction between the solution and the surface in a more dynamic environment, such as in bloodstream or in marine environment [23]. This growth system is very simple and does not require elaborate flow chamber devices, which are costly, complicated, and labor-intensive. Bacterial suspensions of gram positive (*S. aureus)*, gram-negative (*E. coli*) and marine bacteria (*C. marina)* were prepared by dilution in tryptic soy broth (TSB) or marine broth (MB) media. To visualize the adhesion of the bacterial cells on the coated surfaces, LIVE/DEAD BacLight bacterial viability kit was used to differentiate living versus dead bacteria. Figure 5.9 showed the results of the experiments after 10 min incubation of fluorescence dyes followed by three times of rinsing with appropriate growth media. The clean uncoated glass slides were used as a control as they are known to be non-adhesive to bacteria cells. Two different fluorescent dyes presented in the kit stained the bacteria in such a way that live cells were stained green and dead cells are stained red. The figure shows that after 2 days of continuous incubation, very few cells or no cells remain on the polymer coated surfaces. Of the few cells that do stay on K3-QA100-HC coated surfaces, the majority of the cells were dead. It worth noting that several clusters of cells were observed on glass surfaces, which also showed signs of biofilm formation, but on functional polymer coated surfaces, cells were scarce and mainly separated. K3-QA30-PEG70 coated surfaces were almost free of cells for all three bacteria strains tested, indicating the higher effectiveness of this type of dual functionalized copolymers compare to QAS single functional group modified polymers.

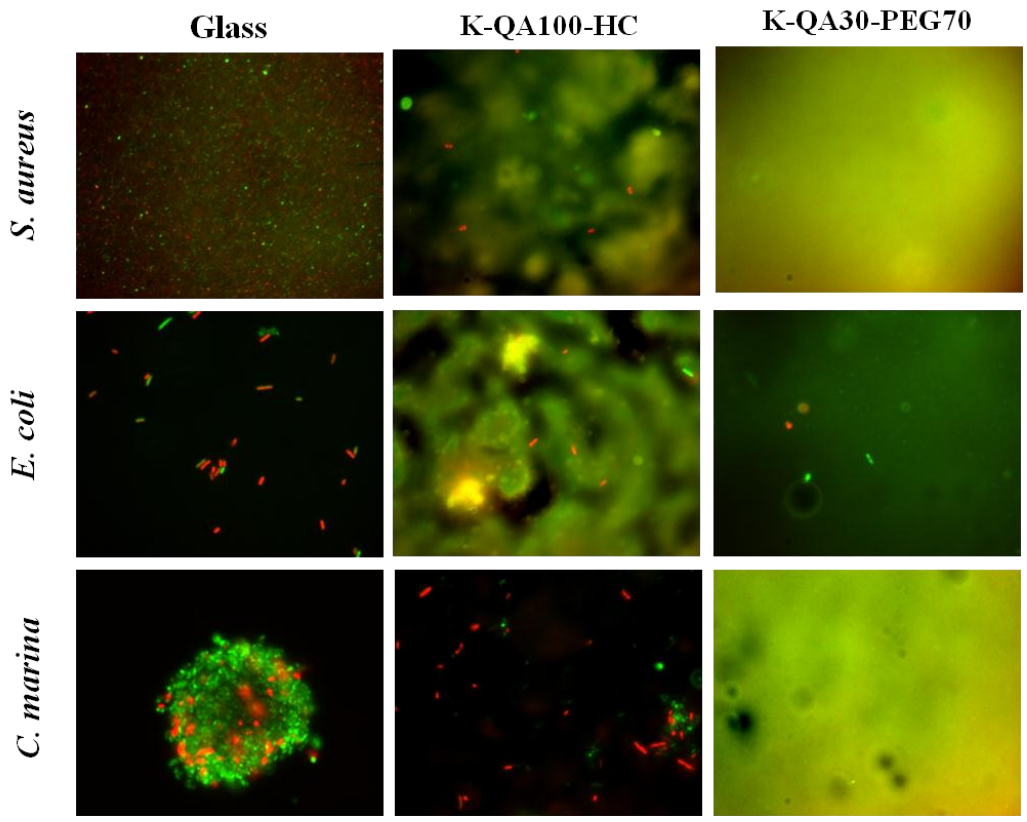

Figure 5.9: Microscopic pictures of functional polymer coated glass surfaces compared to bare glass surfaces after incubated in bacteria solution for 2 days. The cells were stained using LIVE/DEAD BacLight bacterial viability kit, Living bacterial cells exhibit green fluorescence (Syto 9 dye) while dead microorganisms are characterized by a red fluorescence (propidium iodide).

Bacterial growth in the media was also estimated by following the changes in optical density OD_{600} measured using a spectrophotometer. The results showed that the cell growth in the media was largely controlled by the properties of the coated surfaces and bacteria species (Figure 5.10A). Compare to bare glass slides, K3-QA100-HC showed the lowest OD_{600} readings for all three species of bacterial cells. More importantly, it seemed to completely eliminate the growth of *S. aureus*, with OD_{600} almost equal to zero. This result is comparable to the semifluorinated-quaternized PS-*b*-P(E/B)-*b*-PI triblock copolymer that has been shown to inhibit growth of airborne *S. aureus* up to > 99% on the surfaces. The K3-QA100-HC surfaces also

showed significant inhibition of *E. coli* and *C. marina* growth in the media. This is not very surprising, because quaternary ammonium compounds have been known to have a broad spectrum of antimicrobial activity against both gram-positive and gram-negative bacteria [31], and polymers bearing quaternary ammonium moieties with high concentration can manipulate these antimicrobial activities [18]. Also, unlike the soluble polycations, insoluble quaternary ammonium polymers act on the surface of the microbial cell and display their antimicrobial activity only on contact without permeation [19]. In addition, previous studies suggested that upon approach the positively charged surfaces, the structurally essential cations of the cell membrane are relieved of their roles in charge neutralization of the membrane components, and are free to diffuse out of the membrane, thus resulting in a loss of membrane integrity [32]. In this particular case, we hypothesize that the K3-QA100-HC polymer synthesized in this study exhibits this type of membrane-diffusing mechanism in the medium, and that *S. aureus* bacteria (gram-positive) may have been killed before they were able to multiply, resulting in clear growth medium. *E. coli* and *C. marina* (gram-negative) were able to grow at higher density (OD_{600} were 1.8 and 0.5, respectively) after incubating with K3-QA100-HC under the same condition, indicating a different working mechanism of the bacterial species, since gram-negative cell walls are more complex than gram-positive cell walls, both structurally and chemically [33]. Although there were random cells observed on the K3-QA100-HC surfaces for all three species, majority of cells were also dead and numbers were small. K3-QA30-PEG70 coated surfaces showed less cytotoxicity effects on bacterial cells in the growth media, although the OD_{600} readings of *S. aureus* and *C. marina* were lower than those with bare glass surfaces. All cell cultures were able to reach high density (OD_{600} ranged from 0.7 to 2.5), indicating the abundance of cells in the culture media that can generate sufficient contact with polymer coated surfaces.

In addition, the number of cells that adhered to the surfaces were also analyzed and compared. Ten randomly chosen fields of view from LIVE/DEAD BacLight bacterial viability kit staining were imaged using a fluorescence microscope for each sample, and the cells on the surfaces, including both live and dead cells, were counted manually (Figure 5.10 B-D). For *S. aureus* cell culture, all surfaces were relatively free of cells, with only a couple of sparsely separated cells remaining on each surface. K3-QA100-HC seemingly had more cells on the surface but still only about average 5 cells on each random viewed field, and majority of cells was dead. *E. coli* cultures were more resistant to the coated/uncoated glass surfaces (Figure 5.10 C), and grew at higher density in the culture medium, with OD_{600} all close to 2.0. Compared to bare glass surfaces, K3-QA100-HC and K3-QA30-PEG70 showed much lower cell attachment, with K3-QA100-HC showing lowest numbers of *E. coli* cells on the surfaces, partially due to the lower cell density in the culture medium (OD_{600} was 1.8). The *C. marina* culture was very different from both *S. aureus* and *E. coli* species (Figure 5.10 D), where the culture medium (marine broth) formed precipitates after 2 days of cell culture for all tested samples. K3-QA100-HC coated surfaces showed a very uneven distribution of *C. marina* cells, although most fields of view were still free of cells, some fields contained more cells than others due to the non-specific attachment of the particles from the culture nutrients, thus more cells were shown as a result of calculating the average. Again, because of the non-sticky nature of the PEG segments, the K3-QA30-PEG70 surfaces showed better performance than the control glass surfaces for all three species tested, with only few cells adhering to them (~ 2-3 cells in each random field of view) and the numbers are almost negligible.

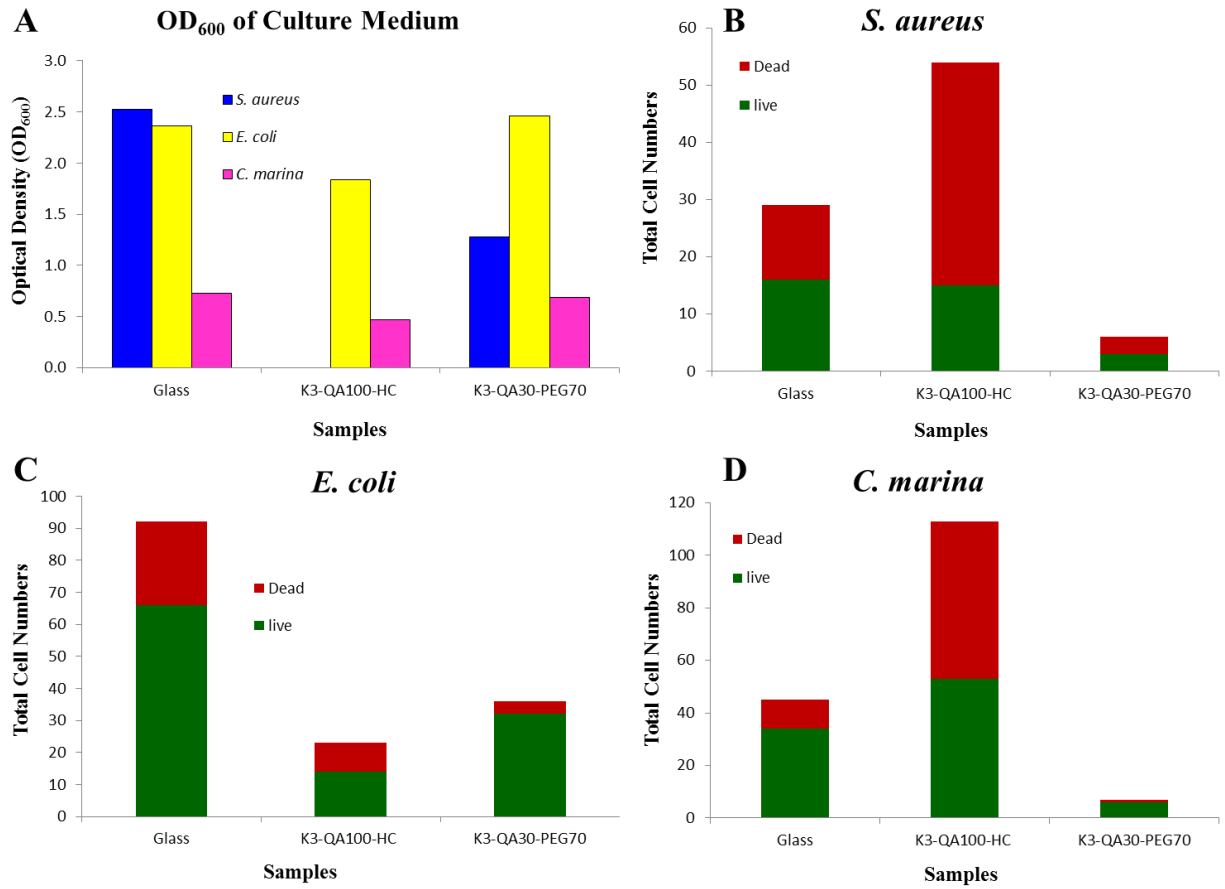

Figure 5.10: A) Optical density (OD_{600}) of the cell culture media after incubated with glass, K3-QA100-HC or K3-QA30-PEG70 samples for 2 days, and average total cell numbers of B) S. aureus, C) E. coli, D) C. marina in 10 random fields on the sample surfaces. Bare glass surfaces were used as controls and each experiment was repeated three times.

The work presented here highlights the antimicrobial effectiveness of surface coatings with different chemical structures. Polymeric coatings containing QAS functionalities alone (K3-QA100-HC) are effective antimicrobials surfaces that can affect both cells in the culture solutions and on surfaces, although their effectiveness can be species dependent, with highest antibacterial activity against *S. aureus* among all three bacteria species tested. Incorporation of PEG segments in similar polymer system (K3-QA30-PEG70) can dramatically reduce the cytotoxic effect of the polymers and obtain higher bacterial repelling on the surfaces. All

bacterial cells tested showed healthy growth in the growth media, and even after contact with bacterial cells at high density for a considerable period of time (48 h), only a few single cells or no cells were observed on those surfaces. Several theories can be used to explain the phenomenon, as previous studies showed that the wettability effect of methoxy-poly(ethylene glycol) (mPEG) may increase the surface energy of the materials and consequently increase bacterial interaction with the bactericide surfaces [34]. Quaternerized polyvinyl pyridine incorporated with hydroxyethyl methacrylate and poly(ethylene glycol) methyl ether methacrylate can elevate antimicrobial activity to 20 times more than the pure quaternized poly(vinyl pyridine). A surface self-concentrating amphiphilic biocide containing both quaternary ammonium and PEG segments was used as an additive for polyurethane surfaces, and the results also showed that this class of polymers are effective antimicrobials against both Gram-positive and Gram-negative bacteria [35]. Interestingly, when the polymers were used in polyurethane resins, contrary to the antimicrobial activities in the solutions (slightly more effective against *E. coli* than *S. aureus*), they were more effective against *S. aureus* than *E. Coli* bacteria. However, it is also possible that the organic components of the nutrient growth medium (NGM) will interact with the positively charged nitrogen atoms and, as a result, deposit on the sample surface and cause the differences (as shown in FTIC-BAS protein absorption testes). NGM can be more significant on K3-QA100-HC coatings, the strong interaction between the coating surfaces and components of the NGM molecules formed another barrier for the direct interaction between cells and coating polymers, which might in fact encourage cells to adhere on the surface despite its cytotoxicity. Furthermore, bacteria can lose membrane integrity upon interaction with highly positively charged surfaces and release cell contents, providing another layer of conditioning film for more cell accumulation and proliferation [6,7]. Bacterial adhesion

and death on the highly quaternized surfaces could also be the reason that semifluorinated-quaternized and fluorinated pyridinium block copolymers did not appear to show promise as either marine antifouling or fouling-release coatings in our previous studies [11,14]. In contrast, K3-QA30-PEG70 can reduce the chance of the NGM molecule deposition and non-specific cell adhesion on the surfaces, and therefore eliminate the interaction between surface proteins and microbial cells [36], and a simple periodic washing would also help to remove the few deposited cells/cell debris and rejuvenate such surfaces.

5.4 Conclusion

In this work, two types of antimicrobial polymers were prepared based on PS-*b*-P(E/B)-*b*-PI triblock copolymers: the first type contained bioactive QAS functionalities and the second type incorporated both QAS and PEG functional units. All QAS and PEG units were covalently attached to the SEBI triblock copolymer backbone through non-hydrolysable amine bonds. This work reported the synthesis and characterizations of all reaction precursors, intermediates and the resulting polymers. The final polymers were further coated on the glass substrate through spray coating techniques and characterized with water contact angles and protein adsorption tests. As an advancement of previous semifluorinated-quaternized SEBI triblock copolymer and fluorinated pyridinium block copolymer coatings prepared in our group, antimicrobial activities of the surfaces were examined against three bacterial species, gram-positive bacteria (*S. aureus*), gram-negative bacteria (*E. coli*) and marine bacteria (*C. marina*). The experiments were also carried out in a simple and effective circulation system for modeling the behavior of bacterial cells both in the culture media and on the polymer coated surfaces. The results showed that the antimicrobial effectiveness was highly dependent on the surface chemical compositions and the

bacterial species. In general, polymers with only QAS functionalities (K3-QA100-HC) showed higher effectiveness to inhibit cell growth in the culture media, and killed most of the cells that did attach to the surfaces. In contrast, polymers containing both QAS and PEG side chains (K3-QA30-PEG70) had less cytotoxic effects on the growth of the cells in the culture media, and cells did not tend to stay on the surfaces. For those cells that did adhere to the surfaces, simple washing steps can be applied to remove the cells/cell debris and to refresh the surfaces. This work emphasizes that the chemical structure of polycationic polymers plays a significant role in their antibacterial activities, and the results suggested that using functional side chains to modify pre-synthesized polymers could be a simple and effective means of producing non-leaching antimicrobial coatings that can be used for various medical and industrial environments.

Acknowledgments

The author would like to thank Dr. David Miller and Dr. Esther R. Angert for help with bacterial culture experiments. This work was supported by the US Department of Defense's Strategic Environmental Research and Development Program (SERDP), grant WP #1454 with additional support from the Office of Naval Research (ONR) through award #N00014-08-1-0010 (JAC and MEC), N00014-02-1-0170 (CKO and EJK). We also acknowledge partial support from the NSF Polymers Program (DMR-0704539) as well as the use of central facilities funded by the NSF-MRSEC program (UCSB MRL, DMR-0520415).

REFERENCES

[1] Nurdin N, Helary G, Sauvet G. Biocidal Polymers Active by Contact .3. Aging of Biocidal Polyurethane Coatings in Water. J Appl Polym Sci. 1993;50:671-78.

[2] Nurdin N, Helary G, Sauvet G. Biocidal Polymers Active by Contact .2. Biological Evaluation of Polyurethane Coatings with Pendant Quaternary Ammonium-Salts. J Appl Polym Sci. 1993;50:663-70.

[3] Kanazawa A, Ikeda T, Endo T. Polymeric Phosphonium Salts as a Novel Class of Cationic Biocides .5. Synthesis and Antibacterial Activity of Polyesters Releasing Phosphonium Biocides. J Polym Sci Pol Chem. 1993;31:3003-11.

[4] Flemming HC, Wingender J. The biofilm matrix. Nat Rev Microbiol. 2010;8:623-33.

[5] Sutherland IW. The biofilm matrix - an immobilized but dynamic microbial environment. Trends Microbiol. 2001;9:222-27.

[6] Qian PY, Lau SCK, Dahms HU, Dobretsov S, Harder T. Marine biofilms as mediators of colonization by marine macroorganisms: Implications for antifouling and aquaculture. Mar Biotechnol. 2007;9:399-410.

[7] Charnley M, Textor M, Acikgoz C. Designed polymer structures with antifouling-antimicrobial properties. React Funct Polym. 2011;71:329-34.

[8] Wach JY, Bonazzi S, Gademann K. Antimicrobial surfaces through natural product hybrids. Angew Chem Int Edit. 2008;47:7123-26.

[9] Park D, Weinman CJ, Finlay JA, Fletcher BR, Paik MY, Sundaram HS, et al. Amphiphilic Surface Active Triblock Copolymers with Mixed Hydrophobic and Hydrophilic Side Chains for Tuned Marine Fouling-Release Properties. Langmuir. 2010;26:9772-81.

[10] Weinman CJ, Finlay JA, Park D, Paik MY, Krishnan S, Sundaram HS, et al. ABC Triblock Surface Active Block Copolymer with Grafted Ethoxylated Fluoroalkyl Amphiphilic Side Chains for Marine Antifouling/Fouling-Release Applications. Langmuir. 2009;25:12266-74.

[11] Park D, Finlay JA, Ward RJ, Weinman CJ, Krishnan S, Paik M, et al. Antimicrobial Behavior of Semifluorinated-Quaternized Triblock Copolymers against Airborne and Marine Microorganisms. Acs Appl Mater Inter. 2010;2:703-11.

[12] Krishnan S, Finlay J, Hexemer A, Wang N, Ober C, Kramer EJ, et al. Interaction of Ulva and Navicula marine algae with surfaces of pyridinium polymers with fluorinated side-chains. Abstr Pap Am Chem S. 2005;230:U4290-U91.

[13] Krishnan S, Wang N, Ober CK, Finlay JA, Callow ME, Callow JA, et al. Comparison of the fouling release properties of hydrophobic fluorinated and hydrophilic PEGylated block copolymer surfaces: Attachment strength of the diatom Navicula and the green alga Ulva. Biomacromolecules. 2006;7:1449-62.

[14] Krishnan S, Ward RJ, Hexemer A, Sohn KE, Lee KL, Angert ER, et al. Surfaces of fluorinated pyridinium block copolymers with enhanced antibacterial activity. Langmuir. 2006;22:11255-66.

[15] Lau C, Anitole K, Hodes C, Lai D, Pfahles-Hutchens A, Seed J. Perfluoroalkyl acids: A review of monitoring and toxicological findings. Toxicol Sci. 2007;99:366-94.

[16] Krafft MP, Riess JG. Perfluorocarbons: Life sciences and biomedical uses - Dedicated to the memory of Professor Guy Ourisson, a true RENAISSANCE man. J Polym Sci Pol Chem. 2007;45:1185-98.

[17] Bleta R, Blin JL, Stebe MJ. Solubilization of various fluorocarbons in a fluorinated surfactant/water system: Relation with the design of porous materials. J Phys Chem B. 2006;110:23547-56.

[18] Kenawy ER, Abdel-Hay FI, El-Raheem A, El-Shanshoury R, El-Newehy MH. Biologically active polymers: synthesis and antimicrobial activity of modified glycidyl methacrylate polymers having a quaternary ammonium and phosphonium groups. J Control Release. 1998;50:145-52.

[19] Tashiro T. Antibacterial and bacterium adsorbing macromolecules. Macromol Mater Eng. 2001;286:63-87.

[20] Gottenbos B, van der Mei HC, Klatter F, Nieuwenhuis P, Busscher HJ. In vitro and in vivo antimicrobial activity of covalently coupled quaternary ammonium silane coatings on silicone rubber. Biomaterials. 2002;23:1417-23.

[21] Nagasaki Y. PEG-Engineering surface having both non-fouling and high-sensing characters. Abstr Pap Am Chem S. 2005;230:U4132-U32.

[22] Zhang ZW, Feng XJ, Luo QM, Liu BF. Environmentally friendly surface modification of PDMS using PEG polymer brush. Electrophoresis. 2009;30:3174-80.

[23] Kuhn DM, Chandra J, Mukherjee PK, Ghannoum MA. Comparison of biofilms formed by Candida albicans and Candida parapsilosis on bioprosthetic surfaces. Infect Immun. 2002;70:878-88.

[24] Liu W, Howarth M, Greytak AB, Zheng Y, Nocera DG, Ting AY, et al. Compact biocompatible quantum dots functionalized for cellular imaging. J Am Chem Soc. 2008;130:1274-84.

[25] Sundaram HS, Cho YJ, Dimitriou MD, Weinman CJ, Finlay JA, Cone G, et al. Fluorine-free mixed amphiphilic polymers based on PDMS and PEG side chains for fouling release applications. Biofouling. 2011;27:589-601.

[26] Daffonchio D, Thaveesri J, Verstraete W. Contact-Angle Measurement and Cell Hydrophobicity of Granular Sludge from Upflow Anaerobic Sludge Bed Reactors. Appl Environ Microb. 1995;61:3676-80.

[27] Bamford CH, Al-Lamee KG. Chemical methods for improving the haemocompatibility of synthetic polymers. Clinical materials. 1992;10:243-61.

[28] Zhao C, Li LY, Wang QM, Yu QM, Zheng J. Effect of Film Thickness on the Antifouling Performance of Poly(hydroxy-functional methacrylates) Grafted Surfaces. Langmuir. 2011;27:4906-13.

[29] Pavithra D, Doble M. Biofilm formation, bacterial adhesion and host response on polymeric implants--issues and prevention. Biomedical materials. 2008;3:034003.

[30] Holmberg M, Hou X. Competitive protein adsorption--multilayer adsorption and surface induced protein aggregation. Langmuir : the ACS journal of surfaces and colloids. 2009;25:2081-9.

[31] Kawabata N, Nishiguchi M. Antibacterial Activity of Soluble Pyridinium-Type Polymers. Appl Environ Microb. 1988;54:2532-35.

[32] Kugler R, Bouloussa O, Rondelez F. Evidence of a charge-density threshold for optimum efficiency of biocidal cationic surfaces. Microbiol-Sgm. 2005;151:1341-48.

[33] Beveridge TJ. Structures of gram-negative cell walls and their derived membrane vesicles. J Bacteriol. 1999;181:4725-33.

[34] Sellenet PH, Allison B, Applegate BM, Youngblood JP. Synergistic activity of hydrophilic modification in antibiotic polymers. Biomacromolecules. 2007;8:19-23.

[35] Harney MB, Pant RR, Fulmer PA, Wynne JH. Surface Self-Concentrating Amphiphilic Quaternary Ammonium Biocides as Coating Additives. Acs Appl Mater Inter. 2009;1:39-41.

[36] Ye SJ, Majumdar P, Chisholm B, Stafslien S, Chen Z. Antifouling and Antimicrobial Mechanism of Tethered Quaternary Ammonium Salts in a Cross-linked Poly(dimethylsiloxane) Matrix Studied Using Sum Frequency Generation Vibrational Spectroscopy. Langmuir. 2010;26:16455-62.

CHAPTER SIX

CONCLUSION

Cell-surface interaction is a crucial part of many biological and physiological processes and represents a prerequisite for a multitude of cellular functions such as movement, growth, differentiation, proliferation and survival. Synthetic polymers are attractive and unique materials that can be used for cell-surface interaction studies, because their scaffold architectures, chemical composition, physical and biochemical properties can be precisely controlled during synthetic steps and each property can also be further optimized for specific biological applications. Both chemical and physical properties of the synthetic polymers play important roles in controlling cell adhesion events and determining the fate of the cells after attaching to the surfaces, and it is important for those polymers to provide all the proper surface cues in order to induce specific cell responses. In recent years, a large number of synthetic polymeric materials have been explored to control cell behavior on material surfaces for different biological applications. They have provided a large degree of surface heterogeneity regarding the type and distribution of chemical functional groups, different surface charges and roughness, and the presence of either hydrophilic or hydrophobic groups. Although a number of contemporary synthetic materials possess excellent characteristics, many still need to be modified in ways that cell attachment, adhesion and spreading on the surfaces can be controlled.

In this thesis, we designed and synthesized functionalized polymers with specific chemical and physical properties to control cell adhesion on material surfaces. For example to promote neuronal cell attachment and growth, the functional monomer 2-methacryloxyethyl trimethylammonium chloride (MAETAC) was chosen to provide tethered neurotransmitter acetylcholine-like functionality, thereby modifying the properties of biocompatible, non-adhesive PEG-based hydrogels. Eleven hydrogel samples (HS-1 to HS-11) were prepared in this study through radical polymerization reactions by mixing MAETAC and PEGMA monomers in

different ratios. Elemental analysis showed that the amount of MAETAC structure presented in the final hydrogels corresponded to the feed ratio of the monomers. The effect of the functional monomer concentration on the physical properties of the hydrogels was systematically studied. In general, increasing the proportion of MAETAC monomer yielded increasing water content, swelling ratio and a corresponding decrease in compressive modulus in the gels. All the hydrogel samples were further evaluated for mice hippocampal neural cell attachment and growth. The results showed that MAETAC in the hydrogels promotes mice hippocampal neuronal cell attachment and differentiation in a concentration-dependent manner, and cells on the hydrogels showed differences in number, length of processes and exhibited different survival rates. Hydrogels with high concentration of MEATAC (greater than 40% v/v, sample HS-1 to HS-5) showed high cytotoxic effects (0% viability), while the gels with relatively low concentration (less than 40% v/v) of MAETAC exhibited statistically reduced toxicity. The sample containing 10% (v/v) MAETAC monomer (HS-9) showed the highest viability (50.9%) and the highest number of neurons among all the eleven samples. In addition, immunocytochemistry analysis indicated that sample HS-7 greatly favored astrocyte adhesion, while sample HS-9 and HS-10 favored neuron attachment, suggesting that the presence of an optimal amount of MAETAC on the hydrogel surface is an important factor in the subsequent behavior of the cells.

By studying these hydrogels, the critical concentration range of functional monomer MAETAC in the system was identified for brain neuronal cell culture (40% to 10% v/v), and this knowledge was important to further optimize the current system. For example, with fewer amounts of crosslinker PEGDA molecules in the prepolymerization solutions, softer hydrogel samples can be easily prepared for the application of brain implantation or cell encapsulation. Also, without adding crosslinker PEGDA in the polymerization solutions, linear soluble

polymers can be prepared with the same components for substrate coating and *in vitro* cell culture studies. Since sample HS-7 favored astrocyte attachment and growth while HS-9 and HS-10 favored neuron attachment and growth specifically, selectively culturing astrocytes or neurons is also possible by properly modifying physical and chemical properties of these types of hydrogels. Furthermore, due to the rich chemistry of the free hydroxyl groups present in the PEGMA monomer, these synthetic hydrogels can be readily modified with other functionalities, such as by linking nerve growth factor, covalently bonding extracellular matrix (ECM) proteins or peptides, for other neuronal tissue engineering applications.

However, hydrogels provide bulky 3-D scaffolds as compared to thin polymer film coated on a substrate to encourage cell adhesion, and thus it is difficult to directly compare hydrogels with standard neuron culture substrates, such as poly(L-lysine) (PLL) or laminin-coated glass coverslips. Moreover, there is an increasing importance in developing biocompatible polymer materials for neuroprosthetic device coatings and in controlling growth of neurites for regeneration in the central nervous system; however, there still remain technical challenges in preparing stable hydrogel coatings on device surfaces and further patterning the surfaces. Polymer brushes, on the other hand, can provide nanometer thickness of functional polymers to modify substrate surface properties without altering their bulk characteristics. Polymer brushes also offer a high degree of synthetic flexibility towards the introduction of a variety of functional groups. In particular, surface-initiated atom transfer radical polymerization (SI-ATRP) reactions can tolerate a wide range of functional monomers, they can also be conducted under less stringent experimental conditions. Therefore, in recent years, SI-ATRP reactions have become one of the most popular routes to control the functionality, density and thickness of the polymer brushes. In addition, polymer brushes can be easily combined with a

wide range of micro- and nano-fabrication techniques (e.g., photolithographic methods) to prepare surfaces with different surface features for cell patterning.

To further explore the potential of biomimetic materials containing acetylcholine functionalities in neural tissue engineering, in chapter three of this thesis, we prepared polymer brushes with functional monomers MAETAC and PEGMA using the "grown from" method through SI-ATRP reactions. The surface properties of the resulting brushes were thoroughly characterized with elliposometry, water contact angles, AFM, ATR-FTIR, XPS and NEXAFS. Results showed that the polymer brushes reached a thickness of 21 $\pm$ 2 nm after 5 h of reaction at room temperature, the brush surfaces were relatively smooth (*Ra* was estimated to be 3 $\pm$ 1.8 nm) and chemically uniform. Mice hippocampal neuronal cell culture on the polymer brush surfaces showed that, after 3 days, the cells maintained comparable viability and number of neurons to standard poly-L-lysine (PLL) coated glass coverslips under the same culture conditions. Also, the neurons possessed the average mean neurite length significantly longer on the brush surfaces than those cultures on the PLL modified control surfaces. In addition, UV photolithographic techniques were used to prepare patterned polymer brushes with different features. The pattern was specifically designed to incorporate both surface chemical and topographic cues in one single visual field. It provides several horizontal lines with different sizes (range from 2 μm to 200 μm, 100 times difference), and all the horizontal lines were connected at one end with a vertical line to provide more curves and another direction (horizontal *vs.* vertical). The pattern was backfilled with non-adhesive PEG-SAM, highlighting the differences between acetylcholine functionalized poly(PEGMA) brush surfaces and surfaces containing only PEG groups for neuronal cell adhesion and growth. To test the pattern, FITC labeled BSA protein (pI is 4.7, negatively charged in PBS buffer) was used to distinguish the difference of polymer brushes

from PEG regions, since BSA protein absorption is much higher on positively charged polymer brush regions. Hippocampal neuronal cell culture tests on the polymer brush patterns showed that both the size and the orientation of the patterns can influence cell behavior on the surfaces. At feature sizes smaller than 12 μm, neurons were not able to follow the patterned lines and establish connections, but they were tightly confined to 25 μm lines. At larger feature sizes (50-200 μm), more neurons can attach to the brush region and they also formed more complicated interconnections and networks. We also noticed that, in this specific pattern, more neurons tend to stay on horizontal lines than vertical lines at the same size scale (100 μm). In addition, neuronal cell morphologies are also strongly influenced by the patterns, for example, at line widths of 100 μm cells exhibited a star-shaped morphology, while at line width of 25 μm cells were extended as line-shaped.

Compared to hydrogel systems with similar chemical composition, polymer brushes enable direct comparison of cell culture results with standard PLL coated surfaces and can be easily patterned through standard photolithography techniques. Studies of BSA protein absorption and hippocampal neuronal cell cultures also indicate that, because of the positively charged nature of the acetylcholine functionalities and the biocompatibility characteristics of PEG units, the random copolymer brushes may also find potential application to pattern other biomacromolecules such as negatively charged DNA, RNA molecules, and to pattern other types of cells such as human endothelial cells. The free hydroxyl terminal groups of the PEG units of the polymer brushes can also be readily modified into various functional groups including chloride, amine, and carboxylic acid groups, and covalently linked to other bioactive molecules for more specific neuronal engineering applications. During cell culture experiments, we noticed that neurons on the polymer brush surface are not as strongly attached as those on the PLL

coated surfaces, and thus cells were more easily washed away and the processes can also be broken during washing steps. This is probably caused by the lower positive charge density on the surface and non-fouling properties of PEG units present in the brushes, which resulted in weaker interactions between the surface and neuronal cells that allows cells to differentiate more easily. High positive charge density in PLL coated surfaces, on the other hand, may lead to stronger interactions which can retard neuronal cell attachment on the surfaces and hinder further differentiation and spreading. Comparing the effect of interaction forces on the neuronal cell growth and morphology on this type of synthetic materials may also help in understanding why the relative length of neurites on brush surfaces is much longer than that on PLL coated surfaces.

Cell adhesion and growth on material surfaces is not always desirable. For example, marine biofouling of various organisms on man-made structures, such as ships and boats, can cause numerous problems including decreased fuel efficiency, lower obtainable speeds and high frequency of required maintenance. Recently, with increased legislation on toxicity requirements of surface coatings, more research has been focused on developing non-leachable, toxin-free, environmentally friendly polymeric antifouling/fouling release materials. To address this problem, in chapter four of this thesis, we described a strategy to prepare amphiphilic polymer coatings using "reversed zonyl" to modify specially designed SEBI triblock copolymer (or K3 polymer) to inhibit fouling of marine organisms. Polymers with amphiphilic structures contain both hydrophobic and hydrophilic components. It was hypothesized that these structures can undergo conformational changes to expose different functionalities corresponding to the surrounding environments to create "ambiguous" surfaces that can deter the settlement and adhesion of a range of cells. The molecular structures of "reversed zonyl" synthesized in this work, feature a short free hydroxyl-terminated fluorinated alkyl chain ($C_{10}H_4F_{16}$) terminated by

monomethylated PEG groups with different lengths (PF-PEG350-OH, PF-PEG550-OH, and PF-PEG750-OH). These macromolecules were then used as side chains to modify the pre-synthesized K3 triblock copolymers through nucleophilic substitution reactions. The chemical structures of the final polymers with amphiphilic side chains were confirmed with NMR and IR spectroscopies and elemental analysis, and the purified polymers were then applied on glass substrates through an established multilayer surface coating technique. Water contact angles showed that the amphiphilic polymer coated surfaces were more hydrophobic in the dry state (water contact angles were higher than 85°), while underwater bubble contact angles showed that the surfaces became more hydrophilic after immersion in water and eventually reached an equilibrium value of 40° after one week. FITC-BSA protein absorption tests on these functional polymer coated glass slides suggested that these coatings can largely reduce the protein absorption on the surfaces, and biofouling assays against green alga *Ulva* showed that there were no signs of toxicity from those surfaces on the cells. Sporelings grew normally on all coatings, but percentage removal of 7-day old sporelings from those coatings was higher than the controlled samples.

The previously described preliminary experiments indicated that the amphiphilic perfluorocarbon/PEG side chain modified triblock copolymers are promising antifouling/fouling release coating materials. However, the major challenge of the current approach is the low attachment yields of side chains (PEG-PF) to the PS-*b*-P(E/B)-*b*-PI (or K3) polymer backbone. A more effective method needs to be identified in order to achieve higher attachment of these functional side chains in the future. Several other methods with improved reaction conditions were also explored in this work to solve this problem, such as using freshly dried solvents and reagents, excess side chain molecules (2-4 times), longer reaction time (3 days to one week), and

different reaction groups (e.g., carbonyl chloride). In addition, epoxidation of isoproprene blocks were prepared to provide active functional groups for polymer backbone modification, and PEG-PF-OH molecules were used to open the epoxy-ring under acid catalyst ($BF_3 \cdot Et_2O$), but as above no improvement was observed. Another strategy we tried was to introduce two extra carbons from ethylene glycol (EG) to eliminate the difficulty of using perfluorocarbon alcohol; these new molecules (PEG-PF-EG-OH) have hydroxyl groups further away from perfluorocarbon block and were used to open the epoxy-rings on polyisoproprene block. Still, only similar amounts of side chains could be attached to the polymer backbones. However, as part of the current progress (not shown), "reversed Brij" (hydrocarbon/PEG or PEG-HC-OH) amphiphilic structures were used to modify K3 block copolymer and the reaction was carried out using PEG-PF-OH molecules to open the epoxy-ring in epoxy-K3 under acid catalyst ($BF_3 \cdot Et_2O$), the reactions obtained much higher attachment ratios compared to reactions with "reversed zonyl" attachment reactions and showed some promising results against both *Ulva* and *Navicula* cell adhesion and release. Compare to "reversed Brij" structures, the difficulty of attaching "reversed zonyl" amphiphilic side chains to the polymer backbones may be caused by the unique chemical and physical properties of perfluorocarbon/PEG compounds, and the steric hindrance of their bulky structures may also deter the completion of the linkage reaction at high yield. As discussed in chapter four, PEGylated semifluorinated surfactants can self-assemble to form micelle structures with a fluorous phase-based inner core. Therefore, the functional groups (-OH groups) can be largely buried in the cores and cannot be efficiently utilized in the reactions. A more careful study of micelle formation and dissociation might provide some useful insights about how to improve its usage in modifying K3 polymer with nucleophilic substitution reactions.

Bacterial adhesion, growth and biofilm formation are also problematic and pose major

concerns in healthcare and many industrial environments. Materials with antifouling and antimicrobial properties are useful in many domains such as food manufacturing, hospitals, building materials and water purification. In particular, those with antimicrobial agents (e.g., quaternary ammonium compounds) covalently attached onto polymer backbones offer good stability and high antimicrobial effectiveness. Since we already established the methods to apply K3 based polymers on glass substrates in the previous chapter, in the last chapter of this thesis (chapter five), we aimed to prepare non-leachable polymer coatings with probable antimicrobial and/or antifouling activities based on modification of K3 triblock copolymer. Two different strategies were reported to introduce quaternary ammonium antimicrobial components on K3 polymer backbone. In the first strategy, antimicrobial quaternary ammonium salts (QAS) alone were attached to the polymer backbones to provide bioactive polymers (K3-QA100-HC) whose quaternary ammonium units were intended to kill bacterial cells. In the second approach, we incorporated both the bioactive moieties (QAS) and the non-adhesive bio-passive moieties (PEG) in the polymer to provide dual function polymers (K3-QA30-PEG70). In both approaches, all the functional moieties were covalently linked to the PS-*b*-P(E/B)-*b*-PI polymer backbone through non-hydrolysable amine bonds. The resulting polymers were characterized with NMR, IR, and elemental analysis. The polymers were then applied to glass surfaces and incubated with several organisms (gram-positive *S. aureus*, gram-negative *E. coli* and marine bacteria *C. marina*) in culture media for a sufficient period of time (2 days) to test their antimicrobial activities in aqueous environments. A simple and effective rocking model system was used for the tests to monitor the of bacterial cells both in the culture media and on the functional polymer coated surfaces, thereby comparing the abilities of different coatings against biofilm formation, without using the elaborate flow chamber devices.

The results of bacterial cell tests emphasized that the chemical structures of polycationic polymers plays a significant role in their antibacterial activities. Polymeric coatings containing QAS functionalities alone (K3-QA100-HC) form effective antimicrobial surfaces that can affect both cells in the culture solutions and on surfaces, although their effectiveness can be species dependent, with the highest antibacterial activity against *S. aureus* among all three bacteria species tested (OD_{600} almost equal to zero). Incorporation of PEG segments in similar polymer systems (K3-QA30-PEG70) can dramatically reduce the cytotoxic effects of the polymers to the cell culture solution and obtain higher bacterial repelling on the surfaces. All bacterial cells tested showed healthy growth in the growth media. K3-QA30-PEG70 polymer also showed better performance than the control glass surfaces for all species tested, even after contact with bacterial cells at high density for a considerable period of time (48 h), only a few cells were observed on the surfaces (~ 2-3 cells in each random field of view) and the numbers are almost negligible.

The detailed mechanism of how the antimicrobial surfaces influence bacterial cells is currently unknown. It is possible that the organic components of the nutrient growth medium (NGM) will interact with the positively charged nitrogen atoms and, as a result, deposit on the sample surface and cause the differences. The effect of the NGM can be more significant on K3-QA100-HC coatings. The strong interaction between the coating surfaces and components of the NGM molecules formed another barrier for the direct interaction between cells and coating polymers, which might in fact encourage cells to adhere on the surface despite its cytotoxicity. Furthermore, bacteria can lose membrane integrity upon interaction with highly positively charged surfaces and release cell contents, providing another layer of conditioning film for more cell accumulation and proliferation. In contrast, the presence of PEG in the K3-QA30-PEG70

polymer can reduce the chance of the NGM molecule deposition and non-specific cell adhesion on the surfaces, and therefore eliminate the interaction between surface proteins and microbial cells. A simple periodic washing would also help to remove the few deposited cells/cell debris and rejuvenate such surfaces. An efficient method that can determine the type of protein on the surfaces and quantify the amount of proteins will also help us understand the roles of those proteins in cell-material interaction. Bacteria cell culture medium should be monitored periodically to understand the cell-surface interaction processes, especially in an environment that can closely mimic complex and dynamic surroundings as in bloodstream or marine water. Those synthetic polymers can also be further optimized to improve their antimicrobial performance. For example, polymers with different lengths of saturated hydrocarbon chains on quaternary ammonium structures or different sizes of PEG chains can be tested and compared for their effectiveness. Furthermore, many structural features in these antimicrobial polymers have not been assessed systematically in the current studies, including the roles of polymer backbone structure, flexibility/rigidity, copolymer microstructure, and macromolecular architectures. More detailed structure-activity studies aimed to delineate delineating the effects of those parameters would improve our understanding of this system and would facilitate future design strategies.

In summary, this dissertation focused on preparation of functionalized polymers with specific chemical and physical cues to control cell-surface interactions. Specifically, hydrogels and polymer brushes with acetylcholine functionalities were prepared to promote mouse hippocampal neuronal cell attachment and to guide neurite outgrowth, while K3 triblock copolymers modified by hydrocarbon/PEG amphiphilic side chains were used as non-toxic marine antifouling/fouling release surface coatings to discourage marine organisms (e.g., *Ulva*) from attaching to the surfaces. In the final chapter, K3 triblock copolymer was functionalized

with quaternary ammonium salts to prepare either bioactive or dual functional polymers as non-leachable antimicrobial coatings.

The functionalized polymers in this thesis open opportunities for future optimization and modification. These polymers may also hold potential applications in other areas which have been separately discussed in each chapter. In all these synthesized polymers, PEGs were used as neutral and non-adhesive components to improve biocompatibility of the materials, while reducing non-specific cell-surface interactions. Also, all hydrogels, polymer brushes and antimicrobial polymer samples contain positively charged quaternary ammonium salts (QAS) to induce specific cell responses. The quaternary ammonium salts in hydrogels and polymer brushes have shorter hydrocarbon terminal groups (one carbon), and they are a part of polymer main chains and presented in either 3D material matrices or thin polymer films on substrates. In contrast, QAS used for antimicrobial coatings have longer hydrocarbon terminal chains (six carbons), and they were attached to K3 triblock copolymer backbone as side groups. The cell culture studies suggest that, despite their structural similarity, polymeric quaternary ammonium compounds can have a broad spectrum of effects on cell behaviors based on the unique properties of the polymers. These effects can range from enhancing neuronal cell adhesion and growth to killing or repelling bacterial cells, which emphasizes the advantages of functional polymers over small molecules with the same functional groups. The results from these studies also indicate that, although the material properties do depend on the functional groups and polymer composition, many other characteristic properties such as scale, connectivity, orientation and specific surface morphology can dramatically influence cell-material interactions. Moreover, there are several interesting challenges remaining to be explained in these polymeric materials. New strategies and methods needed to be developed to help advance and understand

the structure-activity interactions, not only on the effects of chemical properties of the functional groups, but also on the roles of polymer backbone and side chain structures, flexibility, morphology and macromolecular architectures. In particular, experiments focusing on controlling bioactive ligand (e.g., QAS) presentations on surfaces and experimental designs that closely mimic physiological conditions can further our understanding of *in vivo* cell-surface interactions.